Optimal Placement and Sizing of Distributed Generation for Power Loss Minimization and Voltage Profile Improvement in Distribution Network
(Case Study: Kombolcha Distribution System)

Seid Endris Ali

A Thesis Submitted to
The Department of Electrical Power and Control Engineering
School of Electrical Engineering and Computing

Presented in Partial Fulfillment of the Requirement for the Degree of Master's in Electrical Power and Control Engineering (Power System Engineering)

Office of Graduate Studies
Adama Science and Technology University

October, 2023
Adama, Ethiopia

Optimal Placement and Sizing of Distributed Generation for Power Loss Minimization and Voltage Profile Improvement in Distribution Network (Case Study: Kombolcha Distribution System)

Seid Endris Ali

Advisor: Dr. Milkias Berhanu

A Thesis Submitted to
The Department of Electrical Power and Control Engineering
School of Electrical Engineering and Computing

Presented in Partial Fulfillment of the Requirement for the Degree of Master's in Electrical Power and Control Engineering (Power System Engineering)

Office of Graduate Studies
Adama Science and Technology University

October, 2023

Adama, Ethiopia

DECLARATION

I hereby declare that this Master Thesis entitled "Optimal Placement and Sizing of Distributed Generation for Power Loss Minimization and Voltage Profile Improvement in Distribution Network (Case Study: Kombolcha Distribution System)" is my original work and has not been submitted to any university for a similar purpose. All sources of materials that are used for this thesis have been duly acknowledged through a citation.

Seid Endris Ali	________________	________________
Name of Student	Signature	Date

RECOMMENDATION

I, the advisor of this thesis, hereby certify that I have read the revised version of the thesis entitled "Optimal Placement and Sizing of Distributed Generation for Power Loss Minimization and Voltage Profile Improvement in Distribution Network (Case Study: Kombolcha Distribution System)" prepared under my guidance by Seid Endris Ali submitted in partial fulfillment of the requirements for the degree of Master's of Science in Power System Engineering.

Therefore, I recommend the submission of a revised version of the thesis to the department following the application procedure.

Dr. Milkias Berhanu	_________________	_________________
Advisor	Signature	Date

APPROVAL SHEET

I, the advisor of the thesis "Optimal Placement and Sizing of Distributed Generation for Power Loss Minimization and Voltage Profile Improvement in Distribution Network (Case Study: Kombolcha Distribution System)" and developed by Seid Endris, hereby certify that the recommendation and suggestions made by the board of examiners are appropriately incorporated into the final version of the thesis.

Dr. Milkias Berhanu	______________________	__________________
Advisor	Signature	Date

We, the undersigned members of the board of Examiners of the thesis by Seid Endris have read and evaluated the thesis entitled "Optimal Placement and Sizing of Distributed Generation for Power Loss Minimization and Voltage Profile Improvement in Distribution Network (Case Study: Kombolcha Distribution System)" and examined the candidate during the open defense. This is, therefore, to certify that the thesis is accepted for partial fulfillment of the requirement for the degree of Master of Science in Power System Engineering.

Dr. Tefera Terefe	__________________	______________
Chairperson	Signature	Date
Dr. Prathibah E.	__________________	______________
Internal Examiner	Signature	Date
Dr. Firew	__________________	______________
External Examiner	Signature	Date

Finally, approval and acceptance of the thesis are contingent upon submission of its final copy to the Office of Postgraduate Studies (OPGS) through the Department Graduate Council (DGC) and School Graduate Committee (SGC).

____________________	__________________	______________
Department Head	Signature	Date
____________________	__________________	______________
School Dean	Signature	Date
____________________	__________________	______________
Office of Postgraduate Studies, Dean	Signature	Date

ACKNOWLEDGMENT

First and foremost, I take this chance to thank **ALLAH**, the lord of the universe, the most beneficent and merciful for helping me to complete this thesis work. It would have been impossible without the help of him.

Secondly, I would like to express my deepest gratitude, thanks, respect, and appreciation to my advisor **Dr. Milkias Brahanu** for his guidance, and support kindly. His invaluable mentorship, suggestions, and constructive comments supported completing my thesis.

Thirdly, I would like to thank and acknowledge those who helped me in providing the necessary data used for this thesis, mainly **Mr. Bedru**, **Mr. Hussein**, **Mr. Selemon**, and other Kombolcha-I substation and Kombolcha EEU workers for their kindly cooperation for providing all the required data that are useful to accomplish this thesis.

Finally, I would like to take this opportunity to thank all my beloved families, especially my mother **Aregash Adem** and my best friend **Mr. Assen Besher Alyu** for their encouragement, patience and endless prays, and their outstanding support during the different phases of my work.

Thank you all!

Seid Endris Ali

CONTENTS

LIST OF TABLES

LIST OF FIGURES

FIGURE PAGE

LIST OF ACRONYMS AND ABBREVIATIONS

AAC	All Aluminum Conductor
AC	Alternative Current
BCBV	Branch Current Bus Voltage
BFS	Backward Forward Sweep
BIBC	Bus Injection Branch Current
BPSO	Binary Particle Swarm Optimization
CAS	Cross-sectional Area of Conductor
CB	Circuit Breaker
CBE	Commercial Bank of Ethiopia
CIGRE	International Council on Large Electric Systems
CSA	Crow Search Algorithm
CT	Current Transformer
CVD	Cumulative Voltage Deviation
DC	Direct Current
DER	Distributed Energy Resource
DG	Distributed Generator
DLF	Distribution Load Flow
DS	Distribution System
DT	Distribution Transformer
ECI	Equivalent Current Injection
EEP	Ethiopian Electric Power
EEU	Ethiopian Electric Utility
EPRI	Electric Power Research Institute
ETAP	Electrical Transient Analyzer Program
FACTS	Flexible AC Transmission System
GA	Genetic Algorithm
GMR	Geometric Mean Ratio
IEEE	Institute of Electrical and Electronic Engineer
KCL	Kirchhoff's Current Law
KM	Kilo Meter
KV	Kilo Volt
KVL	Kirchhoff's Voltage Law

MOF	Multi-Objective function
NTL	Non-Technical Loss
PSO	Particle Swarm Optimization
PU	Per Unit
PV	Photovoltaic
RDS	Radial Distribution System
USD	United State Dollar
VSI	Voltage Sensitivity Index
WOA	Whale Optimization Algorithm

ABSTRACT

The continuous power demand increment and increasing rate of urbanization need a good quality and reliable power supply system to satisfy the customer's interest. On the other hand, the fast-increasing power demand cannot be met by the current passive distribution system or the expensive power transmission system from generation. The significant issues faced by the Ethiopian power distribution system, such as high-power loss, frequent power interruptions, and inadequate voltage magnitude, severely affect productivity of individual customers. This thesis presents the technique how to improve the performance of the distribution system by reducing the system power loss and enhancing the voltage profile through optimal allocation of distributed generation (DG) at Kombolcha-I substation outgoing distribution feeder three (L3). The feeder has 138 buses, and 74 loads. To assess the selected feeder's system power loss and voltage profile, the feeder was modeled in the MATLAB computational toolbox, and its load flow analysis was simulated using the backward/forward sweep (BFS) approach. From the BFS load flow results of the base case system, the total system real and reactive power loss of the selected feeder are 400.9144 kW and 404.8814 kVAr respectively and the magnitude of most of the buses are below the minimum standard limit. The objective function of this thesis work was to minimize both real and reactive power loss and enhance the voltage profile of the feeder by integrating the optimal DG size in the optimal location. This research uses a hybrid genetic algorithm and particle swarm optimization (GA-PSO) algorithm to find the optimal size and allocation of DG. The findings of this study demonstrate that proper DG sizing and placement enhance the performance of the distribution system. From the simulation results the active power loss percentage reduction was 45.944%, 51.0277%, 58.7234%, and 58.8331%, while the reactive power loss percentage reduction was 52.267%, 59.279%, 62.9945%, 62.4686% for1-DG, 2-DG, 3-DG, and 4-DG installation respectively. And also, the base case minimum voltage was improved from 0.9155p.u to 0.95016p.u, 0.95341p.u, 0.95489p.u and 0.9571p.u. For all cases, the bus voltage of the system was within the acceptable standard range. Th multi objective function (MOF) value was 0.02295, 0.02129, 0.021022, and 0.02082 for the integration of 1-DG, 2-DG, 3-DG, and 4-DG respectively. Furthermore, a comparison analysis has also been done to investigate the effectiveness of the proposed hybrid GA-PSO algorithm with other algorithms. The results obtained from the comparison indicate that, almost in all cases the hybrid GA-PSO method gives a better system performance by minimizing the system power loss, voltage profile improvement, and better fitness values. The cost analysis of DG integration showed that integration of 3-DG in the system needs an initial capital cost of 206,302,896.8 birr with a payback period of 4.782 years and it is an optimum solution.

Keywords: *Distributed generation, Distribution system, GA, Power loss reduction, PSO, Voltage profile improvement.*

CHAPTER ONE

1. INTRODUCTION

1.1 Background of the Study

An electric power system consists of several interconnected components that work together to generate, transmit, distribute, and deliver electricity. It has three fundamental components those are generation system, transmission system, and distribution system. Power generation involves the production of electricity from various renewable and nonrenewable energy sources. The transmission system is another power system component responsible for transporting generated power across great distances from power plants to distribution substations. End-users, such as residential, commercial, and industrial consumers, are supplied with energy by the distribution system from the substations. The distribution system is the largest and the most complex part of the power system, which is typically radial in configuration, has less cost, simple in construction, and is the most critical connection among the rest of the electrical power system components. The radial distribution system is well known for its high resistance-to-reactance ratio and high voltage drops that could cause significant power losses along the feeder. The power loss experienced in the distribution system is typically greater than that in the transmission system. The power distribution system experiences significant power losses that necessitate the utilization of various techniques to minimize it as much as possible (Khetrapal et al., 2020). Power losses happen at each stage of the power distribution process. In heavily loaded distribution systems, high-load currents may lead to an increase in power loss and inefficient performance due to the reduction in voltage magnitude and increase in distribution system losses. Compared to other systems, the distribution system is the most inclusive part and is mainly responsible for system power loss since it operates at low voltage (Marneni et al., 2015). Power loss has a substantial impact on the operational efficiency of distribution systems. Therefore, it is imperative to minimize power loss in the distribution system to the greatest extent possible (Muhammad et al., 2020). Changes in load demand have long been a problem for power distribution systems, leading to voltage oscillations outside the range allowed by fluctuations at various buses and power losses (Ntombela et al., 2022). In recent times, researchers and professionals in the power industry have devoted their attention to discovering novel methods for enhancing the efficiency of distribution systems. Two primary approaches have emerged as potential solutions to overcome those problems. The first way is to expand the network infrastructure. The second and most efficient technique is integrating distributed generation (DG) into the current distribution system. However, the expansion of distribution networks is hindered by high costs and environmental concerns, making it impractical in many cases. Consequently, the most practical and feasible solution involves the integration of DG units within the existing system (Zaheer et al., 2022).In recent years, renewable-based DG units have seen rapid development worldwide due to their promising ability to minimize power loss and reduce harmful carbon emissions. However, there are challenges associated with utilizing DG for power loss reduction and voltage profile improvement, specifically in terms of determining the proper location and appropriate size of the units. If the size of the DG unit is not chosen correctly, it can lead to increased losses compared to a scenario without DG. Therefore, achieving the optimal location and size of DG units within a radial distribution system (RDS) is crucial to maximizing the benefits derived from DG integration into the RDS (S et al., 2016). Power engineers are exploring the transformation of existing passive power distribution systems due to their limited flexibility in meeting power demand. Consequently, there is a growing interest in converting passive distribution systems into active distribution systems, which enable bidirectional power flow instead of the traditional unidirectional flow. Passive systems fail to meet consumer expectations for reliable and high-quality power supply. The incorporation of new generation stations and transmission lines is capital-intensive and time-consuming. However, this challenge can be mitigated by incorporating renewable distributed energy sources. Renewable-based energy sources offer several advantages over non-renewable alternatives, including environmental friendliness and lower operational costs. Renewable-based energy sources like wind and PV (photovoltaic) have taken the attention of the power world to reduce the effect of other energy sources on the environment (Mandefro & Bantiyrga, 2020). Small power generating facilities close to the consumer end known as distributed generation, dispersed generation, or embedded generation have also started to appear as a result of the rise of renewable energy and the steady depletion of fossil fuels. DG is an active power source that supplies energy to the load and is located near the point of consumption. DGs benefit us in many ways such as electricity cost savings, system loss reduction, voltage profile enhancement, system reliability improvement, power quality enhancements, and so on. In today’s modern distribution system, DG is used to enhance the system. However, to gain high benefits from DGs, proper siting and sizing is necessary (Et. al., 2021; Rani & Reddy, 2019). Optimal placement of DG within the electric power distribution system (EPDS) is crucial for improving reliability, power quality, and voltage profile, and minimizing system power loss. Non-optimal DG placements can lead to increased system loss, over voltage, harmonic distortions, and potential instability in the system (Prakash & Lakshminarayana, 2018). In a distribution system, DG must be installed optimally such that it reduces system power losses and enhances the voltage profile of the system. Integrating DG units have various technical and economic advantages such as (Alam et al., 2018; Shaaban & El-Saadany, 2012):

- Minimized system losses in the power system
- Enhancements of the voltage profile
- Maximizing energy efficiency
- Improving the reliability of the system
- Improving power quality and security
- Lower operating cost because of peak shaving
- Enhanced productivity
- Deferred investment for upgrade facilities

However, it is important to note that if DG units are not strategically placed and integrated optimally, it can potentially have a negative impact and worsen the system's performance compared to the existing state or it reverse the desired outcomes (Ms. Rekha C M, 2022).

1.2 Problem of the Statement

A distribution system is a network of electrical components and infrastructure that delivers electric power from the transmission system to medium voltage and low voltage electric power to customers. The sensitivity of distribution networks to issues with power quality, which could make it unstable to distribute the same amount of power generated at the load, is well-known. The resistance-to-reactance ratio for the distribution system is high compared to other parts of the power system, causing large amount of system power losses and a poor voltage profile along radial distribution system. The main existing problems at Kombolcha (case study area) distribution network are high-power loss, high voltage drops, and high-power interruption. As a result, economic loss will be seen at the end user. Due to variations in living standards, electrical power demand is rapidly increasing from time to time, increasing of urbanization, and the building up of different industries in Kombolcha town. Feeder-3 of Kombolcha-I substation distribution network has high amount of power loss and voltage drop due to long-distance coverage of around 41.2km length and has high peak load demand. A significant number of consumers located at the farthest end of this feeder have been encountering issues related to low voltage levels and high-power loss. Finding loss minimization and voltage profile enhancement techniques for distribution system of the Kombolcha-I substation feeder three is a pressing issue. Another issue is ensuring that the chosen mechanism is properly sized and placed within the distribution system, as improper use of compensating devices makes the system worse than existing. One of the best techniques to minimize system power loss and improve the voltage profile of the distribution system is incorporating distributed generation. Proper incorporation of renewable-based DG minimizes the system loss and enhances the voltage profile of the system. For minimization of system power loss and voltage profile improvement for feeder-3 of the Kombolcha-I substation outgoing feeder, optimal placement and sizing of distributed generation using a hybrid GA-PSO algorithm are used.

1.3 Objective of the Thesis

1.3.1 General Objective

The main goal of the thesis work is optimal placement and sizing of distributed generation for reduction of power loss and voltage profile improvement in the power distribution network using a hybrid Genetic algorithm and Particle swarm optimization method.

1.3.2 Specific Objectives

The following are specific goals of this thesis:

- To model the distribution system network for a selected feeder.
- To carry out the system power loss and voltage profile analysis of the distribution system before DG integration using the BFS load flow method.
- To determine the optimal location and size of DG using a hybrid GA-PSO algorithm for power loss reduction and voltage profile improvement.
- To integrate/incorporate optimized DG size in the optimal location for the selected distribution feeder and execute BFS load flow.
- To analysis the economic impact of DG integration to the system.
- To compare the result of power loss and voltage profile before and after the installation of DG integration.

1.4 Scope and Limitation of the Study

The study focuses on the power loss minimization and voltage profile enhancement of distribution systems through optimal DG allocation and sizing using a hybrid GA-PSO algorithm and economic analysis of DG integration. In this thesis, the effects of harmonics and phase imbalance are not considered.

1.5 Significance of the Study

This thesis may serve as a guide and a foundation for future research on enhancing voltage profiles and reducing power loss by other researchers.

The main importance of this project work are:

- Minimization of system power loss in the distribution system.
- Maintaining the voltage profile in a permissible standard voltage range.
- Inspire both consumers and utilities to utilize renewable energy sources.
- Delaying the expenses associated with replacing distribution feeders.

1.6 Organization of the Thesis

This thesis work is organized into five chapters as arranged follows;

In **Chapter One**, discussed introduction about the power system especially the distribution system, and problems observed on the distribution feeder. In addition to this the main and specific objective, scope, and limitation of the research, importance of the study, and the organization of the thesis were summarized. **Chapter two**, explained the theoretical background, distribution system power loss and voltage drop, techniques for power loss minimization and voltage profile improvements, and literature reviews of related works. In **Chapter Three**, system descriptions and the methodologies followed to conduct this thesis which comprises problem formulation, data collection, and data analysis, description of the study area, backward/forward load flow analysis, optimization problem formulation, modeling of distributed generation and optimization techniques have been discussed very well. In **Chapter Four**, results and discussions were discussed. The effect of integrating DG on power loss minimization and improving voltage profile of the system is discussed. In **Chapter Five**, the conclusion, recommendations, and suggestions for future works were discussed.

CHAPTER TWO

2. THEORETICAL BACKGROUND AND LITERATURE REVIEW

2.1 Electrical Power Distribution System

The electric power system has three fundamental components, which are generation system, transmission system, and distribution systems. Generation stations are located away from customers and generate electricity. Through transmission and distribution networks, the generated electric power is delivered to customers. Bulk power is delivered from the generating station to the load center via transmission lines, which take power from generating stations to transmission substations. A distribution network is then used to deliver electricity to a huge number of small and large customers. The voltage is reduced to a level suitable for domestic appliances by distribution transformers and then fed to a large number of customers via secondary distribution lines. The distribution transformer is usually placed near the customer's address to supply quality service, to minimize power loss that can happen due to long distance. Distribution substation is used to step down the voltage level to 33 kV and 15 kV and distribute through outgoing feeders which are connected mostly in radial structure.

In general, the electrical system between the customer meters and the substation fed by the transmission system is referred to as the distribution system. The distribution system has three main components. Those are feeders, distributors, and service main. It must be able to meet the unique requirements of each customer, including those related to energy demand, efficiency, and power quality (Thakur & Chawla, 2015).

A feeder is a conductor that connects the area where power will be transmitted from a substation or localized generating station. The most crucial element to consider when building a feeder is its current carrying capability. In most cases, no taping is done, therefore the current in the feeder remains constant.

A distributor is a conductor where taps are taken to supply customers. Because tapping is taken from the distributor the flow of current in it is not constant. Unlike the feeder, in designing the distributor the most important thing that should be considered is voltage drop in it since the permissible range for voltage deviation at the customer’s terminals is ±5% of the rated value. In Figure 2.1-line AB, BC, CD, and DA represent a distributor.

The service main is another component of the distribution system and it is a conductor or cable that connects the distributor to the customer’s terminals.

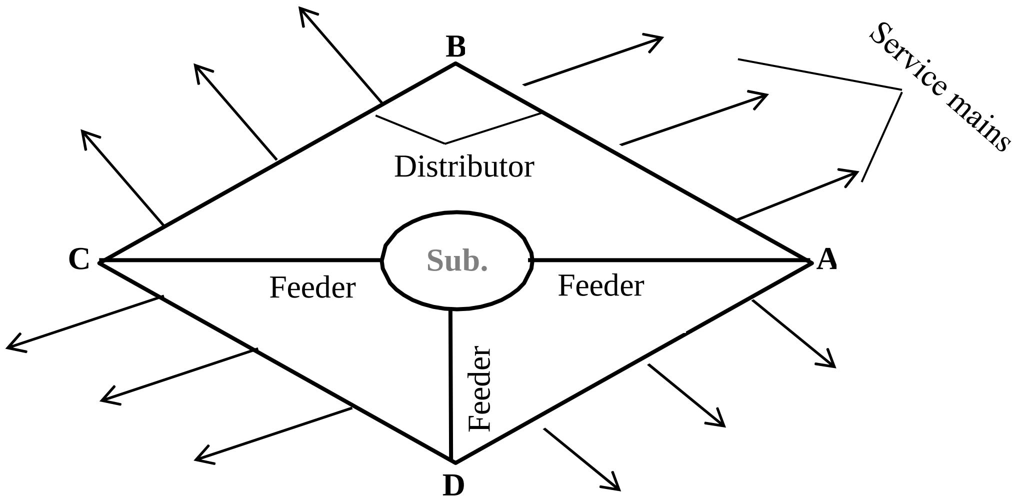

Figure 2.1: Components of distribution system (Alemante, 2017)

2.1.1 Classification of Distribution System

The distribution network can be categorized into various categories, taking into account different factors (Alemu, 2020).

Based on the nature of the current distribution system can be divided into;

- AC distribution system
- DC distribution system.

Based on the type of construction DS can be divided into;

- Overhead distribution system
- Underground distribution system

Depending on the scheme of the operation DS may be divided into;

- Radial delivery distribution network
- Ring main distribution system
- Interconnected distribution system

2.1.1.1 Radial System

This type of DS is made up of separate feeders that radiate from a single substation and feed the distributors at one end only. The primary or source node transmits electricity to the sub-branches, which are then divided along the line. This configuration is the most economically efficient but also the least secure. A single-line diagram of a radial system for d.c. and a.c. distribution is shown in Figures 2.2 a and 2.2 b. respectively. As compared to others radial distribution system is cost-effective and simple in contraction.

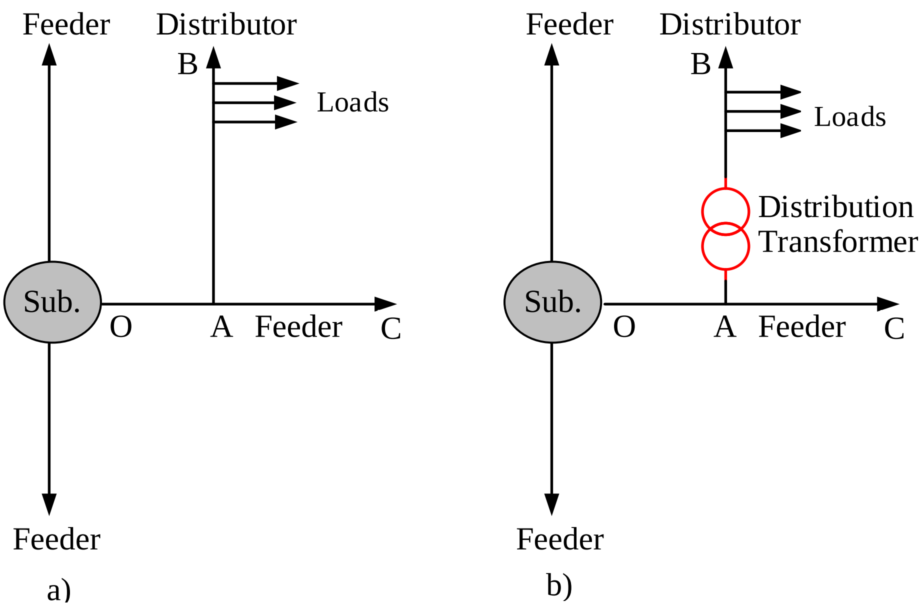

Figure 2.2: Radial distribution systems (Alemu, 2020)

However, the radial-type distribution system has the following disadvantages:

- The major disadvantage of the radial system is, the end of the distributors closest to the feeder point is subjected to heavily loaded.
- The customers are reliant on a single distributor and feeder. As a result, any fault that occurs on the feeder causes services to be interrupted for customers on the fault side.
- When the load on the distributor changed, the consumers at the far end would experience significant voltage variations.

2.1.1.2 Ring System

In these arrangements of the system, the primaries of DT form a loop. The loop circuit originates from the substation bus bars, forms a loop throughout the designated area it serves, and then returns to the substation. The single line schematic of the ring main system for a.c. distribution, with substation supplies going to the closed feeder LMNOPQRS, is shown in Figure 2.3. Through distribution transformers, distributors are tapped from different locations M, O, and Q of the feeder. The ring main system tends to incur higher costs compared to the radial system due to its increased need for switches and conductors.

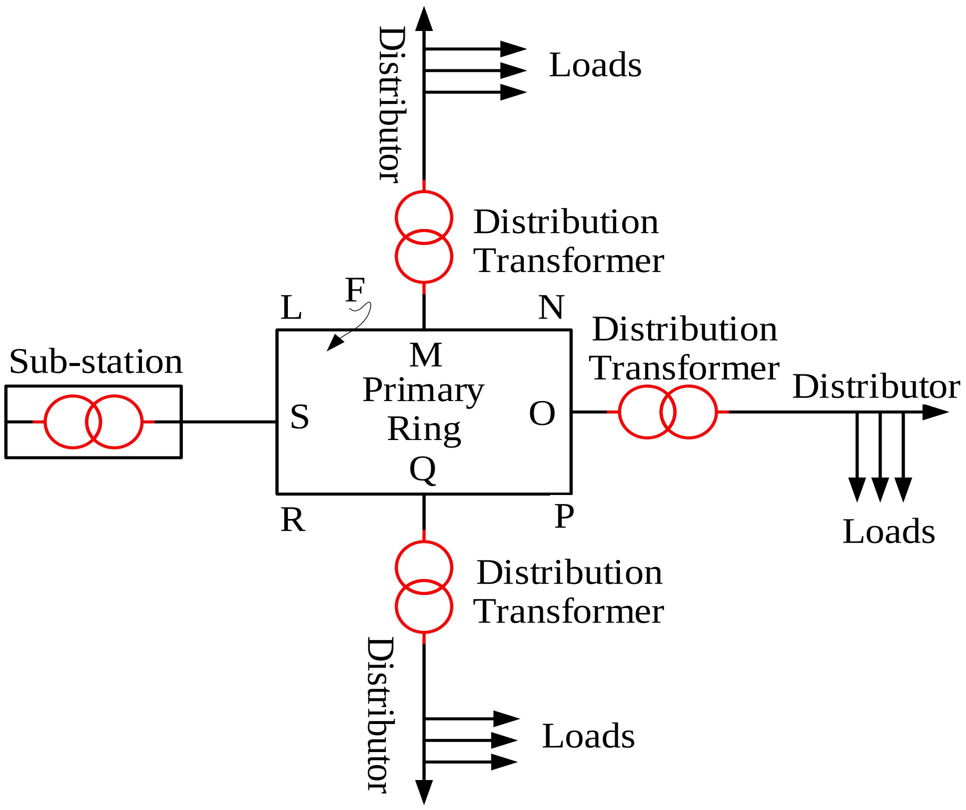

Figure 2.3: Ring main systems (Alemu, 2020)

The benefits of the ring main system are listed as follows:

- The ring main DS is more reliable than the radial DS since each distributor is fed via two feeders. Since each feeder is fed by two feeders, the supply is retained in the event of a problem on any component of the feeder. For instance, suppose there is a problem at point F of section SLM of the feeder. The feeder's section SLM can then be shut down for repairs while still providing uninterrupted service to every customer through feeder SRQPONM. At the customer’s terminal, there are less voltage fluctuation.

2.1.1.3 Inter-Connected System

An interconnected DS is characterized by a feeder ring that receives power from two or more generation stations or substations. The closed feeder ring ABCD in Figure 2.4 is fed by two substations S1 and S2 at locations D and C, respectively, in an interconnected distribution system. Distribution transformers connect the distributors to the feeder ring's points O, P, Q, and R.

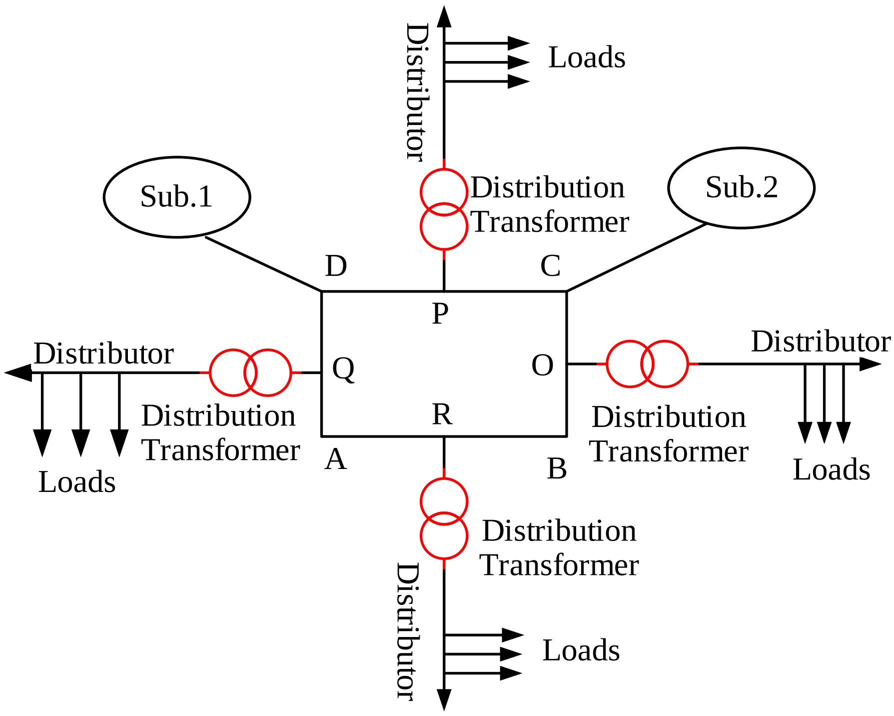

Figure 2.4: Interconnected system (Alemu, 2020)

The benefits of the interconnected system are listed as follows:

- It maximized reliability of the services.
- During peak load hours, any region that receives power from one generating station can be supplied by another generating station. This minimizes the need for excess power reserves and enhances system efficiency.
- Good voltage regulation is achievable.

2.1.2 Distribution System Power Loss and Voltage Drop

The DS sector requires an affordable and efficient method to deliver electrical energy at a reasonable cost for their customers while minimizing system power loss and enhance voltage profile. However, electrical power distribution networks experience both technical and non-technical losses. Technical losses are associated with energy distribution and occur due to the physical characteristics of the power system's equipment, including the conductor, transformer, switch, and generator losses. Non-technical losses, on the other hand, result from issues in the customer service process, such as meter inaccuracies and unauthorized usage in collaboration with utility personnel. Voltage drops and power loss in distribution systems are primarily caused by the resistance and reactance of overhead lines. While complete elimination of power loss and voltage drop is challenging, various techniques can be employed to minimize these issues. These techniques include integrating capacitors, reconfiguring of the network, incorporating distributed generation, and utilizing flexible alternative current transmission systems (FACTS)devices. By implementing these strategies, it becomes possible to mitigate power loss and voltage drop to enhance the efficiency of the distribution system.

2.1.3 Types of Losses in the Distribution System

At every level of the power distribution process, there are electricity losses. It is widely recognized that power systems experience losses that have an impact on customers' economic efficiency. Due to a variety of reasons, it is a well-established truth that not all of the energy sent to a distribution utility is used by the final users. A significant portion of the energy is lost within the DS, and these losses can be categorized into two major types: technical losses and non-technical losses or commercial losses (Hammerschmitt et al., 2020).

a) Technical Losses

Technical losses in the power system arise from the inherent characteristics of the power system components. The loss of power dissipated in transmission lines and transformers as a result of internal electrical resistance is the most prominent example. Nevertheless, they can be diminished through the utilization of innovative technologies and by implementing preventive, corrective, and predictive maintenance practices. Technical losses consist primarily of power dispassion in electrical system components such transmission lines, power transformers, etc. Technical losses are naturally occurring losses (produced by action inside to the power system) (Keoliya & Vaidya, 2013). The following sorts of losses are produced by technical losses that result from current passing through the electrical network;

- Copper losses: These are brought on by I2R losses, which are present in all inductors due to the conductor's finite resistance.
- Dielectric losses: are losses that happen because the dielectric material between conductors heats up.
- Induction and radiation losses: the electromagnetic fields that surround conductors cause induction and radiation losses.

b) Non-technical losses

Non-technical losses (NTL) in the DS refer to the unaccounted-for energy or revenue losses that occur due to reasons other than technical factors. The most likely reasons for non-technical losses are fraud-related, including changing the accuracy of meters, using unbilled energy without using utility meters, and tapping low-voltage connections. The system operators frequently fail to account for these losses, therefore there is no information captured as a result (Chandel, 2016; Leite & Mantovani, 2016; Messinis & Hatziargyriou, 2018)

2.1.4 Distribution System Voltage Drop

A voltage drop refers to an abrupt decrease in the voltage level from its normal operational value to a range between 0.9 per unit and 0.1 per unit of the specified nominal value. In an ideal scenario, the voltage at the receiving end of a power transfer system, whether it's a transmission line or an electric circuit, should be the same as the voltage magnitude at the sending end. However, in practical situations, the receiving end voltage is not identical to the transmitting end voltage due to voltage drop along the line which is caused by the combined effect of resistance and reactance of conducting instruments. Although the utility system's equipment is built to operate at a specified voltage, it is practically impossible to deliver the nameplate voltage to every customer. This is due to voltage drops that occur across different sections of the power system, spanning from generation to the customer's meter (Danishmal et al., 2022; Thakur & Chawla, 2015).

2.1.4.1 Factors Affecting Voltage Drop in Distribution System

Voltage variance and distribution feeder losses in distribution networks are increasing for several reasons. The voltage drop of a line is primarily determined by two factors; this being the current passing the wire and line impedance. As a result, an increment in either current or impedance values will lead to a corresponding voltage drop. The main factors that affect voltage drops and the distribution feeder loss are poor jointing and termination, conductors that are too small, using different sorts of conductor materials, the main feeder loads, distribution feeder length, unbalanced phase, harmonics, distribution transformer’s location (Chen et al., 2012; Taye, 2019).

2.1.5 Techniques for Power Loss Reduction and Voltage Profile Improvements

Many techniques are developed over the years that help to minimize power loss and enhance the voltage profile of DS (Kalambe & Agnihotri, 2014; Taye, 2019). Some of the techniques include network reconfiguration, network conductor grading, reactive power compensation, distribution transformer locating and sizing, integrating distributed generation, using highly effective transformers, using high voltage distribution systems, etc. These strategies are covered in the following section.

A) Network Reconfiguration

Network reconfiguration involves modifying the arrangement of feeder lines by adjusting the open or closed status of sectionalizing switches and tie switches. Typically, networks are reconfigured to minimize system power loss and alleviate network overloads (Rao et al., 2013). This involves transferring loads from heavily loaded feeders to lighter ones, and from higher-resistance routes to lower-resistance ones to achieve system minimal loss. Such transfers not only cut power losses and reduce loads on the switched feeder but also enhance the voltage profile of the feeders and lower overall system power losses (Kumar, 2020). This method is cost-effective if and only if the distribution feeder is automated and not far apart from each other. For fare-apart and unautomated feeders, it is not recommended due to its cost (Sultana et al., 2016).

B) Conductor Grading

It is the process of replacing the feeder's current conductor with a conductor of the optimal size for the optimal (in terms of cost) length in order to minimize resistance. To reduce electrical resistance and save energy, small conductors can be replaced with larger ones or supplemented with additional conductors to work in parallel. However, these methods can be expensive and are typically only used when necessary, such as when an existing conductor becomes insufficient due to significant increases in load demand. The cost of purchasing and installing new conductors is usually higher than the energy savings achieved through this technique. It is particularly beneficial in developing nations where population growth rates and energy demand are high. Conductors are selected in these situations to reduce power loss and voltage drop inside the DS.

C) Reactive Power Compensation

Reactive power compensation refers to the control and regulation of reactive power to enhance the operation and efficiency of an alternating current (AC) power system. Typically, it is included to provide or absorb reactive power, so influencing the reactive power balance in a desired way. Reactive power compensation in transmission and distribution systems offers various advantages such as maintaining consistent voltage profile, improving system capacity through regulation of reactive power flow using capacitors, and minimizing power losses (Kanojia & Rajyaguru, 2019). In general, reactive power compensation is a crucial approach for improving the voltage profile and reducing losses in a distribution network when it is appropriately sized and strategically positioned.

D) Make Use of a High-Voltage Power Distribution System

Implementing a high-voltage DS is one of the best method to decrease losses and voltage fluctuations within the distribution network. This technique involves extending high-voltage lines closer to the load, substituting large transformers with multiple smaller-rated transformers, and converting existing low-voltage distribution systems into high-voltage systems. By doing so, technical losses can be reduced and power quality can be improved due to the low current in high-voltage devices.

E) Locating and Sizing of Distribution Transformers

Although the secondary of a transformer may be kept at an acceptable voltage level, if DTs are not placed strategically concerning customers, those located furthest away will experience significant voltage drops. This can result in greater losses throughout the DS. To minimize these issues, it is advisable to position distribution transformers as close to the load center as possible.

F) Making Use of High-Efficiency Transformers

Utilizing highly efficient transformers can effectively minimize losses in the distribution system. One such example is the use of amorphous core transformers which exhibit excellent magnetic susceptibility and electrical resistance. The large resistance in these transformers helps reduce losses caused by eddy currents, resulting in lower overall losses.

G) Use of Distributed Generation

DG is one of the newest power system trends being employed to meet the rising demand. DG is an electrical source of power, which is directly linked to the customer side of the meter or the distribution system to supply power. Although there are various definitions of DGs, a variety of terminology, including distributed energy resources (DER), embedded generation, dispersed generation, decentralized generation, and embedded generation, are used in the literature. Less than a kW to tens of MW are the dimensions of the DG, according to the Department of Energy (DOE). According to the Gas Research Institute, DG's power output ranges from 25 kW to 25 MW. According to the Electric Power Research Institute (EPRI), the DG can be anywhere from a few kW and 50 MW. The DG range, according to the International Council on Large Electric Systems (CIGRE), ranges from 50 kW to 100 MW. For interfacing at any point in the system network, IEEE defines the DG as the production of electrical power by facilities that are relatively small in comparison to central generating plants (Verma & Kashyap, 2021). The advancement in power electronics since the mid-2000s has been instrumental in enhancing the efficiency of DG systems based on renewable energy sources. This advancement has led to increased costs associated with device integration. Additionally, there is significant interest in utilizing renewable-based DG systems due to the growing global concern regarding climate change, which has gained prominence worldwide. The selection of the type of renewable resource depends on the availability of the source in the specific place we want to integrate. The penetration of DG units in power systems gets increased due to the high increment in using green energy sources to replace fossil fuels. Green power is generated through DG which utilizes renewable resources like hydro, solar, wind, biomass, ocean, and geothermal heat. The use of such power sources has a minimal effect on greenhouse gas emissions, making them an environmentally friendly option. Utility companies see benefits in having intermittent renewable DG units (such as wind and solar) situated near loads in DS, including economic, environmental, and technical benefits.

DG units can be modeled as induction generators for wind and micro hydropower units, as synchronous generators for small hydropower, geothermal power, and combustion turbine units, and as power electronic inverter generators for micro gas turbine, solar power, PV power, and fuel cell units. According to their terminal characteristics in terms of active and reactive power-delivering capability, DG can be categorized into 4 as follows (Kashyap et al., 2018; Verma & Kashyap, 2021; Werkie & Kefale, 2022):

Type-1: This type of DG unit supplies or injects active power only. For instance, solar energy is converted into electricity via photovoltaic systems, which produce DC power.

Type-2: This type of DG unit supplies or injects both P and Q power. This type of DG uses interfaced power electronics to produce both P and Q power and it can include fuel cells and synchronous generators.

Type -3: This type of DG can supply P and it can consume Q power and wind turbines which are the induction generators are categorized in this type.

Type-4: DG units supplying or delivering reactive power only. Certain DG types provide only the Q to enhance the power system conditions and they are synchronous condensers.

The integration of renewable-based DG units into the power system has a number of technical and financial advantages as presented as follows;

The main technical benefits of using DG in a power system are;

- Minimization of power losses
- Enhanced system voltage profile and power quality
- Improved energy efficiency
- Increased system security and reliability

In addition to its technical benefits, DG has an economic advantage. Some of the economic benefits of using DG in power systems are:

- Investing that has been postponed for facility upgrades
- Decreased fuel expenses because of maximized overall efficiency
- Reduced operational expenses as a result of peak shaving
- Reduced reserve requirements and the associated costs

2.2 Literature Review

Several studies have conducted different methods for minimization of system power loss and voltage profile enhancements in DS. Some reviews of research output on the incorporation of distributed generation on distribution system by different authors are mentioned below.

Irfan et al., (2018) provided a solution for the optimal sizing and simultaneous placement of DG units of multiple types for reduction of real power loss and voltage profile improvements based on chaos-assisted gravitational search algorithm. The objective of optimization was to reduce the real power loss and reduce voltage deviation. Three conventional IEEE test systems (12-, 33-, and 69-bus) and a radial distribution feeder in Pakistan, Lahore Electric Supply Company (LESCO), were used to evaluate the viability of proposed methodology. From all results, placement of PV units with capacitors at the same time or induction generators and individual placements of synchronous generators result in a significant reduction of power loss and voltage profile improvements. The proposed technique was compared with other optimization techniques like PSO and analytical methods, and it was shown that the proposed techniques yield better results. This paperwork doesn't include reactive power loss reduction in the objective function and also it doesn't analyze the cost of DG integration in the DS.

Ankaliki et al., (2021) proposed, the hybrid algorithm which includes Binary Particle Swarm Optimization (BPSO) and Whale Optimization Algorithm (WOA) was used for optimal allocation and sizing of DG for performance enhancements of the distribution system. In this study voltage sensitivity index (VSI) was used initially to identify the most sensitive buses and this result was sent to a new hybrid BPSO-WOA method to determine the optimal allocation and capacity of DG. This approach was simulated using MATLAB software on the standard IEEE 33-bus systems, which demonstrates an enhancement in the voltage profile and minimizes system loss when compared to other methods of optimization. This paperwork doesn't give constraints about DG generation in the DS and cost analysis.

Avchat & Mhetre, (2020) proposed the use of particle swarm optimization (PSO) for the proper allocation of DG to minimize system losses and enhance the voltage profile. For the modeling of the network ETAP 12.6 software was applied and the power flow analysis was analyzed by using Newton-Raphson power flow methods. The load flow result was further sent to PSO which find out the optimal DG location. After analyzing the load flow out of 73 buses 10 buses were identified as candidate buses for the DG location. After the incorporation of 25 MW DG in the network the power loss was reduced from [37.817MW, 239.832MVar] to [17.543MW, 119.842MVar] and the voltage profile became within the standard limits. The work doesn't say anything about how it was found 25MW DG and its location in the distribution system. And also, it doesn't give the constraints in the DG integration process except voltage limit constraints.

Ray & Gupta, (2022) proposed the use of a sine cosine algorithm to determine the optimal allocation and best capacity of DG. The main objective of the paper was power loss reduction with voltage profile enhancements. In this paper work the effect of varying pf from 0.85 to 0.95 and for optimal pf for minimization of system loss and voltage profile enhancement have been analyzed using IEEE 15, 33, and 69 buses. After integrating DG in different cases, problems of power quality have been rectified and the voltage profile comes within permissible range and improved very well. The work didn't give brief information about how it determines the optimal placements of DG and its capacity in the given selected tested IEEE bus system and doesn't analyze the cost of DG integration in the distribution systems.

Seet* et al., (2019) proposed analytical method for power loss minimization and voltage profile improvements through optimal allocation and sizing of fixed DG size of 500 kW up to 4500 kW of single P-type DG. In this paper, the analysis was divided into four scenarios. Out of the four scenarios, the fourth (i.e., integrating 3000 kW type I or P-type DG units at bus 7) experienced better performance. The work didn't have any reason for the selection of DG size and didn't give any constraints in the optimization process. And also, the work didn't use any mathematical or intelligent techniques for placement and size as well as cost analysis of DG.

Pandey & Kirmani, (2019) proposed new metaheuristic optimization algorithm which is the Crow search algorithm (CSA) to find out the optimal allocation and size of multiple photovoltaic (PV) units for minimizing the system power loss. This research work also explains the mathematical modeling of probabilistic PV generation, time-varying load modeling, loss calculation, voltage stability, and optimal PV size calculation. The validation of the proposed method was tested on IEEE 30 and 57 bus test systems. Finally, the proposed method was compared with other optimization methods like GA and PSO and the result confirmed that the CSA method gives better performance. Nevertheless, this analysis did not include voltage profile improvement and cost analysis.

Salman et al., (2022) proposed that the influence of DG along with several techniques for the reduction of power loss and voltage profile improvement was examined. For the validity of the proposed technique, an 11kV residential test feeder was selected and modeled in the Electrical Transient Analyzer Program (ETAP). Results were compared by injecting different types of DG and without DG, considering the voltage profile. Out of all cases injecting of 2.5MW synchronous generator at bus 6 shows better performance for power loss minimization and voltage profile improvements. Finally, the impact of injecting un-deterministic DG and high cross-section conductors was examined.

Hussain et al., (2021), the researchers tried to enhance the efficiency of radial distribution by reducing real power loss using distributed generation. For validity analysis, they used three 11 kV feeders (located at Bannu) as a case study. The results have been analyzed mathematically, and at the end, the simulation was taken by Electrical Transient Analyzer Program (ETAP).

Maduforo et al., (2020) proposed a sensitivity-based technique for the optimal allocation of a DG in a distribution system to improve the voltage profile and reduce real power loss. In this study, both loss sensitivity and voltage sensitivity methods were applied separately. To demonstrate the proposed techniques 11kV feeder of Gwagwalada injection sub-station, Abuja Nigeria was used. Out of the two proposed methods, the loss sensitivity-based method provides better performance in terms of real system loss minimization and voltage profile improvements than the voltage sensitivity-based method. However, this study doesn't consider the reactive power loss in the objective function.

According to the literature review stated above, there is a possibility to enhance the performance of the DS through optimal allocation and sizing of DG using different optimization algorithms. As stated above all of the related works have their own gaps. Such as considering single objective function, they didn't consider real and reactive power, voltage profile, and economic impact of DG integration in the distribution system simultaneously, didn't give necessary constraints, some of the papers doesn't give a reason for how they were select DG location and size in their optimization and almost all of the study work takes IEEE bus system as a case study rather than using the real system, etc. This research work is targeted to fill the above-listed gaps. This thesis addresses the optimal sizing and placement of renewable DG for the reduction of real power loss, reactive power loss, and voltage deviation by considering it as a multi-objective function using weighting factors using hybrid GA-PSO algorithm. And also, the economic analysis of DG integration in the network is analyzed. This thesis work employs the efficient load flow analysis approach (backward/forward sweep), which is preferred for radial distribution systems.

CHAPTER THREE

3. SYSTEM DESCRIPTIONS AND METHODOLOGY

3.1 Introduction

In this chapter methods that have been used to accomplish the thesis work, a description of the case study area with its resource feasibility analysis, the necessary data to analyze the existing problem of the selected feeder, and the proposed methodology to find a solution for identifying the problem are explained. The necessary data include the duration and frequency of interruption, feeder length, segment impedance, the real and reactive power, peak, and average, minimum load of the feeder, numbers, and ratting of distribution transformers. This chapter also covers the modeling of DG and the BFS load flow method, the formulation of optimization problems with the objective function, and different constraints. Finally, the implementation of a hybrid genetic algorithm and particle optimization (GA-PSO) method for solving the formulated optimization problem which is optimal siting and sizing of DG are discussed.

3.2 Methods

To accomplish this thesis work, the following steps have been undertaken as part of the research process.

Literature reviews: Several published sources about distribution system power loss reduction and voltage profile improvements using DG in journals, articles, books, and thesis have been read first.

Data collection and analysis: Various input data for modeling the selected feeder and formulation of optimization problems were gathered from the Ethiopian Electric Utility (EEU) at Kombolcha district, Kombolcha-I substation, Ethiopian Electric Power (EEP) North East Region transmission substation, operation, and maintenance at Dessie. Data collection for this research involved physically observing the substation and distribution system and conducting interviews with substation and utility workers and reading the recorded data which exist at the above aforementioned organizations. The collected data were then analyzed to develop models of the selected feeder and simulations of the system.

Modeling, optimization problem formulation, and power flow analysis: Modeling of the selected feeder for the case study has been done using the collected data. And then, the objective function, which is subjected to reduce the total active and reactive power losses and cumulative voltage devotion was done considering both the equality and inequality constraints.

Analysis of the result: After the load flow analysis with each case has been computed, the optimal DG size and allocation have been determined. That is, total active and reactive power loss, commutative voltage deviation and the appropriate DG penetration level are computed. In conducting this research, software tools used are mainly MATLAB/2021a and Microsoft Visio 2019, and Math Type for equation editor are used.

Conclusion: Finally, make a conclusion based on the outcomes of the research work/outputs and compare the outcomes with the base or existing system.

3.3 Description of the Case Study Area

Kombolcha town is found in Amhara regional state in the south Wollo zone and it is the capital city of Kallu woreda. It is located on the main road from Addis Ababa to Dessie - Woldiaya and is far from 364 km from Addis Ababa in the northern direction. Kombolcha is one of the industrial towns, and many industries are found in it. And also, the urbanization rate of Kombolcha town is growing up rapidly. Many textiles, steel, bear, food complex, etc. factories are found in Kombolcha town. And also, there is a big industry park, its name is Kombolcha Industry Park. The latitude and longitude of Kombolcha is 11°5'5.76"N 39°43'45.06"E with elevation between 1842 and 1915 meters above sea level. Kombolcha-I substation supply electric power to Kombolcha town and the nearby areas and it receives power via 132 kV power lines from Kombolcha-II substation. 132 kV voltages are stepped down into 132/66/15 kV by using three winding transformers. Kombolcha-I substation have eight 15 kV, two 66 kV, and one 132 kV outgoing feeder. Out of eight 15 kV outgoing radial feeders of Kombolcha-I substation, six of them are distribute power in the Kombolcha town distribution system, and remain the two 15 kV feeders are going to Bati and Harbu out of Kombolcha town and the two 66 kV out gonging feeders are directly going to Dessie town. 132 kV feeders are directly supplied to the Aksta substation without step-down.

The following are lists of Kombolcha-I substation feeders;

- **L1 (Kombolcha-II):** It is used to supplies 15 kV to Yegof school, Mekelakeya gebi, Derekwodeb, Doroerbata, Yeshearege flour mill, Hospital, Seneside hotel, Amhara bretabret, Biraro, Tekur abay, Dessie ber condomonum, Arhebu duket, Kuteba, Agmase foam factory, etc.
- **L2 (Bati):** It supplies 15 kV to customers for Bati town and around it.

- **L3 (Kombolcha-I):** It supplies 15 kV to customers to condominium, TVT collage, Aragaw flour mill, Service center, Commercial Bank of Ethiopia (CBE), Donat, Milnic, Dewye, China civil construction, Addis mender, Tulu Adame health station, Yegof hotel, Kuasmeda, Habitat, Borchale Kuteba, Meja, etc.
- **L4 (Kemissie):** It supplies 15 kV to customers for Kemissie town and around it.
- **L5 (BGI):** It supplies 15 kV to the BGI beer factory.
- **L6 (Textile 1):** It supplies 15 kV to the Textile share company.
- **L7 (Textile 2):** It supplies 15 kV to the Textile share company.
- **L8 (Industry Mender):** It supplies 15 kV to Industry Mender customers.
- **L9 (Dessie outgoing I):** It supplies 66 kV to Dessie town and nearby city.
- **L10 (Dessie outgoing II):** Also, it supplies 66 kV to Dessie town and nearby cities.
- **L11 (Aksta substation):** It supplies 132 kV to the Aksta substation and nearby city.

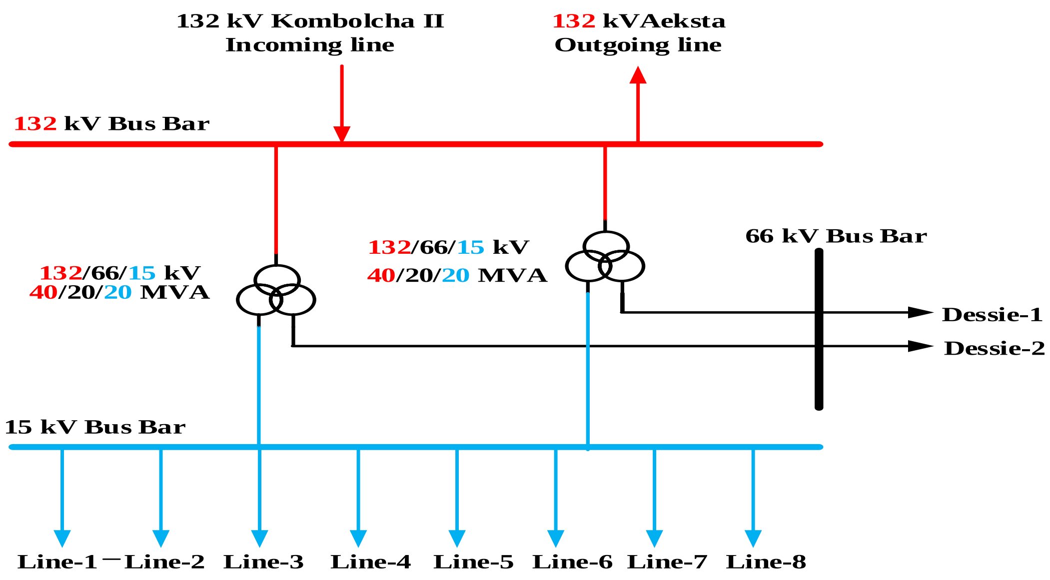

Figure 3.1: Single line diagram of Kombolcha-I substation

3.4 Wind and Solar Power Resources Feasibility Analysis for Kombolcha

3.4.1 Wind Power Resources Feasibility Assessment of Kombolcha

Now a days, a large number of studies are being focused on alternative sources of energy to supply electric power for customers. As the conventional energy sources are continue to decline time to time, focusing on renewable-based sources like wind energy is one of the most promising sources to provide electrical power using wind turbines (Saeidi et al., 2011). The increment in the use of this type of energy requires greater attention must be paid to wind speed, installation, and especially the per unit cost of energy produced by wind turbines

(Abdulla et al., 2015). As the output power of wind depends on the wind speed which is stochastic in nature, a feasibility study before the installation of wind-based DG is needed. In this case study area, for wind power feasibility analysis the recorded data at Ethiopia Meteorological Institute East Amhara Metrological Service Center Kombolcha records the wind speed of Kombolcha City at 2 m was used. By using this recorded data, the feasibility of the wind power plant in the case study site is analyzed. With an increase in height, the wind speed increases noticeably. The surface conditions have the biggest impact on how quickly wind speed increases with height. The following is the empirical formula for calculating wind speed at various heights (Tizgui et al., 2017);

$$v_2 = v_1 \left(\frac{h_2}{h_1} \right)^{\alpha} \tag{3.1}$$

Where, v_2 is the wind speed to be determined at height h2; v_1 is the wind speed measured at anemometer height h1; α is ground surface friction coefficient. For Urban areas with tall building the value of the α ground surface friction coefficient α is 0.4 (Resen et al., 2020; Yeh & Wang, 2008). In this research, a wind speed data record by Ethiopia Meteorological Institute East Amhara Metrological Service Center Kombolcha starting from 2013-2022 at 2 m above the ground is used and converted to the desired height (65m) using equation 3.1.

Table 3.1: Monthly average wind speed (m/s) of Kombolcha at 2m

Monthly average wind speed (m/s) at 2 meters for 10 years from 2013-2022 G.C												
Month	JAN	FE.	MA	AP	MA	JUN	JUL	AU	SEP	OCT	NO	DEC
2013	0.54	0.66	0.67	0.64	0.52	0.69	0.48	0.25	0.23	0.18	0.28	0.35
2014	0.44	0.44	0.40	0.45	0.36	0.49	0.47	0.28	0.22	0.26	0.50	0.69
2015	0.84	0.88	0.89	0.99	0.85	0.88	0.92	0.78	0.62	0.59	0.59	0.69
2016	0.74	0.86	0.84	0.76	0.75	0.93	0.80	0.67	0.58	0.61	0.66	1.18
2017	0.76	0.82	0.85	0.83	0.68	0.94	0.95	0.69	0.59	0.47	0.58	0.81
2018	0.81	0.79	0.81	0.72	0.81	0.81	0.76	0.74	0.59	0.58	0.59	0.67
2019	0.76	0.93	0.79	0.68	0.79	0.87	0.82	0.61	0.61	0.55	0.60	0.65
2020	0.76	0.77	0.81	0.75	0.68	0.78	0.71	0.65	0.57	0.58	0.67	0.72
2021	0.79	0.78	0.88	0.87	0.74	0.81	0.73	0.64	0.55	0.52	0.55	0.61
2022	0.63	0.74	0.77	0.79	0.82	0.87	0.51	0.49	0.46	0.38	0.50	0.56
Average	0.707	0.78	0.68	0.79	0.7	0.807	0.715	0.58	0.502	0.47	0.55	0.693

By using equation (3.1) the monthly average wind speed (m/s) at 65m for ten consecutive years starting from 2013-2022 can be found as shown in table 3.2.

Table 3.2: Monthly average wind speed (m/s) of Kombolcha at 65m

Monthly average wind speed (m/s) at 65 m for 10 years from 2013-2022												
Month	JAN	FEB	MAR	APR	MAY	JUN	JUL	AUG	SEP	OCT	NOV	DEC
Average	2.85	3.14	2.74	3.18	2.82	3.25	2.88	2.34	2.03	1.89	2.22	2.79

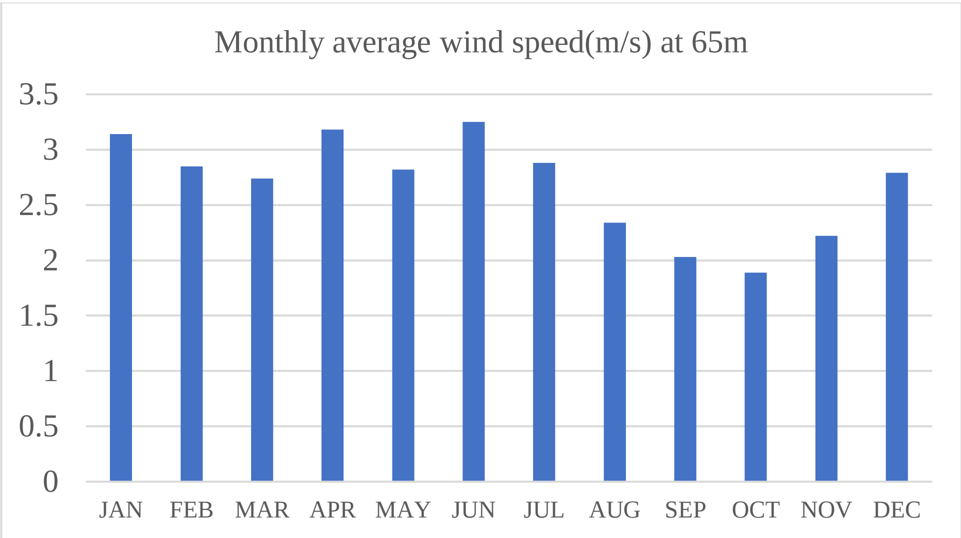

Figure 3.2: Monthly wind speed of Kombolcha at 65m height

The feasibility study of wind power resources for Kombolcha City shows that installation of the wind power plant in Kombolcha City is not feasible, since the monthly average wind speeds for the majority of the month are below the minimum wind speed requirement or cut-in speed (3-5 m/s) to generate electrical power from wind (Chatbordin & Kulyos, 2013).

3.4.2 Solar Power Resources Feasibility Assessment of Kombolcha

Similar to wind resources feasibility analysis, before deciding to install solar-based DG in the selected site, the first work should have to be analyze the feasibility of the source, since the output of solar-based DG depends on the solar irradiance. Accurate information on solar radiation is essential to the development of solar energy-based projects. Furthermore, to estimate long-term solar system performances, monthly mean daily data are required (Muzathik et al., 2011). Solar irradiation must be sufficient for PV cells to produce energy, as well as an hour of sunshine. A minimum of 4-5 hours of sunlight each day is required to provide enough power (Mandefro, 2020). Different models can be used to calculate the solar irradiance from given number of solar sunshine hours, but the Angstrom-Prescott estimating model provided a result that was relatively close to the measured values. The following equations provide the original Angstrom-Prescott type regression equation's monthly average daily solar irradiance to clear day solar irradiance in a certain place and average proportion of potential sunshine hours (Gana & Akpootu, 2013; Muzathik et al., 2011).

$$\frac{H}{H_o} = a + b\left(\frac{S}{S_o}\right) \tag{3.2}$$

Where H is the monthly average daily global solar irradiance on a horizontal surface (MJ/m² /day), H_o the monthly average daily solar extraterrestrial irradiance on a horizontal surface (MJ/m² /day), S is the monthly average daily hours of bright sunshine, S_o the monthly average day length (maximum possible sunshine duration), and “a” and “b” values are known as Angstrom constants and they are empirical. The following equation (3.3) can be used to calculate the average daily extraterrestrial irradiance on a horizontal surface for a given month.

$$H_o = \frac{24}{\pi} I_{sc}(1 + 0.033\cos\frac{360n}{365}) * (\cos\phi\cos\delta\sin\omega_s + \frac{2\pi\omega_s}{360^\circ}\sin\phi\sin\delta) \tag{3.3}$$

Where I_{sc} is the solar constant(=1367W m-2), ϕ is the site's latitude, δ the sun's declination, ω_s is the average sunrise hour angle for the specific month, and n the number of days in the year, starting from January 1. The sun's declination (δ), and the mean sunrise hour angle (ω_s) can be determined by the following equations (3.4), and (3.5) respectively.

Where, $$\delta = 23.45^\circ \sin(360^\circ \frac{284 + n}{365}) \tag{3.4}$$

$$\cos\omega_s = -\tan\phi\tan\delta \tag{3.5}$$

Equation (3.6) can be used to calculate the maximum possible sunshine duration (monthly average day length) S_o for a given month.

$$S_o = \frac{2}{15}\omega_s \tag{3.6}$$

Then, the monthly average daily global radiation H was normalized by dividing it by the monthly average daily extraterrestrial radiation H_o. According to the relationship given in equation (3.7) and equation (3.8), regression coefficients a and b for the computed monthly average global solar radiation can be obtained respectively.

$$a = -0.11 + 0.235\cos\phi + 0.323\left(\frac{S}{S_o}\right) \tag{3.7}$$

$$b = 1.449 - 0.553\cos\phi - 0.694\left(\frac{S}{S_o}\right) \tag{3.8}$$

Table 3.3: Monthly average sunshine hour (hr.) data of Kombolcha

Monthly average sunshine hour (hr.) for 10 years from 2013-2022												
Month	JAN	FE.	MA	AP	MA	JUN	JUL	AU	SEP	OCT	NO	DEC
2013	9.3	9.8	8.6	8.5	8.3	5.9	5.6	5.5	7.4	7.8	8.5	9.7
2014	8.4	6.7	8.2	8.4	8.3	8.5	6.6	5.8	6.4	7.5	8.4	9.3
2015	8.6	9.7	9.4	10.1	8.3	6.7	7.3	6.1	6.8	8.7	8	6.5
2016	5.7	9.1	8.3	6.3	7.9	7.6	5.6	6.1	6.4	8.8	9.1	9.2
2017	10.6	7.3	8.9	9.4	7.4	8.5	6.6	5.6	6	7	8.5	8.2
2018	8.2	8.4	9.3	8.7	8.4	7.7	5.6	4.9	6.3	7.5	7.6	9.2
2019	10.3	9	8.8	7.5	8.6	7.8	6.4	4.7	5.2	7.6	7.3	7.9
2020	7.1	7.9	7.6	10.1	8.7	7.1	4.2	1.2	6.4	9.2	9.1	9.2
2021	9.8	7.6	10.2	8.4	7.6	6.8	3.6	4.9	6.4	7.9	8.4	8.1
2022	9.4	9.1	8.8	9.5	10	10.4	4.8	4.5	6.2	6.6	8.5	7.1
Average	8.74	8.46	8.81	8.69	8.35	7.7	5.63	4.93	6.35	7.86	8.34	8.44

As shown in Table 3.3, the monthly average sunshine hour data of the selected site meets the required standard for solar power plant installation. By using the above mathematical formula and using the data recorded from Ethiopia Meteorological Institute East Amhara Metrological Service Center Kombolcha the monthly average solar radiation of Kombolcha has been calculated for ten consecutive years starting from 2013-2022 as shown in Table 3.4.

Table 3.4: Monthly average insolation (kWh/m^2/day***)*** of Kombolcha

Monthly average insolation (kWh/m^2/day) for 10 years from 2013-2022												
Month	JAN	FE	MAR	AP	MAY	JU	JUL	AU	SE	OC	NO	DE
Average	6.12	5.8	6.16	6.08	5.4	4.7	4.29	4.12	4.46	4.9	5.3	5.79

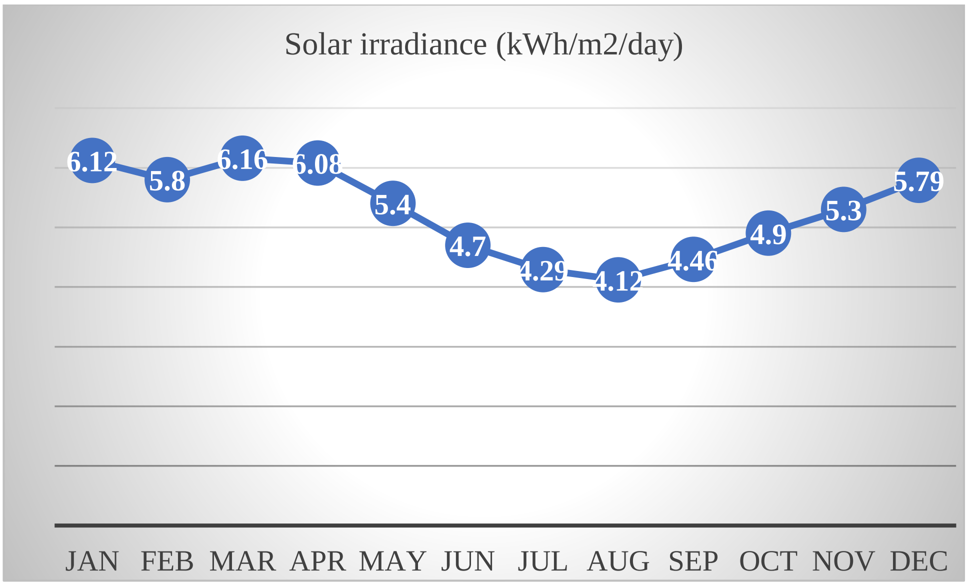

Figure 3.3: Monthly average insolation of Kombolcha

Based on the analysis of the resource data which are presented above, the feasibility analysis of wind power shows that it is not feasible to install wind-based DG in Kombolcha City because the monthly average wind speed for the majority of the month is below cut-in speed (3-5 m/s) (Chatbordin & Kulyos, 2013). The only feasible source at Kombolcha City is solar-based DG since average solar radiation varies between 4.12 to 6.16 kWh/m2/day indicating good solar potential of producing electricity using renewable-based solar energy conversion system (Podder et al., 2014; Yadav & Chandel, 2015). Therefore, for this thesis solar based DG with unity power factor is considered.

3.5 Data Collection and Analysis of the Kombolcha Distribution System

3.5.1 Data Collection

To find a solution for the problem found in the selected case study site different data have been gathered from various sources while doing this research on the selected distribution outgoing feeder. The important data specified to select the outgoing feeder and analyze the performance are gathered from the Ethiopian Electric Power (EEP), northeast region, and the Ethiopian Electric Utility (EEU), Kombolcha. Those important data are collected by direct observation of the Kombolcha-I substation control room, and also making an interview with the operator of the substation and the technician of the utility. The data collected from the panel board or control room are the number of feeders and their voltage level, the current transformer (CT) ratio of each feeder, and circuit breaker types for each feeder. The other necessary data collected from EEU are; the number of distribution transformers and their rating, conductor type (AAC-25, AAC-50, and AAC-95), the branch length, load data of the selected feeder, feeder topology, distribution line configuration (triangular arrangements), pole data(height, type, and spacing). And also, for doing this research work different websites and recorded documents related to the distribution system are used.

For this research work feeder three (L3) is selected because of the following reasons;

- ✓ Long-distance coverage
- ✓ High peak load/demand
- ✓ High power interruption

Interruption data of 2013 E.C and 2014 E.C for 15 kV outgoing feeders of the Kombolcha-I substation are given the Appendix A.

Table 3.5: Six-month peak load current in (A) of Kombolcha-I substation 15 kV outgoing feeder in 2022 G.C

Feeder Name	July	August	September	October	November	December
L1 (Kombolcha-II)	187.6	184.4	193.8	227.4	223.8	216
L2 (Bati)	171.6	162.4	234.6	192	181.4	194.6
L3 (Kombolcha-I)	289.9	332	298.4	288	295	362.8
L4 (Harbu)	181.8	138.2	190.2	241.1	165	170.4
L5 (BGI)	189	89.1	126.6	97.2	136	147
L6 (Textile 1)	143.2	149.6	156.8	156	168.8	168
L7 (Textile 1)	148	162.4	158	151.2	168	150.4
L8 (Industry Village)	198	197	194	197	209	236

Table 3.6: Six-month peak load power in (MW) of Kombolcha-I substation 15 kV outgoing feeder in 2022 G.C

Feeder Name	July	August	September	October	November	December
L1 (Kombolcha-II)	3.895	3.828	4.024	4.721	4.646	4.484
L2 (Bati)	3.563	3.372	4.871	3.986	3.766	4.039
L3 (Kombolcha-I)	6.018	6.892	6.195	5.979	6.124	7.532
L4 (Harbu)	3.774	2.869	3.949	5.005	3.426	3.538
L5 (BGI)	3.924	1.849	2.629	2.018	2.824	3.052
L6 (Textile 1)	2.973	4.190	3.256	3.239	3.504	3.488
L7 (Textile 1)	3.076	3.372	3.280	3.139	3.488	3.123
L8 (Industry Village)	4.111	4.089	4.028	4.089	4.339	4.899

As indicated in Table 3.5 and Table 3.6 line 3 (Kombolcha-I) has high peak load than other feeders which means the feeder is more sensitive to power interruption due to overloading of the system.

3.5.2 Capacity of Kombolcha-I Substation Outgoing of Feeders

Table 3.7 shows information about Kombolcha-I substation outgoing feeders such as voltage rating, length of feeders, circuit breaker (CB) type, types of cable used, the capacity of each feeder, and current transformer (CT) ratio.

Table 3.7: General data of the eight outgoing feeders of the Kombolcha-I substation

Feeder Names	Voltage rating (KV)	Length (km)	Circuit breaker type	Cable		CT Ratio		
				Type	C.S.A (mm^2)	Ratio	A	MW
Line-1	15	15.75	Vacuum CB	Al	1 X 120	300/5	300	7.014
Line-2	15	---	Vacuum CB	Al	1 X 120	300/5	300	7.014
Line-3	15	41.2	Vacuum CB	Al	1 X 120	300/5	300	7.014
Line-4	15	---	Vacuum CB	Al	1 X 120	300/5	300	7.014
Line-5	15	1	Oil CB	Al	1 X 120	150/5	150	3.5
Line-6	15	0.5	Vacuum CB	Al	1 X 120	400/5	400	9.352
Line-7	15	0.5	Vacuum CB	Al	1 X 120	400/5	400	9.352
Line-8	15	10	Vacuum CB	Al	1 X 120	600/5	600	14

3.5.3 Single Line Diagram Representation of Kombolcha-I Substation of Feeder Three

The radial configuration of Kombolcha-I substation feeder three (L3) consists of 138 buses, 137 branches, seventy-four (74) distribution transformers, sixty-three (63) common tapping nodes, and out of these buses, bus-1 is taken as swing/slack or reference bus. The feeder is constructed from aluminum conductor of size (AAC-25, AAC-50 & AAC-95) with a total length of 41.2 km. This overhead line (feeder) is used to distribute medium voltage (15 kV) using the wooden pole. The single-line diagram of the selected feeder is developed in Microsoft Visio 2019 software as shown in Figure 3.4. The line and load data of this feeder are found in Table 3.10.

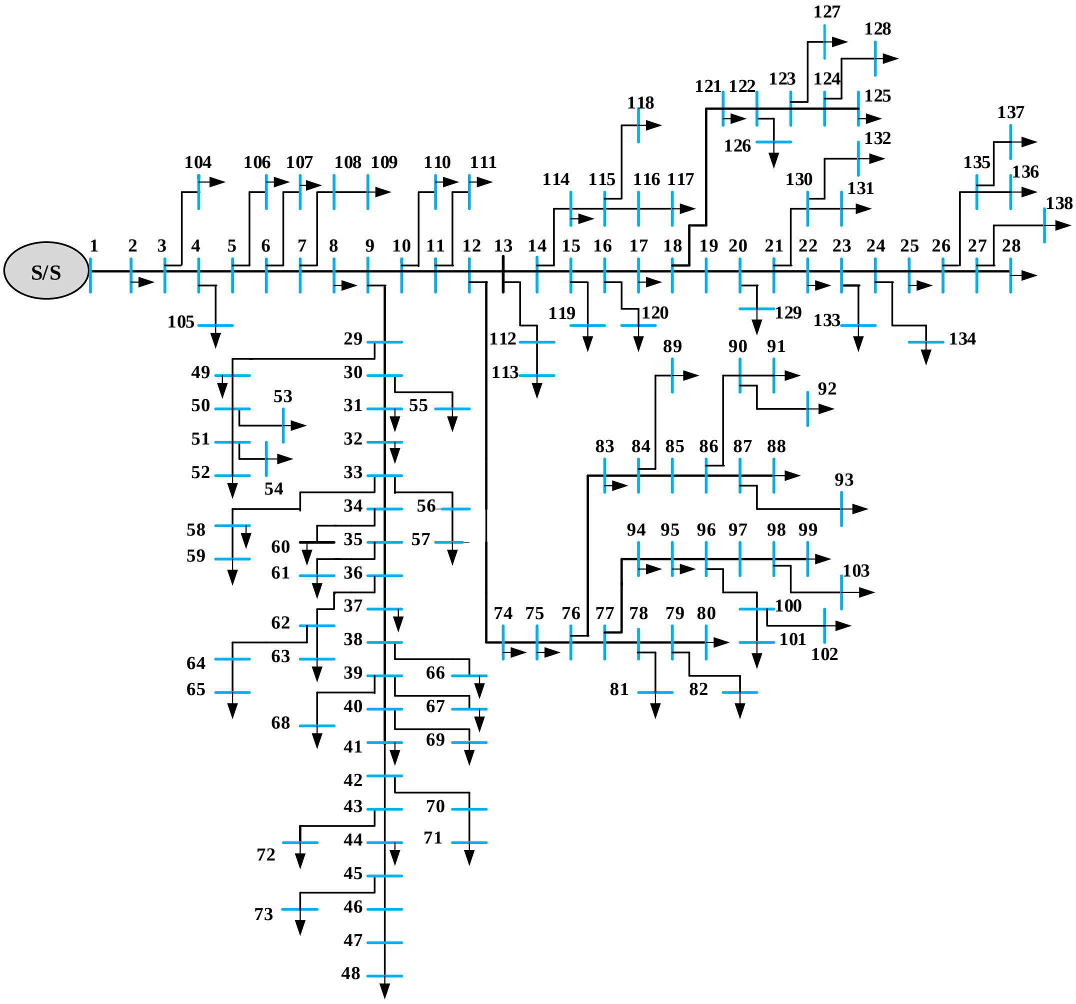

Figure 3.4: Single line diagram of Kombolcha-I substation feeder three (L-3)

3.5.4 Kombolcha-I Overhead Distribution Line Arrangements

For overhead distribution conductors, it is essential to have a symmetrical arrangement or maintain equal distances between them. This ensures that the flux linkages and inductance for each phase are similar. If the conductors' arrangement is unsymmetrical, the inductance will be different which results in unequal voltage drops in the three-phase even if the current in the conductor is balanced. To ensure equal voltage drops across all conductors, it is a usual practice to either arrange the conductors symmetrically or periodically interchange their positions along the line. This way makes, each conductor occupies the original position of other conductors over an equal distance, promoting balanced voltage distribution. The overhead conductor arrangement for the Kombolcha-I feeder three is shown in Figure 3.5 and the impedance value (R & X) of the selected line is determined accordingly.

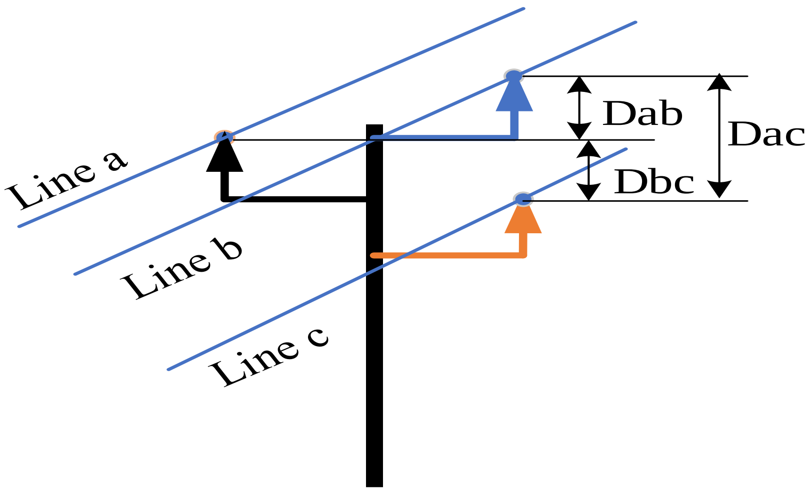

Figure 3.5: Overhead conductor arrangement of Kombolcha-I feeder three

3.5.5 Impedance Calculation of Overhead Distribution Lines

For load flow studies the line data of the distribution system is very important. The line impedance value (resistance and reactance) of each branch should be known. The impedance can be computed using Carson's equation, which does not rely on assumptions, or it can be estimated from tables with different assumptions, depending on the desired level of accuracy. Conductor material used at the Kombolcha distribution system are all aluminum conductors (AAC). AAC conductors have a relatively low specific mechanical resistance, take less space, are simple to install, and are typically employed for shorter spans rather than long distances. The overhead conductor parameters are presented in Table 3.8, and the resistance of the conductor is obtained from the standard overhead conductor data sheet and the GMRs are calculated using equation (3.11). All aluminum conductors (AAC-25 mm2 & AAC-50 mm2) with 7 stranded and (AAC-95 mm2) with 19 stranded are used as distribution line conductors for the Kombolcha-I feeder three. The inductive reactance value is obtained at a frequency of 50 Hz, and at a distance of one kilometer. Thus, line impedances are given by;

$$Z_a = R_a + j0.06283\ln(\frac{D}{GMR_a})\frac{\Omega}{km} \tag{3.9}$$

$$D = \sqrt[3]{D_{ab} * D_{bc} * D_{ac}} \tag{3.10}$$

Due to the conductor material used in distribution feeders are stranded conductors and thus for stranded conductors, the GMRa is given by:

$$GMRa = k * r \tag{3.11}$$

Where: GMRa =Geometric mean ratio of conductor a, k = the GMR factor

r = actual conductor radius, Za = impedance of conductor a in Ω/km

Ra = resistance of conductor a in Ω/km, D = distance between conductors in meter D_{ab}=Distance between conductors a and b in meter, D_{bc}=Distance between conductors b and c in meter, Dac=Distance between conductors a and c in meter

Table 3.8: Standard of conductor

Conductor type	Nominal area (mm2)	Real area (mm2)	Stranding and wire diameter	Overall diameter (mm)	Actual diameter (mm)	GMR	Resistance (ohm/km)	Reactance (ohm/km)
AAC	25	24.2	7/2.1	6.3	5.56	1.88	1.181	0.3736
AAC	50	49.5	7/3	9	7.9377	2.88	0.5785	0.3470
AAC	95	93.5	19/2.5	12.5	10.8975	4.13	0.3085	0.3244

Based on Tables 3.8 and 3.9 the impedance of the conductor can be evaluated as the following:

1) For AAC-25 mm^2 conductor type the positive sequences impedance can be calculated using equation 3.9 as follow;

$$Z_a = R_a + j0.06283\ln(\frac{D}{GMR_a})\frac{\Omega}{km}$$

$$Z_a = 1.181 + j0.06283\ln(\frac{0.72135}{2.0172*10^{-3}})\frac{\Omega}{km}$$

$$Z_a = 1.181 + j0.06283\ln(\frac{0.72135}{2.0172*10^{-3}})\frac{\Omega}{km}$$

$$= 1.181 + j0.37367 \Omega/km$$

2) For AAC-50 mm^2 conductor type the positive sequences impedance can be calculated as follows;

$$Z_a = R_a + j0.06283\ln(\frac{D}{GMR_a})\frac{\Omega}{km}$$

$$Z_a = 0.5785 + j0.06283\ln(\frac{0.72135}{2.88*10^{-3}})\frac{\Omega}{km}$$

$$= 0.5785 + j0.34702 \Omega/km$$

3) For the AAC-95 mm^2 conductor type the positive sequences impedance can be calculated as follows;

$$Z_a = R_a + j0.06283\ln(\frac{D}{GMR_a})\frac{\Omega}{km}$$

$$Z_a = 0.3085 + j0.06283\ln(\frac{0.72135}{4.1285*10^{-3}})\frac{\Omega}{km}$$

$$= 0.3085 + j0.3244\Omega/km$$

For the three-phase, three conductors the line impedance value of each conductor is similar (i.e., Za = Zb = Zc). Therefore, the positive sequence impedance of conductors is calculated by multiplying the impedance per kilometer by its length. The shunt admittance of overhead lines is neglected because the distribution line is relatively short.

Table 3.9: GMR Factor (k) and Strand Relationship for AAC conductor

Strands	GMR factor, k
1	0.7788
3	0.6778
7	0.7256
19	0.7577
37	0.7678
61	0.7722

To analyse the performance of a distribution line, several crucial parameters need to be considered, including resistance, reactance, segment distance, and active and reactive power demand. The distance of each segment and the types of conductors used are the two important things for positive sequence impedance calculation. The impedance values or resistance and reactance values can be manually calculated based on the segment distance and conductor type used at the time of installation of the Kombolcha-I feeder three using equation 3.9. All buses, from bus, to the bus, conductor type, distance of each line segment, reactance, resistance, active and reactive power are given in Table 3.10.

Table 3.10: Line and load data of 138 buses Kombolcha-I feeder three

Bus	Sending End	Receiving End	Conductor type	Length of conductor (km)	Resistance (ohm)	Reactance (ohm)	Pload (kW)	Qload (kVAr)
1	1	2	AAC-95	0.05	0.01542	0.0162	0	0
2	2	3	AAC-95	1	0.3085	0.3244	149.94	92.9
3	3	4	AAC-95	0.12	0.0372	0.03893	0	0
4	4	5	AAC-95	0.48	0.14808	0.15572	0	0
5	5	6	AAC-95	0.9	0.2776	0.2919	0	0

6	6	7	AAC-95	0.2	0.0617	0.0648	0	0
7	7	8	AAC-95	0.65	0.2	0.2108	0	0
8	8	9	AAC-95	0.75	0.2314	0.2433	372.7	223.24
9	9	10	AAC-95	0.158	0.0488	0.0513	0	0
10	10	11	AAC-95	0.192	0.0593	0.0623	0	0
11	11	12	AAC-95	0.14	0.04319	0.04542	0	0
12	12	13	AAC-95	0.25	0.0771	0.0811	0	0
13	13	14	AAC-95	0.85	0.263	0.2757	0	0
14	14	15	AAC-95	0.4	0.1234	0.12976	0	0
15	15	16	AAC-95	0.35	0.10798	0.1135	0	0
16	16	17	AAC-95	0.1	0.03085	0.03244	0	0
17	17	18	AAC-95	0.25	0.07712	0.0811	40.8	25.3
18	18	19	AAC-50	0.11	0.0637	0.0382	0	0
19	19	20	AAC-50	0.24	0.13884	0.0833	0	0
20	20	21	AAC-50	0.25	0.14463	0.08675	0	0
21	21	22	AAC-50	1.45	0.8388	0.503	0	0
22	22	23	AAC-50	1.2	0.6942	0.4165	689	412.68
23	23	24	AAC-50	0.25	0.1446	0.0867	0	0
24	24	25	AAC-50	1.01	0.5843	0.3505	0	0
25	25	26	AAC-50	0.8	0.4628	0.2776	32.6	24.37
26	26	27	AAC-50	0.3	0.17355	0.10411	0	0
27	27	28	AAC-50	1.05	0.60743	0.3644	0	0
28	9	29	AAC-50	0.15	0.0868	0.0521	23.8	14.756
29	29	30	AAC-50	0.1	0.05785	0.03471	0	0
30	30	31	AAC-50	0.248	0.14347	0.0861	0	0
31	31	32	AAC-50	0.111	0.0643	0.03852	36.12	22.4
32	32	33	AAC-50	0.141	0.08157	0.04893	6.8	4.216
33	33	34	AAC-50	0.234	0.13537	0.0812	0	0
34	34	35	AAC-50	0.23	0.13055	0.07982	0	0
35	35	36	AAC-50	0.116	0.06711	0.04023	0	0
36	36	37	AAC-50	0.114	0.06595	0.0396	0	0
37	37	38	AAC-50	0.05	0.02893	0.01735	34.4	21.06

38	38	39	AAC-50	0.186	0.1076	0.06455	0	0
39	39	40	AAC-50	0.52	0.30082	0.18045	0	0
40	40	41	AAC-50	0.318	0.1839	0.1103	0	0
41	41	42	AAC-50	0.386	0.2233	0.13394	226	119.72
42	42	43	AAC-50	0.364	0.21057	0.12632	0	0
43	43	44	AAC-50	0.2	0.1157	0.0694	0	0
44	44	45	AAC-50	0.11	0.06364	0.0382	21.34	16.72
45	45	46	AAC-50	0.61	0.5314	0.16812	0	0
46	46	47	AAC-50	0.152	0.0879	0.0528	0	0
47	47	48	AAC-50	0.08	0.04628	0.02776	0	0
48	29	49	AAC-50	0.116	0.067106	0.040254	6.8	4.216
49	49	50	AAC-50	0.105	0.06075	0.0365	113.6	89.59
50	50	51	AAC-50	0.229	0.13248	0.07947	0	0
51	51	52	AAC-50	0.06	0.03471	0.02082	0	0
52	50	53	AAC-50	0.15	0.08676	0.05206	152.78	89.52
53	51	54	AAC-50	0.55	0.31818	0.19086	121.36	66.24
54	30	55	AAC-50	0.05	0.02893	0.01735	81.6	50.6
55	33	56	AAC-50	0.242	0.1399	0.08398	157.78	90.23
56	56	57	AAC-50	0.109	0.06306	0.03786	0	0
57	33	58	AAC-50	0.543	0.31413	0.18843	29.98	21.43
58	58	59	AAC-50	0.056	0.0324	0.0195	285.56	139.04
59	34	60	AAC-50	0.3	0.17355	0.1041	34	21.08
60	35	61	AAC-50	0.06	0.03471	0.0204	6.8	4.216
61	36	62	AAC-50	0.8	0.4628	0.2776	364.12	214.35
62	62	63	AAC-50	0.2	0.11577	0.0694	0	0
63	62	64	AAC-50	0.282	0.1631	0.0979	184.21	114.2
64	64	65	AAC-50	0.418	0.24181	0.14505	0	0
65	38	66	AAC-50	0.35	0.20245	0.121457	6.8	4.216
66	39	67	AAC-50	0.498	0.28809	0.1728	47.6	29.5
67	39	68	AAC-50	0.15	0.08678	0.05205	108.8	67.5
68	40	69	AAC-50	0.2	0.1157	0.0694	65.9	40.9
69	42	70	AAC-50	0.26	0.1504	0.0903	6.8	4.216

70	70	71	AAC-50	0.12	0.06942	0.04164	0	0
71	43	72	AAC-50	0.06	0.03471	0.02082	34	21.08
72	45	73	AAC-50	0.13	0.0752	0.04512	57.76	41.34
73	12	74	AAC-50	0.693	0.4	0.2404	106.08	65.8
74	74	75	AAC-50	0.157	0.0908	0.0545	63.24	39.2
75	75	76	AAC-50	0.45	0.2603	0.156	27.6	23.6
76	76	77	AAC-50	0.14	0.0809	0.0486	0	0
77	77	78	AAC-50	0.35	0.2024	0.12145	0	0
78	78	79	AAC-50	0.11	0.0637	0.03817	0	0
79	79	80	AAC-50	0.766	0.4431	0.2658	0	0
80	78	81	AAC-50	0.1	0.0579	0.0347	154.4	129.5
81	79	82	AAC-50	0.3	0.17355	0.1041	116.08	66.9
82	76	83	AAC-50	0.15	0.0868	0.05205	34	21.08
83	83	84	AAC-50	0.12	0.06942	0.04164	40.8	16.8
84	84	85	AAC-50	0.15	0.08678	0.0521	0	0
85	85	86	AAC-50	0.264	0.1527	0.0916	0	0
86	86	87	AAC-50	0.134	0.0775	0.0465	0	0
87	87	88	AAC-50	0.116	0.0671	0.0403	0	0
88	84	89	AAC-50	0.1	0.05785	0.03244	122.4	75.9
89	86	90	AAC-50	0.121	0.0699	0.0412	403.28	223.43
90	90	91	AAC-50	0.5	0.28925	0.17351	0	0
91	90	92	AAC-50	1.115	0.64503	0.38693	34.78	22.39
92	87	93	AAC-50	0.114	0.06595	0.03956	31.5	26.89
93	77	94	AAC-50	0.3	0.17355	0.1041	6.8	4.216
94	94	95	AAC-50	0.75	0.4339	0.2603	103.36	64.08
95	95	96	AAC-50	0.33	0.19099	0.11452	6.8	4.216
96	96	97	AAC-50	0.18	0.10413	0.06246	0	0
97	97	98	AAC-50	0.12	0.06942	0.04164	0	0
98	98	99	AAC-50	0.336	0.1944	0.1167	0	0
99	96	100	AAC-25	0.327	0.386187	0.1222	128.52	79.68
100	100	101	AAC-25	0.45	0.5314	0.16812	0	0
101	100	102	AAC-25	0.69	0.8149	0.2578	40.8	16.8

102	98	103	AAC-25	0.14	0.16534	0.04858	6.8	4.216
103	3	104	AAC-50	0.04	0.02314	0.01389	160.65	99.6
104	4	105	AAC-50	0.05	0.02893	0.0174	61.2	37.9
105	5	106	AAC-50	0.3	0.17355	0.10411	63.4	39.79
106	6	107	AAC-50	0.1	0.05785	0.0347	149.94	92.9
107	7	108	AAC-50	0.3	0.17355	0.104106	29.76	24.56
108	108	109	AAC-50	0.056	0.0324	0.01944	0	0
109	10	110	AAC-50	0.15	0.0868	0.05205	30.78	26.52
110	11	111	AAC-50	0.1	0.05785	0.034702	71.34	54.32
111	13	112	AAC-50	0.15	0.0868	0.05205	171.36	106.24
112	112	113	AAC-50	0.1	0.05785	0.034702	0	0
113	14	114	AAC-50	0.25	0.14463	0.0868	65.28	40.47
114	114	115	AAC-50	0.107	0.0619	0.03713	217.04	129.36
115	115	116	AAC-50	0.293	0.1695	0.101676	0	0
116	116	117	AAC-50	0.1	0.05785	0.034702	0	0
117	115	118	AAC-50	0.15	0.0868	0.05205	129.2	80.1
118	15	119	AAC-50	0.15	0.0868	0.05205	6.8	4.216
119	16	120	AAC-50	0.1	0.05785	0.034702	57.8	35.84
120	18	121	AAC-50	0.35	0.2024	0.12145	81.6	50.6
121	121	122	AAC-25	0.43	0.5078	0.1606	92.5	57.34
122	122	123	AAC-25	0.12	0.14172	0.04484	0	0
123	123	124	AAC-25	0.26	0.30706	0.09714	0	0
124	124	125	AAC-25	0.25	0.2953	0.0934	0	0
125	122	126	AAC-25	0.1	0.1181	0.0374	6.8	4.216
126	123	127	AAC-25	0.06	0.07086	0.02242	98.8	57.5
127	124	128	AAC-25	0.74	0.8739	0.2764	30.6	18.97
128	20	129	AAC-50	0.2	0.1157	0.0694	68	42.16
129	21	130	AAC-50	0.3	0.17358	0.10411	28.9	17.918
130	130	131	AAC-50	0.11	0.0636	0.03817	0	0
131	130	132	AAC-50	0.1	0.05785	0.0347	36.72	14.33
132	23	133	AAC-50	0.557	0.3223	0.1933	100.64	62.4
133	24	134	AAC-50	0.5	0.2893	0.1735	68	42.16

134	26	135	AAC-50	0.546	0.3158	0.1894	51.6	32.04
135	135	136	AAC-50	0.3	0.17355	0.10411	0	0
136	135	137	AAC-50	0.05	0.02892	0.0174	53.78	36.23
137	27	138	AAC-50	0.2	0.1157	0.0694	128.52	79.68
138							23.8	14.756

The selected distribution feeder has a 6.456 MW total active power demand and 3.822 MVAr total reactive power demand as shown in Table 3.10.

3.5.6 Per Unit (p.u) Value Determination

Per unit (p.u) is a method of expressing quantities in a normalized or relative manner in power systems. It is the ratio of the actual value in any quantity and the base or reference value in the same unit. It is a useful technique for simplifying calculations and analysing power system parameters.

The p.u value of any quantity is defined as:

$$\text{Per unit(p.u)}=\frac{\text{The actual value of the quantity}\left(\text{in any unit}\right)}{\text{The base/reference value in the same unit}} \tag{3.12}$$

The per-unit system used in power system analysis relies on both basic base values and derived base values. The basic base values refer to the power and voltage levels within the system, while the derived base values encompass the current and impedance values, which are calculated based on the basic base values. Given the four base values, per unit quantity is calculated as follows:

$$V_{pu}=\frac{V_{actual}}{V_{base}}, I_{pu}=\frac{I_{actual}}{I_{base}}, S_{pu}=\frac{S_{actual}}{S_{base}}, Z_{pu}=\frac{Z_{actual}}{Z_{base}} \tag{3.13}$$

The base values for apparent power and voltage are selected appropriately. Sbase = 100 MVA (common power), Vbase = 15 kV (system voltage as common).

The determination of the base values for impedance and current in a power distribution system is dependent on the chosen base values.

$$Z_{base}=\frac{V^2{}_{base}}{S_{base}}=\frac{15^2}{100}=2.25\Omega \tag{3.14}$$

$$I_{base}=\frac{S_{base}}{V_{base}}=\frac{100*10^3}{15}=6.667kA \tag{3.15}$$

3.5.7 Load Models: Load models can be categorized into two; static and dynamic. Since power flow studies is mainly performed for steady states of the power system, only static load is considered in this thesis work. Constant power model (constant active and reactive), in which the load power is constant with the voltage magnitude. This system is modeled as constant power. Constant power loads describe real and reactive power absorbed by the system so these are modeled as positive power injections at the buses. Loads can be categorized into three classes based on load characteristics, as outlined below (Khushalani et al., 2006).

a) **Constant power:** in these types of load the active and reactive power injections at the bus are remains constant.
b) **Constant impedance:** these load types are used to model huge industrial loads. The impedance of the load is calculated by the specified real and reactive power at a nominal voltage and is remains constant.
c) **Constant current:** In these types the magnitude of the load current is determined by the specified real and reactive power at a nominal voltage and is remains constant.

3.6 Radial Distribution Power System Load Flow Analysis

A load flow study, also known as power flow analysis, is a fundamental analysis performed in power systems engineering. A standard and efficient load flow technique is required for real-time applications such as planning, control, operation, optimization of networks, and so on. It involves calculating the voltage magnitude and its phase angles at each node, the currents and power loss in each branch, and the total power loss in the feeder. Since load flow is a non-linear problem, it must be solved iteratively, which requires one of the following methods including backward/forward sweeping, Gauss-Seidel, Newton Raphson, and Fast Decoupled methods. Traditional load flow techniques like Gauss-Seidel, Newton Raphson, and Fast Decoupled methods are not preferred for radial distribution networks because the RDS networks have some features like high resistance to reactance ratio, a wide range of values of reactance and resistance, unbalanced distribution of load (Khushalani et al., 2006; Rupa & Ganesh, 2014).The backward/forward sweep (BFS) method is the best technique for radial DS because of no need for a Jacobian matrix and has good computational efficiencies and system accuracies.

3.6.1 Bus Classification

In an electric power system, a bus is a node at which one or more lines, generators, and loads, are connected. Each bus is associated with four parameters: voltage magnitude, voltage phase angle, active and reactive power, of which two are known and other two are to be determined. Depending on the quantities to be specified the buses are classified into three categories.

- **Load bus:** This bus is also known as the P-Q bus and no generator is connected. The voltage magnitude and phase angle are calculated for this bus, where the real (P) and reactive (Q) power are given.
- **Generator bus or Voltage-controlled bus:** In these kinds of buses, the true or active power (P) that corresponds to its rating and the voltage magnitude that corresponds to the generating voltage are both given. The bus voltage's phase angle and reactive power (Q) must be calculated.
- **Slack/swing/ reference bus:** In this type of bus the real and reactive power are typically computed by solving equations, given the voltage magnitude and phase angle at this bus.

3.6.2 Backward/Forward Sweeping for Radial Distribution Load Flow Analysis

Load flow analysis is a fundamental thing for planning future power system expansion and analyzing the performance of the existing system. The BFS algorithm is one of the most used techniques for distributing system load flow because of its simplicity, speed, robust convergence, and minimal memory needs for processing with efficiency and solution accuracy (Devi & Geethanjali, 2014). The backward/forward algorithm contains three stages based on Kirchhoff's law. Those stages are nodal current calculation, backward sweep, and forward sweep matrix (Jain et al., 2014).

Algorithm for Backward-Forward Sweep Load Flow:

In the backward /forward algorithm, equivalent current injections (ECI), bus injection to the branch-current matrix (BIBC), and branch current to bus voltage (BCBV) are employed to facilitate the calculations. For distribution system networks, the ECI-based model is more common.

- **Nodal current calculation:**

For bus f, the complex load S_f is expressed as;

$$S_L(f) = P_L(f) + jQ_L(f) \tag{3.16}$$

Where f=1, 2, 3…N

From the specified complex S_f at bus f the equivalent current injection is expressed as follows.

$$I_L(f) = \left[\frac{P_L(f) + jQ_L(f)}{V(f)} \right]^* \tag{3.17}$$

For the load flow solution, the ECI at the kth iteration at the f^{th} node is calculated as;

$$I_L(f)^k = \left[\frac{P_L(f)+Q_L(f)}{V(f)^k}\right]^* \tag{3.18}$$

Where: f=1, 2…. N, k =1, 2,…. Maxiter

I_L (f) is the load currents at the bus 'f', V (f) is the bus voltages at the bus 'f'

P_L & Q_L are the real and reactive power load demand and N is the number of buses.

❖ **Formation of BIBC Matrix/Backward Sweep:**

A backward sweep is carried out with the calculation of the current start from the end node and back to the first node or reference node. For each iteration k, branch currents are aggregated from load to sources. Iteration is stopped when the mismatch between voltage is very low or less than the pre-defined value and maximum iteration occurs (Ouali & Cherkaoui, 2020). First current injected to each bus using equation 3.17 and bus-injection to branch-current is determined. Next by applying Kirchhoff's current law (KCL) to the distribution system, the relation between branch currents and the bus current injection at each bus is obtained as shown in Figure 3.6.

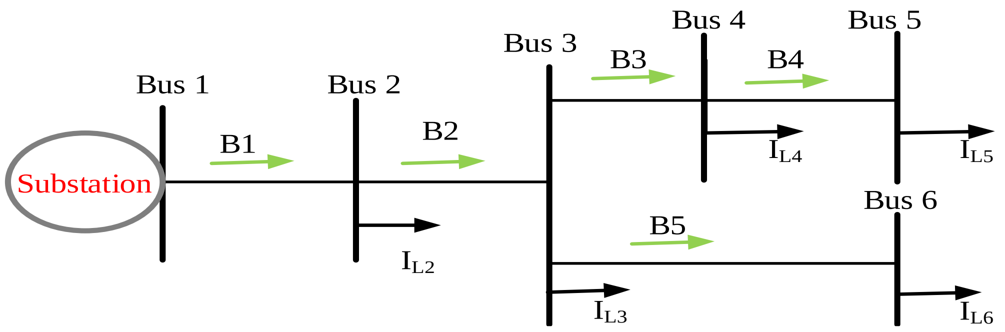

Figure 3.6: Simple radial distribution system

The branch currents B1, B2, B3, B4 and B5 can be found as:

$$\begin{aligned} B_5 &= I_{L6} \\ B_4 &= I_{L5} \\ B_3 &= I_{L4} + I_{L5} \\ B_2 &= I_{L3} + I_{L4} + I_{L5} + I_{L6} \\ B_1 &= I_{L2} + I_{L3} + I_{L4} + I_{L5} + I_{L6} \end{aligned} \tag{3.19}$$

Thus, branch currents and bus current injections can be related as follows;

$$\begin{bmatrix} B1 \\ B2 \\ B3 \\ B4 \\ B5 \end{bmatrix} = \begin{bmatrix} 1 & 1 & 1 & 1 & 1 \\ 0 & 1 & 1 & 1 & 1 \\ 0 & 0 & 1 & 1 & 0 \\ 0 & 0 & 0 & 1 & 0 \\ 0 & 0 & 0 & 0 & 1 \end{bmatrix} \begin{bmatrix} I_{L2} \\ I_{L3} \\ I_{L4} \\ I_{L5} \\ I_{L6} \end{bmatrix} \tag{3.20}$$

The general form of equation (3.20) can be expressed as:

$$[B]=[BIBC][I_L] \tag{3.21}$$

$$[BIBC]=\begin{bmatrix} 1 & 1 & 1 & 1 & 1 \\ 0 & 1 & 1 & 1 & 1 \\ 0 & 0 & 1 & 1 & 0 \\ 0 & 0 & 0 & 1 & 0 \\ 0 & 0 & 0 & 0 & 1 \end{bmatrix} \tag{3.22}$$

Where: BIBC is a bus injection to branch current matrix for the given sample network, I_L is the load currents at the bus 'f'.

- **Formation of BCBV matrix/Forward Sweep:**

Forward sweep carried out with voltage calculation starts from the first node and goes to the last node iteratively. Using previously calculated branch currents vector B and BCBV, nodal voltage vector V is updated from the origin to loads in accordance with Kirchhoff's voltage law (KVL). The relationship between bus voltage and branch currents in a radial distribution system is known as the BCBV matrix. Figure 3.6 illustrates the link between bus voltages and branch currents.

$$\begin{aligned} V_2 &= V_1 - B_1 Z_{12} \\ V_3 &= V_2 - B_2 Z_{23} = V_1 - B_1 Z_{12} - Z_{23} \\ V_4 &= V_3 - B_3 Z_{34} = V_1 - B_1 Z_{12} - Z_{23} - B_3 Z_{34} \\ V_5 &= V_4 - B_4 Z_{45} = V_1 - B_1 Z_{12} - Z_{23} - B_3 Z_{34} - B_4 Z_{45} \\ V_6 &= V_3 - B_5 Z_{36} = V_1 - B_1 Z_{12} - Z_{23} - B_3 Z_{34} - B_5 Z_{36} \end{aligned} \tag{3.23}$$

Where: -V_f is the voltage of bus f, and Z_{fj} is the line impedance between bus f and bus j

The network's bus voltage can be expressed as a function of branch currents, line parameters, and main substation voltage from equation (3.23).

$$\begin{bmatrix} V_2 \\ V_3 \\ V_4 \\ V_5 \\ V_6 \end{bmatrix} = \begin{bmatrix} V_1 \\ V_1 \\ V_1 \\ V_1 \\ V_1 \end{bmatrix} - \begin{bmatrix} Z_{12} & 0 & 0 & 0 & 0 \\ Z_{12} & Z_{23} & 0 & 0 & 0 \\ Z_{12} & Z_{23} & Z_{34} & 0 & 0 \\ Z_{12} & Z_{23} & Z_{34} & Z_{45} & 0 \\ Z_{12} & Z_{23} & 0 & 0 & Z_{36} \end{bmatrix} \begin{bmatrix} B_1 \\ B_2 \\ B_3 \\ B_4 \\ B_5 \end{bmatrix} \tag{3.24}$$

Where BCBV is the branch current to bus voltage which is provided by the sample network.

$$[BCBV] = \begin{bmatrix} 1 & 0 & 0 & 0 & 0 \\ 1 & 1 & 0 & 0 & 0 \\ 1 & 1 & 1 & 0 & 0 \\ 1 & 1 & 1 & 1 & 0 \\ 1 & 1 & 0 & 0 & 1 \end{bmatrix} \begin{bmatrix} Z_{12} & 0 & 0 & 0 & 0 \\ 0 & Z_{23} & 0 & 0 & 0 \\ 0 & 0 & Z_{34} & 0 & 0 \\ 0 & 0 & 0 & Z_{45} & 0 \\ 0 & 0 & 0 & 0 & Z_{36} \end{bmatrix} \tag{3.25}$$

$$[BCBV] = \begin{bmatrix} 1 & 1 & 1 & 1 & 1 \\ 0 & 1 & 1 & 1 & 1 \\ 0 & 0 & 1 & 1 & 0 \\ 0 & 0 & 0 & 1 & 0 \\ 0 & 0 & 0 & 0 & 1 \end{bmatrix}^T \begin{bmatrix} Z_{12} & 0 & 0 & 0 & 0 \\ 0 & Z_{23} & 0 & 0 & 0 \\ 0 & 0 & Z_{34} & 0 & 0 \\ 0 & 0 & 0 & Z_{45} & 0 \\ 0 & 0 & 0 & 0 & Z_{36} \end{bmatrix} \tag{3.26}$$

$$[BCBV] = [BIBC]^T [Z_D] \tag{3.27}$$

Equation (3.27) can be expressed

$$\begin{bmatrix} V_1 \\ V_1 \\ V_1 \\ V_1 \\ V_1 \end{bmatrix} - \begin{bmatrix} V_2 \\ V_3 \\ V_4 \\ V_5 \\ V_6 \end{bmatrix} = \begin{bmatrix} Z_{12} & 0 & 0 & 0 & 0 \\ Z_{12} & Z_{23} & 0 & 0 & 0 \\ Z_{12} & Z_{23} & Z_{34} & 0 & 0 \\ Z_{12} & Z_{23} & Z_{34} & Z_{45} & 0 \\ Z_{12} & Z_{23} & 0 & 0 & Z_{36} \end{bmatrix} \begin{bmatrix} B1 \\ B2 \\ B3 \\ B4 \\ B5 \end{bmatrix} \tag{3.28}$$

$$\begin{bmatrix} V_1 \\ V_1 \\ V_1 \\ V_1 \\ V_1 \end{bmatrix} - \begin{bmatrix} V_2 \\ V_3 \\ V_4 \\ V_5 \\ V_6 \end{bmatrix} = \begin{bmatrix} 1 & 0 & 0 & 0 & 0 \\ 1 & 1 & 0 & 0 & 0 \\ 1 & 1 & 1 & 0 & 0 \\ 1 & 1 & 1 & 1 & 0 \\ 1 & 1 & 0 & 0 & 1 \end{bmatrix} \begin{bmatrix} Z_{12} & 0 & 0 & 0 & 0 \\ 0 & Z_{23} & 0 & 0 & 0 \\ 0 & 0 & Z_{34} & 0 & 0 \\ 0 & 0 & 0 & Z_{45} & 0 \\ 0 & 0 & 0 & 0 & Z_{36} \end{bmatrix} \begin{bmatrix} B_1 \\ B_2 \\ B_3 \\ B_4 \\ B_5 \end{bmatrix} \tag{3.29}$$

$$\Delta V = [BCBV][B] \tag{3.30}$$

$$\Delta V = [BIBC]^T [Z_D][B] \tag{3.31}$$

According to equation (3.24), the bus voltage at the (k+1) th iteration has the following general form:

$$\left[V^{k+1}\right] = [V_1] - [BCBV][B] \tag{3.32}$$

Bus current injections and bus voltages can be relate using equations (3.21) and (3.30) as follows.

$$[\Delta V] = [BCBV][BIBC][I_L] \tag{3.33}$$

$$[\Delta V] = [BIBC]^T [Z_D][BIBC][I_L] \tag{3.34}$$

The distribution load flow matrix (DLF) is formulated as follows:

$$[DLF]=[BCBV][BIBC]=[BIBC]^T[Z_D][BIBC] \tag{3.35}$$

Substituting equation (3.34) into equation (3.35), we have

$$[\Delta V]=[DLF][I_L] \tag{3.36}$$

The stepwise solution for the load flow in the distribution system can be obtained as:

$$[\Delta V^{k+1}]=[DLF][I_L^k] \tag{3.37}$$

$$[V^{k+1}]=[V_1]+[\Delta V^{k+1}] \tag{3.38}$$

Algorithm for Distribution Network Load Flow:

For the load flow solution of distribution networks, the BFS load flow algorithm described above may include the steps listed below:

Step 1: Read the line and bus data of the selected feeder (R and X value for each branch, P and Q value for each bus).

Step 2: Evaluate each node's current injection matrix using equation (3.18).

Step 3: Formulate the BIBC matrix and find out the branch current.

Step 4: Formulate the BCBV matrix using the steps given in the section above.

Step 5: Perform the DLF matrix using equation (3.35).

Step 6: Set iteration counter k = $k+1$, k=0,1, 2…Maxiter

Step 7: Update voltages magnitude using equations (3.37) and (3.38).

Step 8: Find the error in voltage, if max ($|V^{k+1}| - |V^k|$) > tolerance, go to step 6.

Step 9: Once the load flow is converged and the bus voltage and branch currents have been determined, the power loss of each branch in the network must be determined.

Step 10: Display the resulting load flow analysis.

Step 11: Stop

3.7 Modeling of Distributed Generation

The passive distribution system changes into active distribution system when the distributed generator is incorporated into the distribution network. As a result power flow changes as a function of DG penetration level and loading condition (Matos et al., 2021). The distributed generator can be modeled as constant active and reactive (PQ) with currents injected into the node and constant active power and voltage (PV) model in power flow equations. The PQ model is considered a negative load injected into the system (Esmaeilian & Fadaeinedjad, 2014; Khushalani & Schulz, 2006). The new active and reactive power demand at the bus where a DG unit is integrated, suppose at bus k, is updated as follows when incorporating the DG unit into the distribution network (Ganguly & Samajpati, 2017).

$$P_{DGk}^{DG} = P_{Dk}^{base} - P_{DGk} \tag{3.39}$$

$$Q_{DGk}^{DG} = Q_{Dk}^{base} - Q_{DGk} \tag{3.40}$$

Where: P_{DGk}^{DG} and Q_{DGk}^{DG} are new active and reactive power consumed at bus k after DG deployment; P_{Dk}^{base} and Q_{Dk}^{base} are active and reactive power absorbed by the load at bus k before DG deployment; P_{DGk} and Q_{DGk} are active and reactive power of DG but in this research Q_{DGk} is zero since the DG units for this study considered are solar based-DG which inject real power only and operating at unity pf and the PV-DG constant active and reactive power (PQ) models are used. A DG unit doesn't consume or inject reactive power when it works at a unity power factor.

3.8 Problem Formulation

3.8.1 Objective Function

The main targets of DG allocation and sizing in the network are to enhance the performance of the system by minimizing active power loss, and reactive power loss and improving the voltage profile of the system. The objective functions in this study aim to achieve multiple goals, including minimizing real power loss, minimizing reactive power loss, and improving the cumulative voltage deviation (CVD) index in the distribution system. These objectives are considered while accounting both equality and inequality constraints in the optimization process. To address the multi objectives, a weight sum method is employed to change the three single functions into one. By assigning appropriate weights to each objective, a unified objective function is created, allowing for a comprehensive optimization approach.

3.8.1.1 Distribution System with DG Connection

There are many advantages to installing DG units in strategic locations of a distribution system. Reduced line losses, an improved voltage profile, fewer overloads on distribution lines, diminished environmental effects, improved overall energy efficiency, and postponed expenditures in updating current generating, transmission, and distribution systems are a few advantages of distributed generation (Werkie & Kefale, 2022).

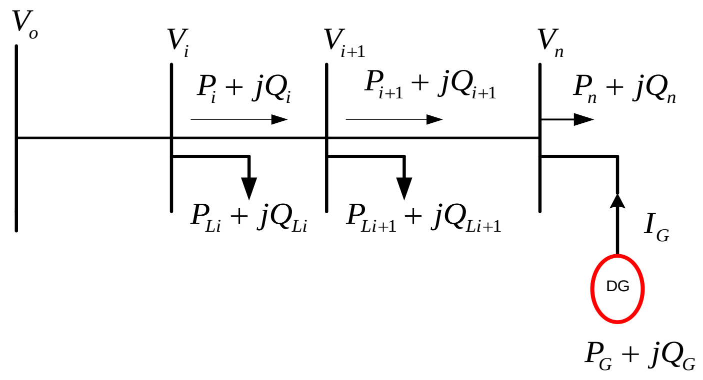

Figure 3.7: Distribution system with DG connection (Werkie & Kefale, 2022)

The real and reactive power loss when DG is integrated at optimal location in the distribution system as shown in Figure 3.7 is given by equations (3.47) and (3.48). Whereas equations (3.43) and (3.44) show active and reactive power losses before DG integration respectively.

$$P_{i+1} = P_i - P_{Li+1} - \frac{R_{i,i+1}}{V_i^2}(P_i^2 + Q_i^2) \tag{3.41}$$

$$Q_{i+1} = Q_i - Q_{Li+1} - \frac{X_{i,i+1}}{V_i^2}(P_i^2 + Q_i^2) \tag{3.42}$$

P_i and Q_i are real and reactive powers flowing out of bus 'i', P_{Li+1} and Q_{Li+1} are the real and reactive power load at bus 'i+1', $R_{i,i+1}$ and $X_{i,i+1}$ are resistance and reactance of the line between buses, i and $i+1$ respectively.

The following formulas can be used to calculate the total active and total reactive power losses in the line section connecting buses i and $i+1$ before DG incorporation.

$$P_{Loss(i.i+1)} = \frac{R_{i,i+1}}{V_i^2}(P_i^2 + Q_i^2) \tag{3.43}$$

$$Q_{Loss(i.i+1)} = \frac{X_{i,i+1}}{V_i^2}(P_i^2 + Q_i^2) \tag{3.44}$$

Then the total active and reactive power losses in the system $P_{T,loss}$ and $Q_{T,loss}$ are given as:

$$P_{T,loss} = \sum_{i=1}^{nb} P_{Loss(i,i+1)} = \sum_{i=1}^{nb} R_i * I_i^2 \tag{3.45}$$

$$Q_{T,loss} = \sum_{i=1}^{nb} Q_{Loss(i,i+1)} = \sum_{i=1}^{nb} X_i I_i^2 \tag{3.46}$$

The power loss equations derived previously equation (3.43) and equation (3.44) can be changed as follows when a DG is incorporated into the distribution system, as shown in Figure 3.7.

$$P_{Loss(i.i+1)} = \frac{R_{i,i+1}}{V_i^2}(P_i^2 + Q_i^2) + \frac{R_{i,i+1}}{V_i^2}\left(P_G^2 + Q_G^2 - 2P_iP_G - 2Q_iQ_G\right) \tag{3.47}$$

$$Q_{Loss(i.i+1)} = \frac{X_{i,i+1}}{V_i^2}(P_i^2 + Q_i^2) + \frac{X_{i,i+1}}{V_i^2}\left(P_G^2 + Q_G^2 - 2P_iP_G - 2Q_iQ_G\right) \tag{3.48}$$

But in this research Q_G is zero since the DG units for this study considered are solar based and operating at unity power factor, it injects only active power.

As a result, the objective function is formulated for reduction of the associated system losses and the voltage deviation for each bus as given below.

1) Loss Minimization

The total active power loss in the distribution system can be computed as follows:

$$f_1 = \sum_{i=1}^{nb} R_i * I_i^2 \tag{3.49}$$

The total reactive power loss in the feeder is given by equation 3.50 and it is considered as the second objective function (f_2) in the optimization.

$$f_2 = \sum_{i=1}^{nb} X_i * I_i^2 \tag{3.50}$$

I_i: is the current of line ‘i’, R_i: is the resistance of the i[th] line

X_i: is the reactance of the i[th] line, nb: is the number of system branches

The total active and reactive power loss reduction can be calculated as follows;

$$\text{Percentage active power reduction} = \frac{P_{\text{total loss}}^{\text{without DG}} - P_{\text{total loss}}^{\text{with DG}}}{P_{\text{total loss}}^{\text{without DG}}} *100 \tag{3.51}$$

$$\text{Percentage reactive power reduction} = \frac{Q_{\text{total loss}}^{\text{without DG}} - Q_{\text{total loss}}^{\text{with DG}}}{Q_{\text{total loss}}^{\text{without DG}}} *100 \tag{3.52}$$

Where; $P_{\text{total loss}}^{\text{without DG}}$, and $P_{\text{total loss}}^{\text{with DG}}$ are total active line losses in the system without and with the installation of DG respectively. Whereas $Q_{\text{total loss}}^{\text{without DG}}$, and $Q_{\text{total loss}}^{\text{with DG}}$ are total reactive line losses in the system without and with the installation of DG respectively.

b) Voltage Profile Improvement

Maintaining bus voltage within the limits is the most important issue since a slight variation in the voltage affects the whole system. Improving the voltage profile of the distribution network which is the commutative voltage deviation (CVD) index is considered as the third objective function (f_3) which is explained as follows:

$$f_3 = \sum_{i=1}^{N} (1 - V_i)^2 \tag{3.53}$$

V_i is the voltage of the i^{th} bus, and N is the number of the system bus.

The weight sum method is used in this thesis work to convert three single-objective function (MOF) into single-objective function. The mathematical illustration of objective function is expressed as follows:

$$Minimize(MOF) = Min(w_1 * f_1 + w_2 * f_2 + w_3 * f_3) \tag{3.54}$$

$$\text{Where, } \sum_{i=1}^{3} w_i = 1$$

3.8.2 Constraints for the Optimization Process

The above multi-objective function will have the following constraints.

1) Equality constraints

The power balance is one of the critical constraints to be fulfilled in the system to maintain the system stable.

$$P_{Grid} + \sum_{i=1}^{np} P_{DG} = \sum_{i=1}^{nl} P_{loss} + P_d \tag{3.55}$$

Where P_{DG} is power supplied by DG, P_d is the total load demand, P_{grid} is the power supplied by the source, P_{loss} is the real power loss in the system, np is the number of DG units and nl is the number of transmission lines in the radial distribution system.

2) Inequality constraints

Bus voltage limits:

As a result of the integration of DG into the distribution network, there is a reverse flow of power and an increase in inrush current, which raises the voltage at the buses. Consequently, the voltage magnitude at each bus must be kept between the permitted minimum and maximum ranges.

$$V_{min} \le V_i \le V_{max} \tag{3.56}$$

Where, V_{min} and are lower and upper voltage limits. Its value is considered as V_{min} =0.95 p.u and V_{max} =1.05 p.u.

Active power limit:

The active power of each DG unit should be selected within a predefined value and the sum of the capacity of all DG units must not be greater than the load demand. DG capacity depends on the availability of resources, technology, and local conditions at the site. In this thesis, the total capacity of DG units is limited to a maximum of 60% of the active power load demand of the selected feeder, with a minimum limit of zero capacity (Arefifar et al., 2014; Juanuwattanakul & Masoum, 2012).

$$\sum_{i=1}^{np} P_{DG}(i) \leq \sum_{i=1}^{n} P_D(i) \tag{3.57}$$

Where P_{DG} and P_D are the real power injected by DG and the active load demand respectively.

Line thermal Limit constraint:

The load rating (current) should be less than or equal to the maximum rating.

$I_k \leq I_{\max,k}$ k=1, 2, …Nb, where Nb is the number of branches. (3.58)

3.9 Optimization Techniques

DG integration at a non-optimal place can lead to an increase in system power loss and voltage drop hence having a negative effect opposite to the desired. There are various optimization methods available to optimize the location and size of DG in DS to minimize power loss and enhance the voltage profile of the system.

3.9.1 Genetic Algorithm

Genetic algorithm (GA) is a general-purpose search approach based on ideas drawn from the genetic and assessment mechanisms found in populations and natural systems of living things. In the genetic algorithm, each chromosome has an m-dimensional real value vector, where m is the number of optimized parameters, and the population has n chromosomes that represent the candidate solution. A genetic search begins with an initial population that is formed at random and in which each member is assessed using a fitness function. According to their fitness values, individuals in this generation and the next generation is either replicated or removed. Further generations are created by applying the GA operator. This eventually leads to a generation of high-performing individuals (Shivarudraswamy et al., 2017). The genetic algorithm (GA) uses a population of points at once, in contrast to the single-point approach used by other methods, which is a more notable distinction between GA and other most traditional optimization methods. The GA repeatedly the modifies population of individual solutions. The genetic algorithm chooses individuals at random from the present population to serve as parents and uses them to create offspring for the next generation at each stage. It improves over time and becomes closer to the optimal answer (Lalitha & Reddy, 2011).

GA Parameters:

The selection of appropriate GA parameters in the optimization process is critical for its convergence. Those GA parameters are population, fitness function, selection, crossover, and mutation (Hailemariam, 2020; Student et al., 2018; Taye, 2019).

A) Initial population

The normal GA operates on a population of N chromosomes simultaneously. These number vectors' starting population is generated at random. Each of these vectors represents one possible solution to the given proposed problems. The population size dictates the number of individuals within a population.

B) Fitness function

The fitness function calculates a person's fitness level (their ability to compete against other people) and provides a corresponding fitness score. The probability of an individual being selected for reproduction is influenced by their fitness value.

C) Selection

This operator enables the transmission of the best individual's genetic material to the next generations in order to focus the search on a promising area and find a suitable answer quickly. The best individual in each group is chosen, which has the objective function. This operator select one or more copies of any individual which has a high fitness value otherwise the individual is removed from the solution pool (Gallego et al., 2009). Many other systems may be used to do this, but roulette wheel selection is the most popular.

Crossover (Recombination)

Crossover is a genetic operator utilized in the genetic algorithm to modify the programming of a chromosome as it transitions from one generation to the subsequent generations. It’s similar to reproduction and biological crossover, which form the fundamental principles of GA. Crossover involves merging multiple parental solutions to generate a new offspring solution. It crossover mated couples with probability crossover, Pc, and develops candidate offspring by marring chromosomes in the mating pool in pairs. Usually, the probability value of the parent chromosome's crossover is assumed between 0 and 1(Hassanat, Almohammadi, Alkafaween, Abunawas, et al., 2019; Kalantari, 2011).

D) Mutation

After performing crossover, some of the genes in the candidate offspring are inverted with probability Pm. The mutation is performed to provide new information about the population (uncover new chromosomes) and also prevent premature convergences. Typically, the probability of mutation (Pm) is assumed to be between 0.01 to 0.1(Hassanat, Almohammadi, Alkafaween, & Abunawas, 2019; Kyule, 2020)

E) Elitism

The worst chromosome in newly generated population is replaced by the best chromosome in the old population if the best number in the new population is lower than the best number in the old population. The purpose of this action is to guarantee convergence of the algorithm. This way of preserving the elite is called elitism.

GA has the following advantages;

- ✓ It can quickly scan a vast solution set for a given formulated objective function
- ✓ They can be resistant to becoming trapped in the local optima

Disadvantages of GA are;

- ✓ It takes more computational times
- ✓ It has a lower convergence rate

GA implementation steps:

Each chromosome in the population of the GA contains an m-dimensional real value vector, where m is the number of optimized parameters, and n chromosomes that each represent a candidate solution. GA implementation has the following steps:

Step 1: Initialization: Set the iteration counter k=1 and generate a random population that contains n chromosomes.

Step 2: Fitness: Using the objective function evaluate each chromosome's fitness in the initial populations.

Step 3: Selection: Choose two parent chromosomes from the population for mating based on the fitness scores of each chromosome and the specified selection method.

Step 4: Crossover and Mutation: After selecting the best two parents using the appropriate selection method, and with a crossover probability, crossover the selected parents to form a new child. Next, by using a predetermined mutation probability, alter the genes in each chromosome of the new offspring.

Step 5: New population: Form a new population by repeating steps 3 and 4 while accepting the newly formed child until the new population is completed.

Step 6: Elitism: Substitute the least effective chromosome in the newly formed population with the most effective chromosome from the previous population.

Step 7: Replacement: Replace the old population with the newly generated population.

Step 8: Iteration upgrading: Upgrade the iteration counter k=k+1.

Step 10: If the stopping conditions are fulfilled go to step 11 else go to step 2.

Step 11: Stop! The chromosome with the highest fitness in the current population is the optimal solution.

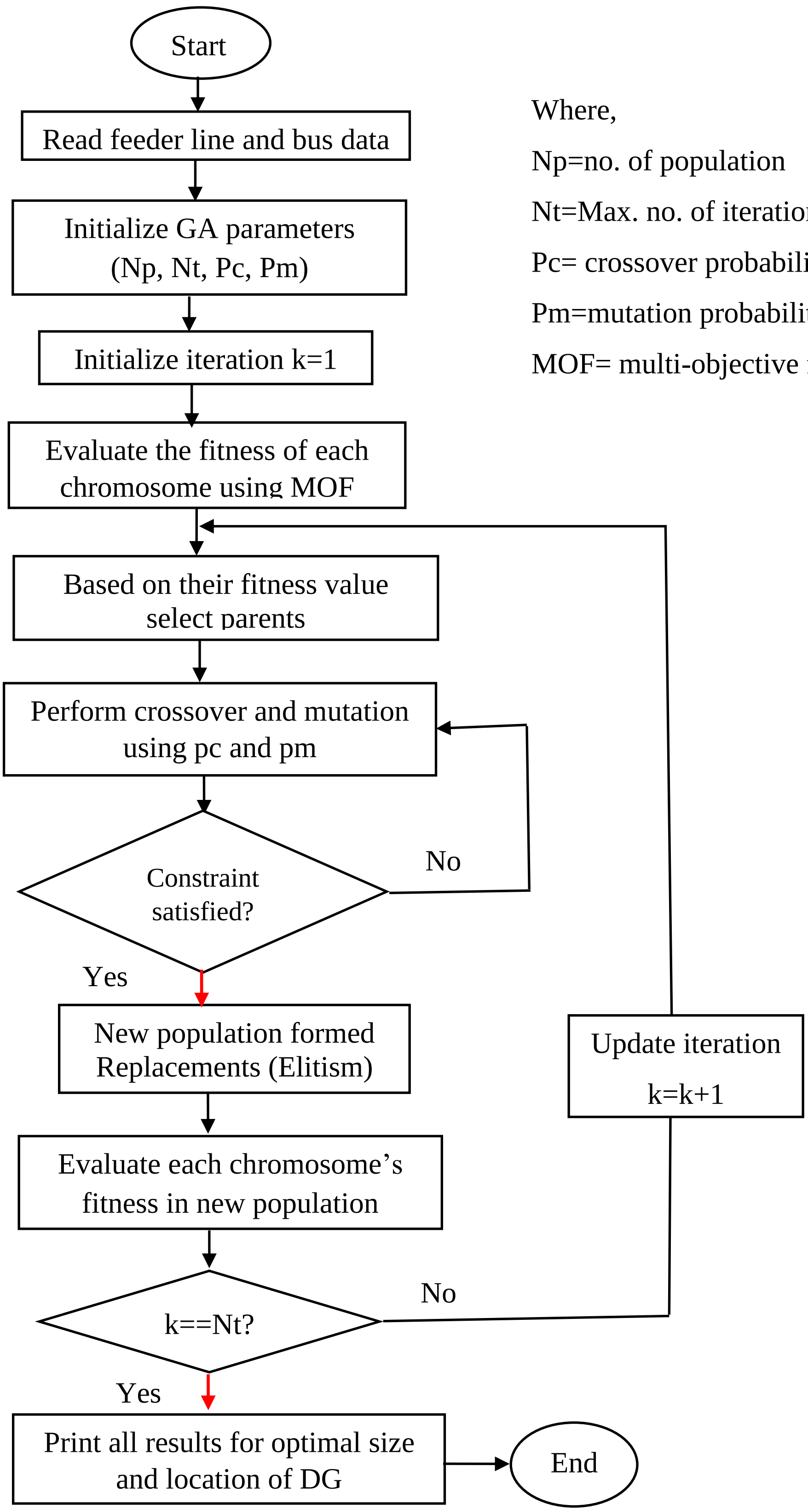

Where,

Np=no. of population

Nt=Max. no. of iteration

Pc= crossover probability

Pm=mutation probability

MOF= multi-objective function

Figure 3.8: Flow chart of genetic algorithm for optimal DG allocation

3.9.2 Particle Swarm Optimization

Particle swarm optimization (PSO) is a population-based swarm intelligent optimization method based on the social behavior of flocks of birds and the schooling of fish, introduced by Kennedy and Eberhart in 1995 (Wang et al., 2017). PSO starts with a random number of particles, or solutions, that are free on the search space. Each particle represents a potential answer to the problem and has a fitness value. A velocity is defined which directs each particle's position and gets updated in each iteration. By coordinating the best placements of all the particles with one another, the swarm's direction modifies the particles' location and velocity dynamically. Before the swarm discovers the optimal solution, all particles attempt to move into better positions (Mohammadi et al., 2011; Rajalakshmi & Durairaj, 2016). The best fitness of each particle, the best fitness of the swarm, and velocity and position updates are the three distinctive characteristics of PSO. Each particle keeps track of its search space coordination, which is connected to the particle's best fitness thus far, which is called personal best (Pbest). Another best value that the PSO tracks of the best value acquired so far by any particle in that particle's vicinity, which is called global best (Gbest) (Niazi & Lalwani, 2017a). The PSO modifies each particle's location and velocity with each iteration. Each particle's position is altered in accordance with their individual flying performance, known as personal best (Pbest), as well as the collective flying performance of all the other particles in group, known as global best (Gbest). The modification process mathematically can be given as follows;

The velocity of the particle (i) is updated as follows;

$$V_i^{k+1} = \omega V_i^k + c_1 r_1 (P_{best,i} - X_i^k) + c_2 r_2 (G_{best} - X_i^k) \quad (3.59)$$

The position of the particle (i) is updated as follows;

$$X_i^{k+1} = X_i^k + V_i^{k+1} \quad (3.60)$$

Where $c1, c2$: acceleration coefficients; $r1, r2$: the random numbers between 0 and 1

ω : inertia weight; V_i^k : the current velocity of the particle i at iteration k,

X_i^k : the current position of the particle i at iteration k; V_i^{k+1} : the modified velocity of particle i ; X_i^{k+1} : the modified position of particle i; P_{best_i} : the personal best position of particle i ; G_{best_i} : the global best position of particle i.

The weighting function is given by the following equation (3.61)

$$w_k = w_{\max} - \frac{w_{\max} - w_{\min}}{t_{\max}} * t \quad (3.61)$$

Where; w_{min} , w_{max} : are the minimum and the maximum inertia weight respectively.

t, t_{max} : are the current and the maximum iteration numbers (Khanday & Malviya, 2019).

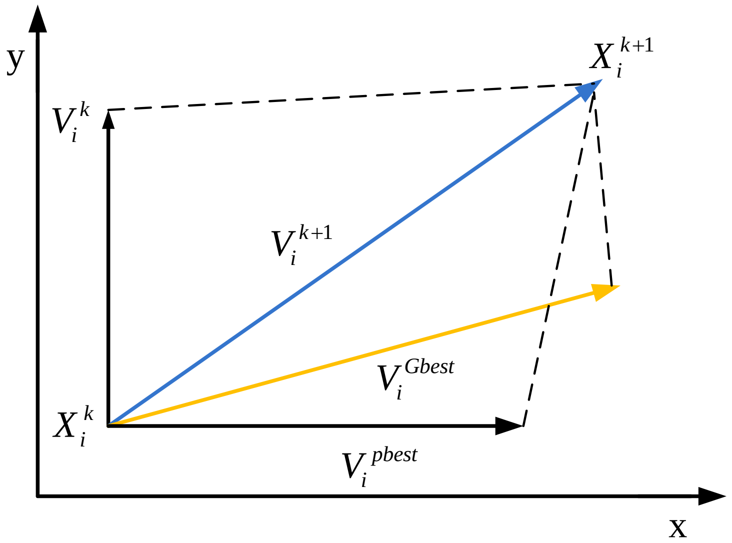

Figure 3.9: Concept of modification of searching points (Venugopal & Jayalaxmi, 2015)

Advantage of PSO

- ✓ Comparatively easy and straight forward to implement
- ✓ Have a few parameters to tune/adjust
- ✓ Fast convergence rate

Disadvantage of PSO

- ✓ The approach is susceptible to partial optimism, which results in less precise control over its speed and direction.

PSO Parameters

For any optimization problem, some of the control parameters in the given algorithm have a considerable impact on its efficiency. The basic parameters of PSO are (Talukder, 2011).

1) Swarm Size:

Swarm size is defined as the number of agents n in the swarm. A large swarm generates larger particles and the maximum search space to be covered per iteration. Using a larger number of agents can reduce number of iterations needed to achieve optimization. However, this increases the computational complexity of each iteration and also makes the process more time-consuming.

2) Particle Velocity

Particle velocity is one of the derived control parameters used in the PSO algorithm. It's worth limited to the bounds. The parameters Vmax and Vmin, which specify which region should be searched between the current position and the target positions, are what determine the fitness. When the value of Vmax is excessively high, particles might fly past good solutions. This is because the particles move in larger steps and the solution reached may be not an optimal solution. Likewise, when Vmax is set too low, particles require an extended period to reach the desired solution. In the majority of PSO interactions, it is common to set the particle's movement range on each axis to around 12-15% of the variable's total range. The agents' velocity is composed of three terms. The three of them are the inertia, cognitive, and social components (Del Valle et al., 2008).

- **Inertia components (V_i^k):** It gives information about the movements in the recent past. This component is utilized to prevent sudden changes in the agent's direction and encourages a tendency to continue moving in the current direction.
- **Cognitive components** $c_1 r_1 (P_{besti} - X_i^k)$ **:** It is used to measure the performance of the agent's relation to their previous performances. It serves as a personal memory of the best position for an agent.
- **Social Component** $c_2 r_2 (G_{besti} - X_i^k)$ **:** It is used to evaluate an agent's performance in relation to a group of agents. Each agent is forced to walk in the direction of the best position found in the agent's neighborhood.

3) Random Number

Random values are in the range [0, 1], it makes easier to achieve the stochastic behavior of PSO.

4) Acceleration Coefficients

The stochastic effects of the social and cognitive components on an agent's velocity are determined by the acceleration coefficients c1 and c2, as well as the randomly generated numbers r1 and r2, respectively. An agent's confidence in themselves is represented by c1, and its confidence in its neighbors is reflected by c2. The properties of c1 and c2;

- When c1= c2, all agents will get attracted towards the average of P_{best} and G_{best}
- When c1>>c2, each agent is heavily influenced by its own best position, which causes it to become locally trapped.
- When c1<<c2, then the global best position has a significant impact on every agent in the swarm, causing every particle to run prematurely to optima (Del Valle et al., 2008).

In many applications c1 and c2 are often constant and their typical values are c1=c2=2 (Niazi & Lalwani, 2017b).

5) Inertia Weight

A suitable inertia weight (w) selection will offer a good mix of global and local searches. Normally, a large beginning value is chosen for the inertia weight, which is subsequently decreased during optimization. This setting enables the PSO to initially explore a vast region at the start of the simulation, when the inertia weight is large, and to refine the search later by using a smaller inertia weight. In general, the inertia weight is modified according to equation (3.61). Appropriate values for W_{max} and W_{min} are 0.9 and 0.4 respectively.

6) Termination Criteria

After the initial phase, several iterations and objective function tolerance for the evaluation steps are performed until a stopping criterion is fulfilled. A predetermined maximum number of iterations or the achievement of certain accuracy in the solution are often the stopping conditions.

PSO Implementation Procedures:

In a PSO optimization algorithm, the population has n particles, each of which represents a candidate solution. Each particle has a k-dimensional real-valued vector, where k is the number of the optimized parameters.

PSO approach has the following implementation steps

Step 1: Initialization: Set the iteration counter k =1, generate a random population that has n particles for objective function evaluation, and PSO parameters like c1, c2 and maximum iteration, $W_{max,}$ and W_{min} are specified.

Step 2: While maxiter >iter or tolerance

Step 3: Objective function evaluation: Calculate the objective function and find its fitness score for each particle.

Step 4: Select the personal best (Pbest) and global best (Gbest) values of particles.

Step 5: Update the velocity and position of particles as follows

The velocity of each particle is modified using the following equation;

$$V_i^{k+1} = \omega V_i^k + c_1 r_1 (P_{best,i} - X_i^k) + c_2 r_2 (G_{best} - X_i^k)$$

Then generate the new particles based on using the following equation

$$X_i^{k+1} = X_i^k + V_i^{k+1}$$

Step 6: Iteration upgrading: Upgrade the iteration counter, k = k+1.

Step 7: If the iteration count reaches the permitted maximum limits go to step 8. Otherwise set iteration counter k=k+1, and return back to step 2.

Step 8: Stop, the most recent particle value produced is the PSO’s optimal solution.

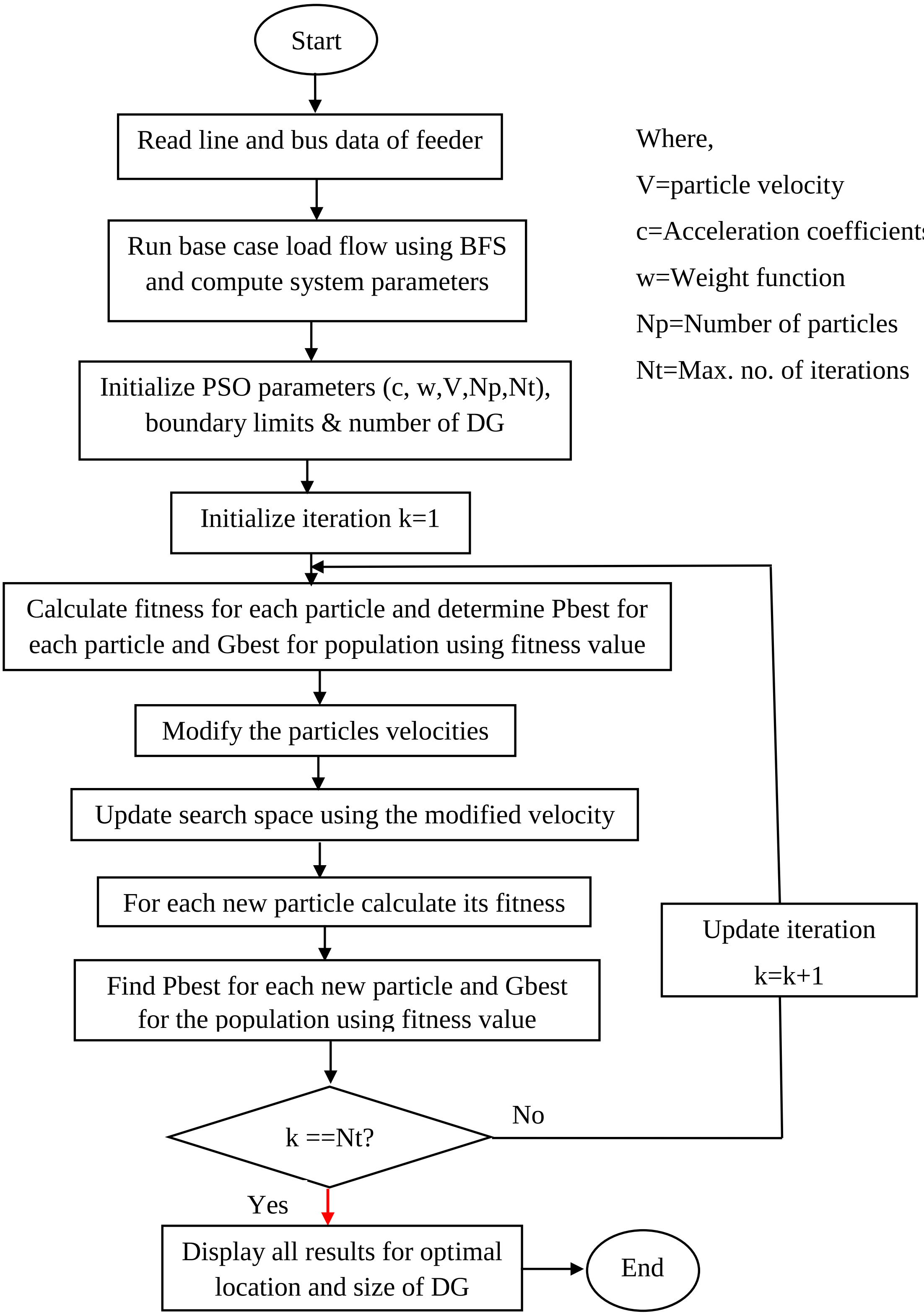

Where,

V=particle velocity

c=Acceleration coefficients

w=Weight function

Np=Number of particles

Nt=Max. no. of iterations

Figure 3.10: Flow chart of PSO for optimal DG allocation

3.9.3 Proposed Hybrid GA-PSO Algorithm

This thesis work proposes the use of hybrid GA-PSO optimization techniques for optimal placement of DG to minimize power loss and voltage profile improvement in the DS. The motivation to develop the hybrid GA-PSO algorithm is to get the combined advantage of genetic algorithms with particle swarm optimization. Each algorithm has its advantages and disadvantages. GA uses a population of points at one time, in contracts to the single point approach by other optimization techniques, and also, GA can resist being trapped in local optima. On the other hand, PSO has good features like a faster convergence rate and low iteration. In GA if individuals are not chosen the information, they possess is lost, but PSO has memory. In contrast, PSO is susceptible to partial optimism, which results in less precise control over its speed and direction. Hence hybridizing the two algorithms gives better optimal results. The optimization problem consists of two parts. The first is the optimal allocation of DG which is the bus number and the second is its optimal capacities of it. The result for the first is an integer which is the bus number where the DG is suggested to be integrated. This needs an integer-based optimization algorithm. The answer obtained from the GA solution is used in the PSO algorithm to optimize the size of DG based on objective function. Generally, GA explores and obtains potential ideas, which are then send to PSO for fine-tuning. The partially optimized GA output result which is handed to PSO comprises some sets of solutions each having DG location and the associated capacities. The optimized GA output results are used as initial particles in PSO. This helps to obtain better-optimized results.

In this thesis work arithmetic crossover and mutation were applied in the proposed hybrid optimization technique. These parameters help in avoiding premature convergence/partial optimism and thus improve the performance of the algorithm.

There are different ways in which these two optimization techniques can be hybridized to come up with a better method to solve the problem at hand. Some of the important tools used in this research are discussed as follows:

Roulette Wheel Selection Method:

Roulette wheel selection, also referred to as fitness proportionate selection, is a genetic operator utilized in proposed algorithms to choose potentially valuable solutions for the crossover process. The idea behind the roulette wheel selection method is to provide every individual with an opportunity to become a parent, which is determined by their fitness level. In other words, the probability of an individual chromosome being chosen as a parent is directly influenced by its fitness i.e., chromosomes with higher fitness scores are more likely to be chosen. If f_i is the fitness of individual i in the population, its probability of being selected is given by;

$$p_i = \frac{f_i}{\sum_{j=1}^{N} f_i} \tag{3.62}$$

Where, N = No of individuals in the population.

It is called roulette wheel selection as the chance of selecting a parent can be seen as spinning a roulette wheel in a casino with the size of the slot for each parent being proportional to its fitness. Those candidate solutions with high fitness values have more probability of being selected.

Arithmetic Crossover and Mutation:

In the proposed hybrid GA-PSO optimization algorithm arithmetic crossover and mutation were utilized. These operators aid in preventing early convergence/partial optimism and thereby enhancing the algorithm's effectiveness. Arithmetic crossover refers to the process of generating two child chromosomes X_{c1} and X_{c2} by combining two parent chromosomes X_{p1} and X_{p2} according to the following procedure (Kilonzi & Odero, 2013).

$$X_{c1} = \lambda X_{p1} + (1-\lambda) X_{p2} \tag{3.63}$$

$$X_{c2} = \lambda X_{p2} + (1-\lambda) X_{p1} \tag{3.64}$$

$\lambda \in (0,1)$ is a random number between 0 and 1 and used to compute the child as shown.

For a given child, $X_{cl}^{k} = X_{l1}^{k},,, X_{lj}^{k},,, X_{lm}^{k}$ Where, $l = 1, 2, \ldots, N$; $j = 1, 2, \ldots, m$.

If the element X_{lj}^{k} is selected for mutation, the resulting offspring is $X_{cl}^{k} = X_{l1}^{k},,, X_{lj}^{k*},,, X_{lm}^{k}$

Where $X_{lj}^{k*} = X_{lj}^{k} + \Delta X_{lj}^{k}$, ΔX_{lj}^{k} is randomly selected from the two possible choices:

$\Delta X_{lj}^{k} = r(X_{lj}^{\max} - X_{lj}^{k})(1 - \frac{k}{k_{\max}})$ or $\Delta X_{lj}^{k} = r(X_{lj}^{\min} - X_{lj}^{k})(1 - \frac{k}{k_{\min}})$.

Where r is a random number in the range between 0 and 1.

Steps for the Proposed Hybrid GA-PSO Algorithm:

The proposed hybrid GA-PSO algorithm is implemented in the following steps:

1. Read the distribution systems bus data and line data, base MVA, base kV, and bus voltage limits.
2. Execute the backward/forward sweep method for load flow studies to determine base

case system power loss and voltage profile for the selected distribution feeder.

3. Set the lower and upper limit constraints, and inputs for both GA and PSO control parameters (population size, C1, C2, W_{max}, W_{min}, Pc, Pm, max. number of iterations)
4. Initialize N random chromosomes which consist of possible DG location and size.

   $X_j = [\text{Size of DG} \quad \text{Location}] = [S \; L],\; j = 1,2,3,...N$

   $X_j(\text{Num\_DG}) = [S_1 \; S_2 \; S_3......S_{\text{Num\_DG}} \;\; L_1 \; L_2 \; L_3.........L_{\text{Num\_DG}}]$
5. Calculate each chromosome's fitness value using the multi-objective function.
6. Set iteration count for GA, i = 1
7. While $i \le i_{max}$
   a) Calculate the fitness value for each chromosome using a multi-objective function.
   b) Using exponential probability and roulette wheel selection select two parent chromosomes (X_{p1} and X_{p2}).
   c) Apply arithmetic crossover and evaluate offspring fitness value.
   d) Apply mutation and evaluate mutant fitness value.
   e) Create a merged population (New population).
   f) Update iteration counter i = i+1.
   g) Stop and pass the current chromosome (partially optimized) to PSO.
   h) Use GA-optimized chromosome as an initial particle to PSO algorithm.
   i) Evaluate the fitness value for each particle using a multi-objective function and identify personal best P_{best} and global best G_{best}.
8. Set iteration count for PSO, k =1.
9. While $k \le k_{max}$
   a) Modify the velocity of each particle as follows

   $$V_i^{k+1} = wV_i^k + c_1 r_1 (P_{best_i} - X_i^k) + c_2 r_2 (G_{best_i} - X_i^k)$$

   b) Then update the new position for each particle as follows

   $$X_i^{k+1} = X_i^k + V_i^{k+1}$$

   c) Apply velocity and position limits.
   d) Calculate the fitness of each particle using a multi-objective function and identify personal and global best.

   $$P_{best(j)}^{k+1} = \begin{cases} X_j^{k+1} & if\ MOF_j^{k+1} < MOF_j^k \\ P_{best(j)}^k & if\ MOF_j^{k+1} \ge MOF_j^k \end{cases}$$

$$G_{best(j)}^{k+1} = \begin{cases} P_j^{k+1} & if\ MOF_j^{k+1} < MOF_j^{k} \\ G_{best(j)}^{k} & if\ MOF_j^{k+1} \geq MOF_j^{k} \end{cases}$$

e) Update iteration counter k=k+1.

10. Stop, the particle that generates the latest G_{best} is the optimal solution which consists optimal location and size of DG.
11. Using the latest generated $G_{best,}$ perform load flow analysis using BFS and display all results for optimal size and location of DG.

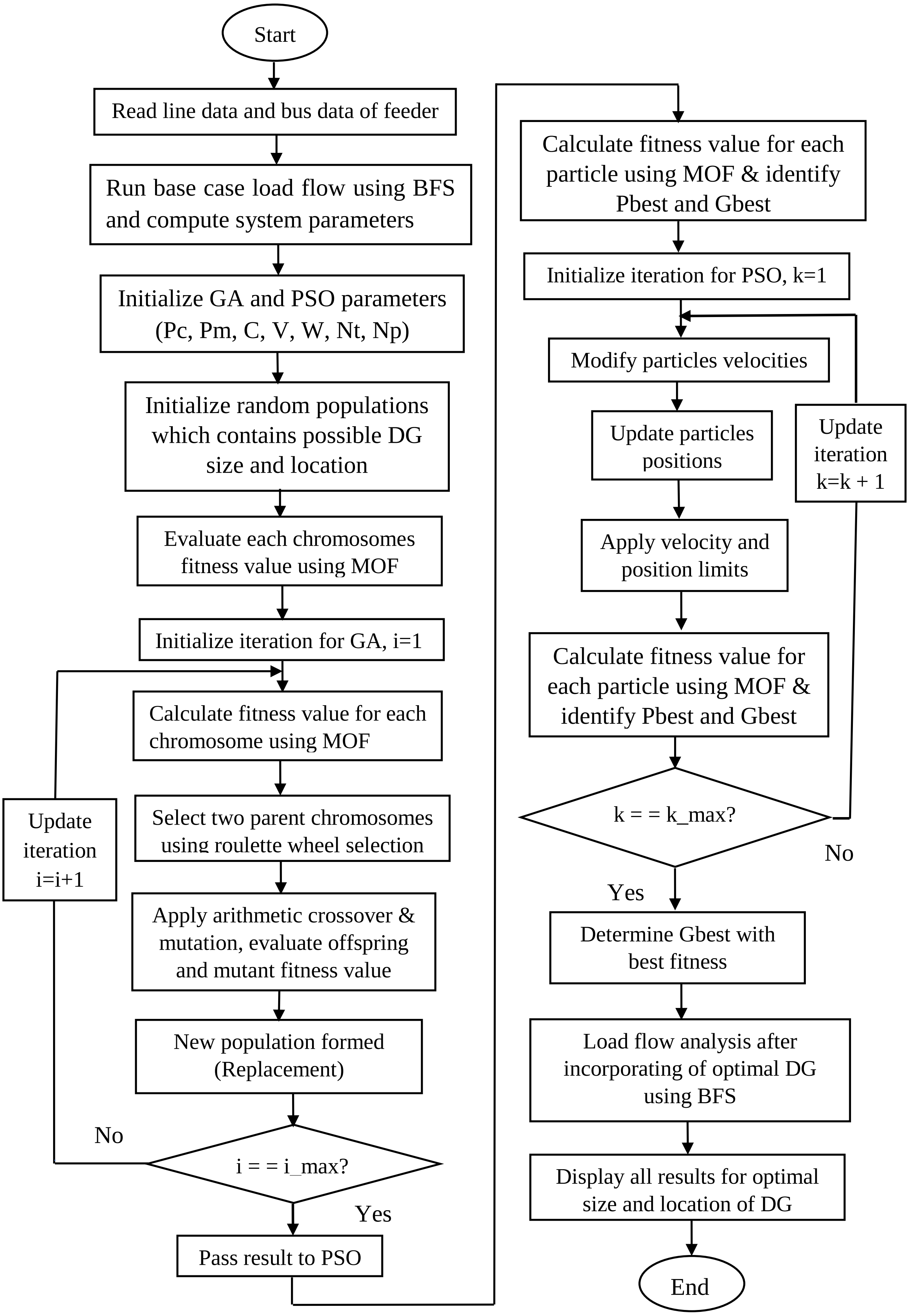

Figure 3.11: Flow chart of proposed hybrid GA-PSO for optimal DG allocation

CHAPTER FOUR

4. SIMULATION RESULTS AND DISCUSSIONS

In this chapter, the results obtained using the BFS load flow method, and a hybrid of GA-PSO methods have been presented. The hybrid GA-PSO algorithm explained in the previous chapter is implemented in MATLAB 2021 software. Comparative analysis of GA, PSO, and proposed GA-PSO algorithms have also been done to show effectiveness of this algorithm in minimizing real and reactive losses and enhancing the voltage profile of the system. The performance parameters of the distribution system like power losses and voltage profile of the system are discussed as the base case and after the optimal allocation of DG.

The simulation results are presented in two scenarios as follows:

Scenario-I: Base case or existing system

Scenario-II: After integration of DG

- Case -1: Integration of one DG
- Case -3: Integration of two DG
- Case -2: Integration of three DG
- Case -4: Integration of four DG

4.1 Scenario-I: Base Case or Existing System

4.2.1 Base Case Simulation Results

Power flow analysis is performed to determine the active and reactive power loss, each bus voltage profile of the selected feeder for the existing system. The load flow analysis has been performed using the backward forward sweep (BFS) algorithm coded in MATLAB 2021a software, using line and bus data. The system input base MVA =100 and base voltage =15 kV are used to change into per unit value and minimum and maximum voltage limit has been taken at 0.95 p.u and 1.05 p.u respectively. The selected feeder's total real and reactive power load demands are 6.456 MW and 3.8218 MVAr respectively. From the base case simulation result, the total active and reactive power loss becomes 400.9144 kW and 404.8856 kVAr respectively. The active and reactive power losses graph for each branch at the base case are shown in Figures 4.1 and 4.2 respectively. And also, the active and reactive power losses for each branch in tabular form at the base case are given in Appendix-E after the backward-forward load flow has been analyzed. The base case voltage profile of buses of the selected feeder is also evaluated using a backward-forward sweep load flow algorithm. The base case simulation result shows that most of the buses are below the minimum voltage level which is 0.95p.u. The minimum voltage value at the base case system was 0.9155p.u which occurs

@ bus 28. The base case voltage profile graph is shown in Figure 4.3 and its voltage magnitude in tabular form for all buses at base case is given in Appendix-F after backward forward load flow has been analyzed. According to the base case voltage profile result, the feeder's voltage profile depends on the distance traveled and the load placed on the lines. As can be observed, voltage decreases grow as the feeder's length increases. It decreases rapidly from 1 p.u to 0.9155 p.u up to bus 28 due to the distance from the source being increased. Again the voltage profile rises to 0.984 p.u at bus 104 since the distance from the source is less. As voltage drops rise as the length of the feeder gets longer, the voltage profile of the buses close to the substation is higher than the bus voltage magnitude further from the source.

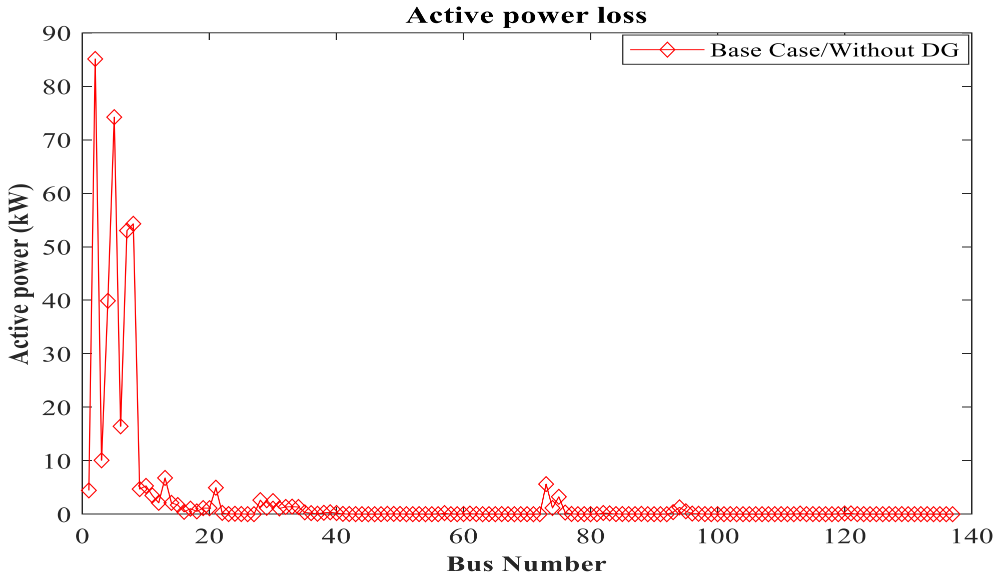

Figure 4.1: Base case active power loss in each branch of Kombolcha L-3 feeder

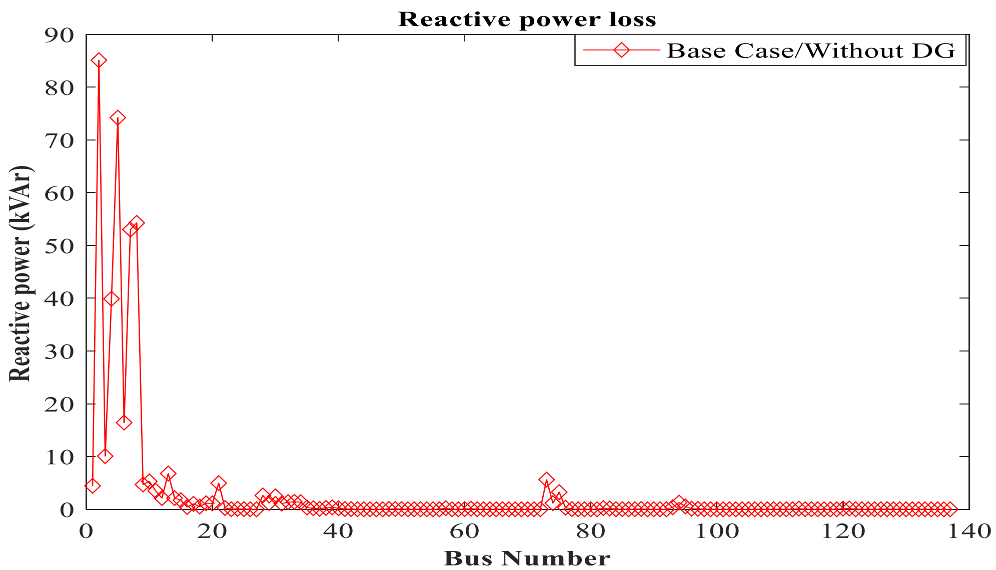

Figure 4.2: Base case reactive power loss in each branch of Kombolcha L-3 feeder

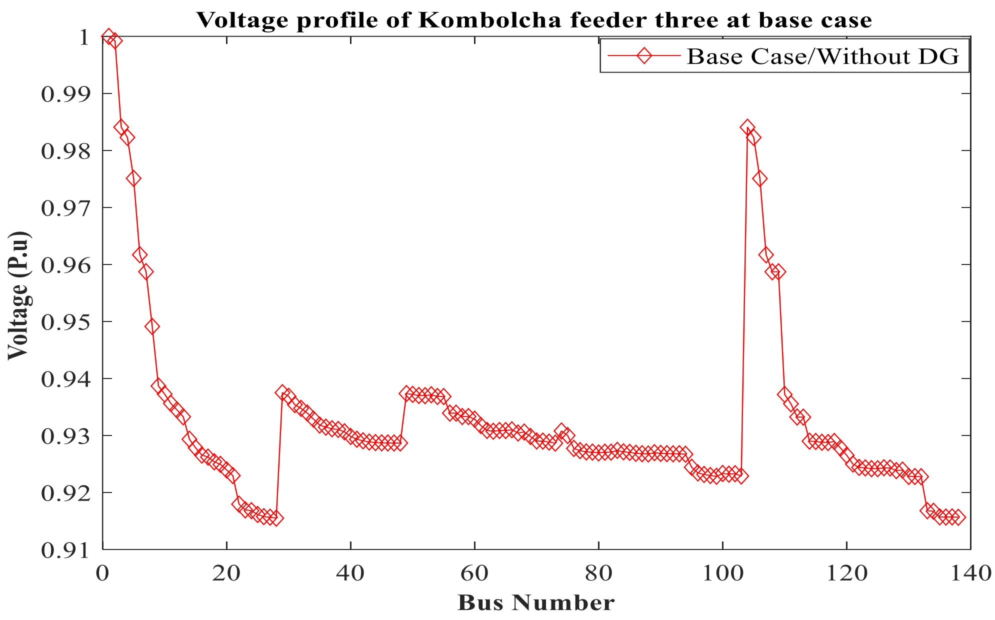

Figure 4.3: Base case voltage profile of Kombolcha L-3 feeder

Table 4.1: Result summary of scenario-I

Performances	Base case result
Active power loss (kW)	400.9144
Reactive power loss (kVAr)	404.8856
Minimum voltage (p.u)	0.9155 @ bus 28
Maximum voltage (p.u)	1
Maximum voltage deviation (%)	8.4696
CVD	0.6655

4.2 Scenario-II: After Integration of DG

Choice of weights value for multi-objective function: The multi-objective function consists of the minimization of real power loss, reactive power loss, and voltage deviation index. The choice of weight factors depends on the researcher's focus on achieving better performance. In this study, active power loss has a weight factor greater than 0.5 since it significantly lowers the overall cost of operation. To determine the best objective function value, various weighting factors are tested, and the results are presented in Table 4.2. Among the tested weighting factors, the combination that yields the minimum best objective value is selected to form the multi-objective function.

Table 4.2: The effect of weights on the fitness value

W1	W2	W3	Best Fitness
0.5	0.1	0.4	0.26861
0.5	0.2	0.3	0.20246
0.5	0.3	0.2	0.13632
0.5	0.4	0.1	0.070173
0.6	0.1	0.3	0.20246
0.6	0.2	0.2	0.13631
0.6	0.3	0.1	0.070169
0.7	0.1	0.2	0.13631
0.7	0.2	0.1	0.070165
0.8	**0.1**	**0.1**	**0.070161**

From the tested weighting factor results, the last case is selected as the weighting factor to form the multi-objective function since it gives the best minimum objective value.

Therefore, the multi-objective function is formulated as follows;

$$MOF = 0.8 * f1 + 0.1 * f2 + 0.1 * f3 \quad (4.1)$$

To obtain the optimal values of the control variables, the GA, PSO, and proposed GA/PSO-based algorithm were run with different optimal control settings. The parameters used in this study are given in Table 4.3.

Table 4.3: GA/PSO Parameters

GA/PSO Parameters	Number of populations (P)		50
	Maximum number of iterations		100
	Inertia weight	Wmin	0.4
		Wmax	0.9
	Acceleration coefficients	C1	2
		C2	2
	Crossover probability (pc)		0.9
	Mutation probability (pm)		0.02

4.2.1 Simulation Result after Integration of DG Using Hybrid GA-PSO Algorithm

The simulation results for DG integration have been discussed in four cases, i.e., case one (1-DG integration), case two (2-DG integration), case three (3-DG integration), and case four (4-DG integration). The simulation results for bus voltage profile, total active and reactive power losses, and convergence curve after integration of DG using the proposed hybrid GA-PSO algorithm for all cases are shown in Figures 4.4, 4.5, and 4.6 respectively.

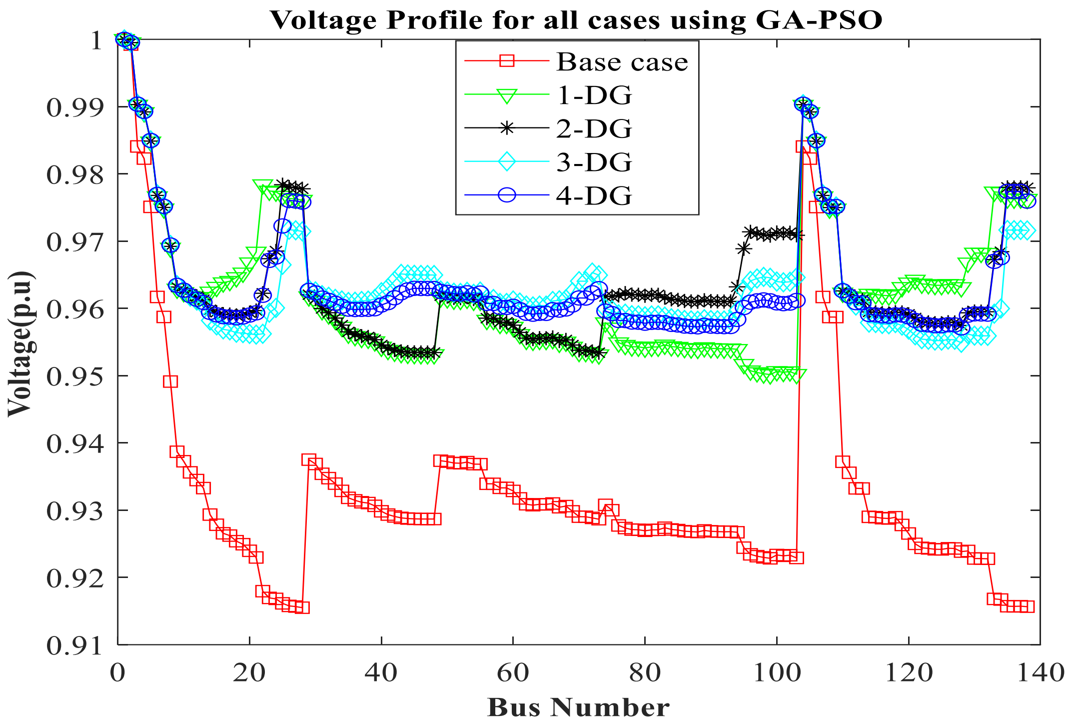

Figure 4.4: Voltage profile for all cases using the GA-PSO algorithm

As shown in Figure 4.4, after the integration of the optimal size of DG in the optimal location voltage profile of all buses is improved very well. The minimum voltage before integration of DG was improved from 0.9155p.u to 0.95016p.u, 0.95341p.u, 0.95489p.u and 0.9571p.u. In all cases, all bus voltages are above the minimum threshold value which is 0.95 p.u. And also, in all cases the buses voltage magnitude at which DG is integrated becomes high(peak). The optimal location and size of DG units using the hybrid GA-PSO algorithm for all cases are shown in Table 4.4. Similar to voltage profile improvements, the optimal allocation of DG minimized the total active and reactive power losses of the system. The active power loss is minimized from 400.9144 kW to 216.7175 kW, 196.3369 kW, 165.484 kW, and 165.0038 kW, while the reactive power loss is minimized from 404.8856 kVAr to 193.2621 kVAr, 164.8733 kVAr, 149.8299 kVAr and 151.9591 kVAr after integration of 1-DG, 2-DG, 3-DG and 4-DG respectively. The percentage reduction of active power loss after integration of 1-DG up to 4-DG is 45.9442 %, 51.0277%, 58.7234%, and 58.8431 % respectively. Whereas the percentage reduction of reactive power loss after the integration of 1-DG up to 4-DG is 52.2675 %, 59.279%, 62.9945 %, and 62.4686 % respectively.

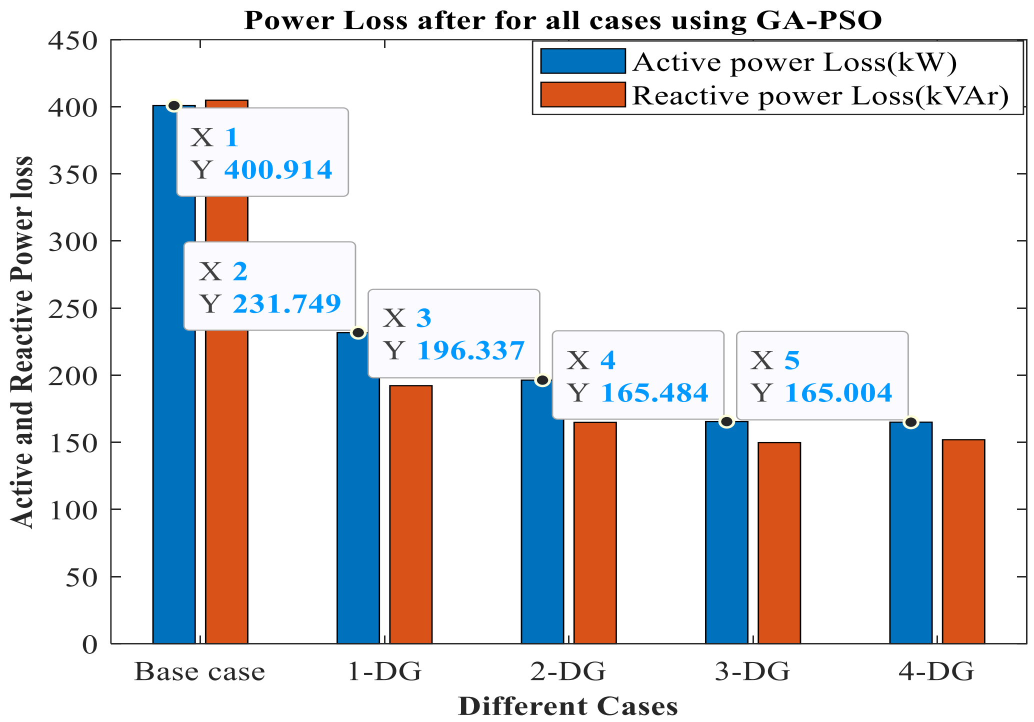

Figure 4.5: Total active and reactive power loss for all cases using the GA-PSO algorithm

The convergence curve for all cases or numbers of multiple DG integration using proposed hybrid GA-PSO method is shown in Figure 4.6. The objective functions (MOF) values are 0.02295, 0.02129, 0.021022, and 0.02082 after the integration of 1-DG, 2-DG, 3-DG, and 4-DG respectively. As shown from the convergence curve the objective function value for case 3 and case 4 have a small difference.

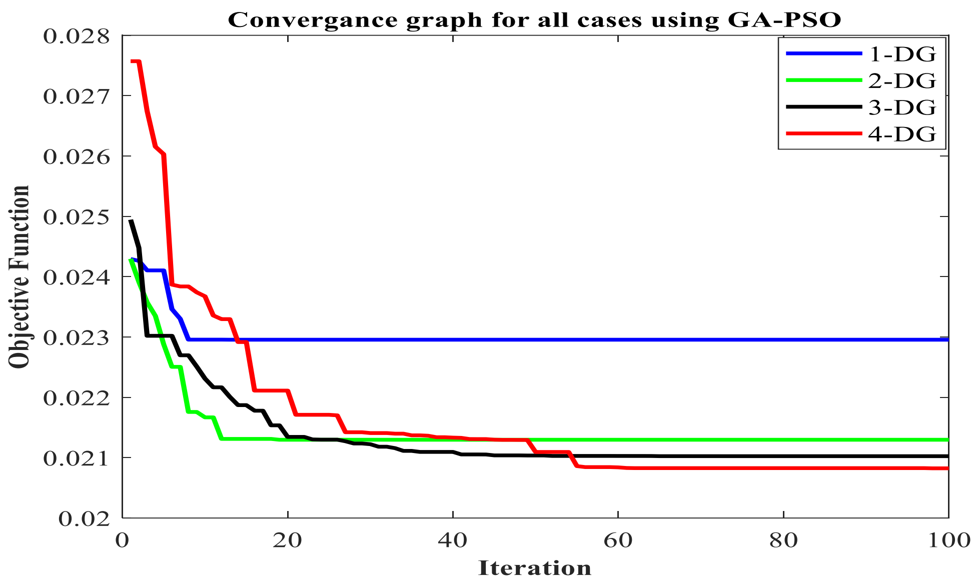

Figure 4.6: Convergence curve for all cases using the GA-PSO algorithm

Table 4.4: Result summary of all scenarios using hybrid GA-PSO

Parameters	**Without DG**	**With 1-DG**	**With 2-DG**	**With 3-DG**	**With 4-DG**
Active power loss (kW)	400.9144	216.717	196.3369	165.484	165.0038
Reactive power loss (kVAr)	404.8856	193.262	164.8733	149.8299	151.9591
Maximum V. devotion (%)	8.4696	4.984	4.6588	4.5113	4.2899
Minimum voltage (p.u)	0.9155 @ bus 28	0.95016 @ bus 99	0.95341 @ bus 73	0.95489 @ bus 128	0.9571 @ bus 128
Active power loss red. (%)	-----	45.944	51.0277	58.7234	58.8431
Reactive power loss red. (%)	--------	52.267	59.279	62.9945	62.4686
MOF	-----	0.02295	0.02129	0.021022	0.02082
DG location	----	22	22	26	23
				72	45
			96	98	98
					135
DG size (kW)	------	3874	1937	1291	968
				1291	968
			1973	1291	968
					968

4.2.2 Comparative Analysis of Proposed GA-PSO With GA and PSO Methods

To investigate the effectiveness of the proposed hybrid GA-PSO method, the results of the proposed model are compared with GA and PSO methods. A comparison result after 1-DG integration is presented in Table 4.5.

Table 4.5: A comparison result summary after 1-DG integration for different algorithms

Methods	Location (size in kW)	P_{loss} (kW)	Q_{loss} (kVAr)	V_{min} (p.u)	V_{Max} dev. (%)	$\%P_{loss}$ red.	$\%Q_{loss}$ red.	MOF
PSO	22 (3874)	216.77	193.26	0.95016	4.984	45.94	52.26	0.2295
GA	95 (3630)	231.74	192.21	0.95001	4.999	52.52	42.19	0.0256
GA-PSO	22 (3874)	216.77	193.26	0.95016	4.984	45.94	52.26	0.2295

As shown in Table 4.5, for integration of 1-DG, the proposed hybrid GA-PSO and PSO algorithms are selected the same bus number and DG size. The percentage real and reactive power loss reduction and MOF value were 45.944%,52.2675%, 0.229551 for the proposed method and PSO method, and 42.195%, 52.5258%, 0.025681 for GA respectively. For all three methods, the bus voltages are above the minimum voltage range, which is 0.95p.u. Simulation results for integration of 2-DG are presented in Table 4.6.

Table 4.6: A comparison result summary after 2-DG integration for different algorithms

Methods	Location (size in kW)	P_{loss} (kW)	Q_{loss} (kVAr)	V_{min} (p.u)	V_{Max} dev. (%)	% P_{loss} red.	% Q_{loss} red.	MOF
PSO	25 (1937)	197.64	170.17	0.95003	4.997	50.701	57.969	0.0219
	44 (1937)							
GA	26 (1763)	208.53	173.24	0.95192	4.808	47.984	57.212	0.0231
	97 (1874)							
GA-PSO	25 (1937)	196.33	164.87	0.95341	4.659	51.028	59.279	0.0213
	96 (1937)							

The simulation result after the integration of 2-DG for different algorithms shows that, the percentage active and reactive power loss reduction and MOF are 51.028%, 59.279%, and 0.02129 for GA-PSO, 47.984%, 57.212%, and 0.02313 for GA and 50.70%, 57.969% and 0.02194 for PSO respectively. The voltage profile graph for 2-DG is shown in Figure 4.7.

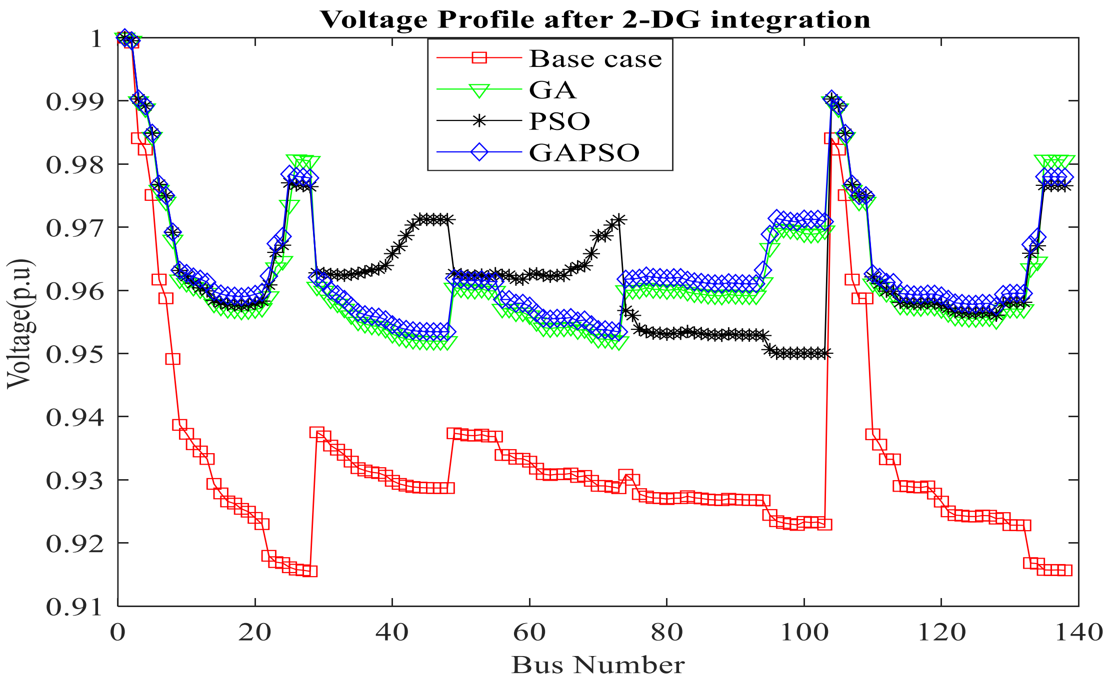

Figure 4.7: Voltage profile of the base case and after 2-DG integration with different algorithms

As shown in Table 4.6 and Figure 4.7 after the integration of 2-DG the proposed hybrid GA-PSO algorithm has better performance in terms of active and reactive power loss reduction, voltage profile improvements, and minimization of the objective function. Similar to case 1 and case 2, comparative analysis was also performed for case 3 and case 4. The comparison results for case 3 are shown in Table 4.7 and in Figure 4.8.

Table 4.7: A comparison result summary after 3-DG integration for different algorithms

Methods	Location (size in kW)	P_{loss} (kW)	Q_{loss} (kVAr)	V_{min} (p.u)	V_{Max} dev. (%)	$\%P_{loss}$ red.	$\%Q_{loss}$ red.	MOF
PSO	26 (1291)	175.12	155.35	0.9536	4.641	56.32	61.63	0.02124
	98 (1291)							
	123 (1291)							
GA	97 (1206)	171.23	156.57	0.9532	4.674	57.28	61.33	0.02267
	73 (1277)							
	27 (1194)							
GA-PSO	26 (1291)	165.48	149.83	0.9549	4.511	58.72	62.99	0.02102
	72 (1291)							
	98 (1291)							

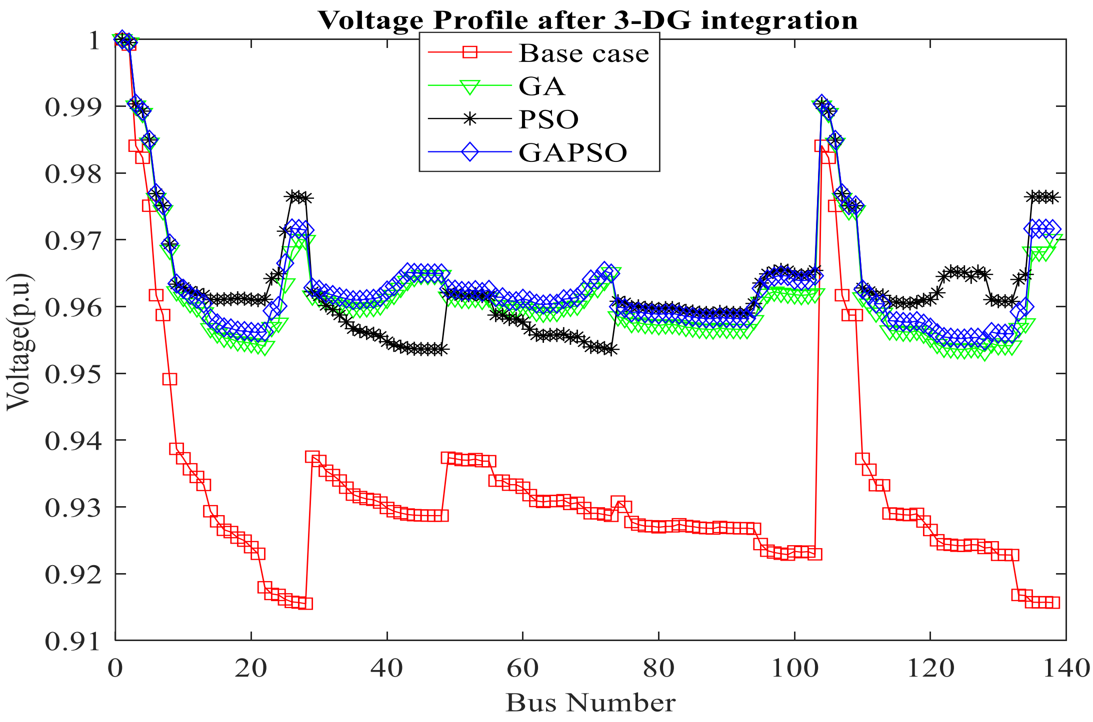

Figure 4.8: Voltage profile of the base case and after 3-DG integration with different algorithms

The simulation result after the integration of 3-DG using different algorithms shows that, the active and reactive power loss percentage reduction and MOF are 58.724%, 62.995, and 0.02102 for GA-PSO, 57.288% 61.329%, and 0.02267 for GA and 56.319%, 61.63% and 0.02124 for PSO respectively. Comparison results after integration of 4-DG are presented in Table 4.8. As shown from the simulation result, the voltage magnitude at the integrated bus is high/peak for all algorithms. The voltage profile graph after integration of 4-DG using different algorithms is shown in Figure 4.9

Table 4.8: A comparison result summary after 4-DG integration for different algorithms

Methods	Location (size in kW)	P_{loss} (kW)	Q_{loss} (kVAr)	V_{min} (p.u)	V_{Max} dev. (%)	%P_{loss} red.	%Q_{loss} red.	MOF
PSO	26(968)	168.74	150.93	0.9537	4.628	57.91	62.72	0.0227
	46(968)							
	96(968)							
	98(968)							
GA	27(861)	158.70	152.87	0.9512	4.879	60.41	62.24	0.0236
	72(940)							
	86(928)							
	98(886)							
GA-PSO	23(968)	165.04	151.95	0.9571	4.289	58.84	62.46	0.0208
	45(968)							
	98(968)							
	135(968)							

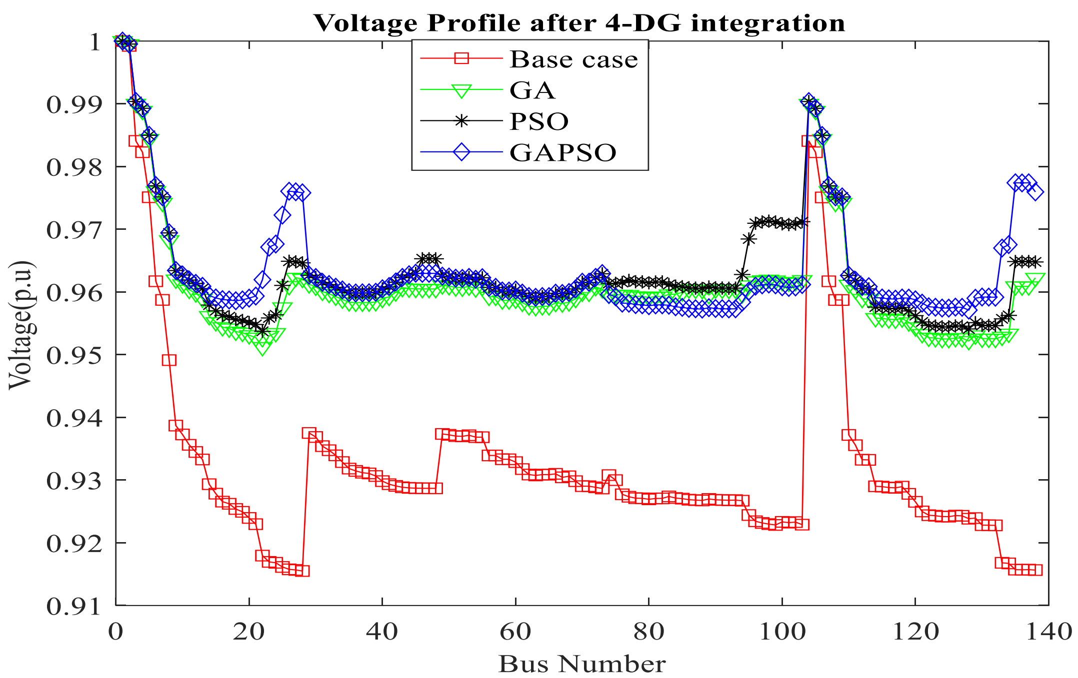

Figure 4.9: Voltage profile of the base case and after 4-DG integration with different algorithms

As shown in Table 4.8, the percentages of active and reactive power loss reduction and MOF are 58.724%, 62.469, and 0.02082 for GA-PSO, 60.415%, 62.242% and 0.02359 for GA, 57.909%, 62.722% and 0.02270 for PSO respectively. The simulation result shows that the proposed hybrid GA-PSO method has better performance in terms of reducing total active and reactive power losses, improving the voltage profile of buses, and has better MOF value than GA and PSO algorithms. The convergence curve for all cases in a given number of iterations obtained during the optimization of multi-objective functions using different algorithms is shown in Figure 4.10.

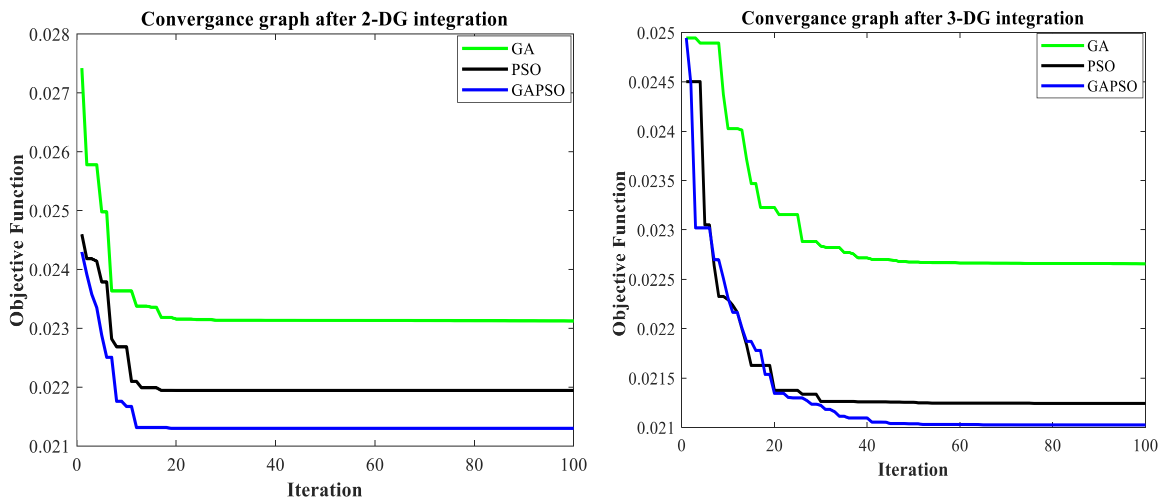

(a) Convergence curve after 2-DG

(b) Convergence curve after 3-DG

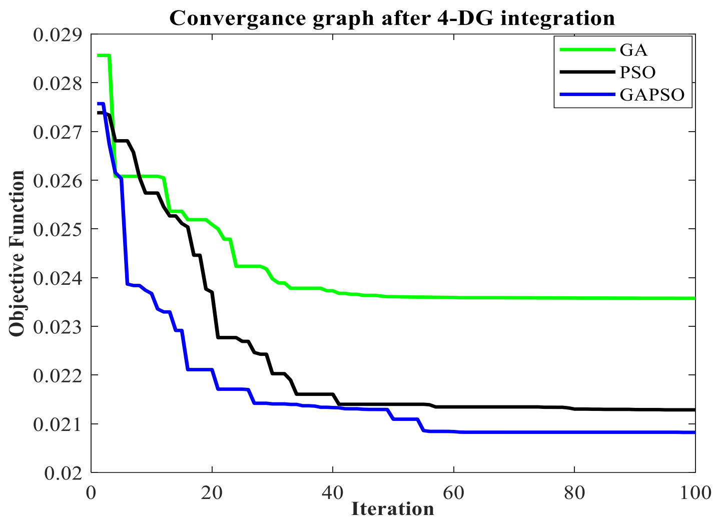

(c) Convergence curve after 4-DG

Figure 4.10: Convergence curve for all cases using different algorithms

As shown from the convergence graph of Figure 4.10, the convergence rate depends on the number of decision variables of the objective function, i.e. DG location and its size. For 2-DG case, it converged rapidly but for 3-DG and 4-DG cases it converged slowly since the number of decision variables are increased. Generally, almost in all cases, the performance of the proposed algorithm is better compared to other two algorithms in terms of minimizing the multi-objective functions (MOF).

4.3 Economic Impact of Integrating DG to the System

After determining the optimal location and size of DG at the selected distribution feeder, the cost it needs for implementation is the next step. As shown from the simulation results, the objective function value for case 3 and case 4 have very small differences. Hence, due to the economic point of view integration of 3-DG is the best optimal option from the second scenario and economic impact of DG integration is carried out for integration of 3-DG. The cost analysis started by finding the total annual energy lost before the integration of DG.

Annual energy loss of Kombolcha-I substation feeder three before DG installation can be calculated as follows;

Annual energy loss before DG installation

= Ploss*8760 hrs.

= 400.9144 kW*8760 hrs.

= 3,512,010.144 kWhr.

Based on the new power tariff's ETB/kWh energy rates for Ethiopian Electric Utility, the financial loss assessment is made. According to the most recent Ethiopian Electric Utility tariff, the average of the first block and general rate is 1.1985 birr/kWh as shown in Appendix-D. Therefore, the annual cost of energy loss of the feeder at base case can be calculated as follows;

Cost of energy loss before DG installation

= Annual energy loss*Cost of energy (E.c)

= 3,512,010.144 kWhr.*1.1985 Birr/kWhr.

= 4,209,144.158 Birr

From the simulation result integrating 3-DG gives better performance than others. After integrating 3-DG in the selected distribution feeder, the active power loss found on the feeder becomes 165.484 kW.

Energy loss of Kombolcha-I substation feeder three after DG installation can be found as;

Annual energy loss reduction after DG installation

= Ploss reduction*8760 hrs.

= (400.9144 -165.484) kW*8760 hrs.

= 235.4304 kW*8760 hrs.

= 2,062,370.304 kWhr.

Cost of energy loss reduction after DG installation

= Eloss reduction * E.c

= 2,062,370.304 kWhr. *1.1985 Birr/ kWhr.

= 2,471,750.809344 Birr

After the installation of DG through Kombolcha-I substation feeder three the annual energy loss cost is reduced from 4,209,144.158 birr to 1,737,393.347 birr per year. This implies that 2,471,750.809344 birr per year can be saved when integrated 3-DG on the feeder. The total installation cost of solar PV-DG varies from time to time, but its rate is decreasing. Depending on the technology and company, the installation cost will vary. Since the end of 2009, the cost of a solar PV module has dropped sharply, reaching between $0.52 and $0.72 per watt in 2015. Costs associated with the balance of the system (BoS) have decreased concurrently. The global weighted average total installed costs of utility-scale solar PV plants decreased by 62% between 2009 and 2015 as a result of falling prices for solar PV modules and the rest of the system. Utility-scale solar PV plant systems might see a 57% drop in cost over ten years, from an average total installed cost of USD 1.8/watt in 2015 to USD 0.8/watt in 2025 (Taylor & So, 2016). Therefore, based on this reference we can calculate the cost of utility-scale solar PV DG in 2023 G.C as follows;

PV DG cost in 2023 ($/W) = (1.8-8/10*57/100*1.8) =0.9792$/W=0.98$/W.

The investment cost of DG is calculated as follows;

The investment cost of PV-DG = DG generated power * cost in dollar/watt

= 3874 kW*0.98$/watt

= 3,796,520 USD

So, the investment cost of solar-based DG in this research work is 3,796,520 USD. Based on the exchange rate of the Commercial Bank of Ethiopia (CBE) on 2-June-2023, (1$ = 54.34 Birr). Therefore, the total investment cost in birr equals 206,302,896.8 birr.

Once the total investment cost of solar PV-DG has been determined, evaluating the economic feasibility of DG integration involves calculating the payback period for the invested finance. The payback period represents the length of time required for the investment cost to be recovered. It is calculated as the ratio of the DG investment cost to the net annual return. The net annual return includes the cost savings from losses and the cost of energy supplied by the DG system (Mithulananthan et al., 2017). Assessing the payback period provides valuable insights into the economic viability of DG integration.

The cost of supplied energy by DG = 3874 kW *8760 hrs* 1.1985 Birr/ kWhr.

= 40,672,583.64 Birr

$$\text{Payback period(yr.)} = \frac{\text{Net investment}}{\text{Net annual return}}$$

$$= \frac{\text{Investment cost of DG}}{\text{Saved energy loss cost} + \text{cost of energy supplied by DG}}$$

$$= \frac{206{,}302{,}896.8}{2{,}471{,}750.809344 + 40{,}672{,}583.64}$$

$$= \frac{206{,}302{,}896.8}{43{,}144{,}334.4493} = 4.782 \text{ years}$$

CHAPTER FIVE

5. CONCLUSION, RECOMMENDATION, AND FUTURE WORK

5.1 Conclusion

In conclusion, this study demonstrated the development and application of a hybrid genetic algorithm and particle swarm optimization (GA-PSO) method to minimize power losses and improve the voltage profile in a power system by optimizing the location and size of multi-type DG(s). A backward/forward sweep load flow method was applied to find bus voltage, active and reactive power loss. A multi-objective function comprising total active power loss, reactive power loss, and cumulative voltage devotion improvement was formulated for the optimization algorithms.

The base case simulation results indicate that the selected feeder has a total active power loss of 400.9914 kW and 404.8816 kVAr reactive power loss. And also, most of the bus voltages magnitude are out of the acceptable range (0.95p.u-1. 05p.u). The simulation results were analyzed by considering two scenarios which are the base case or existing system and after DG integration. After integrating multiple DG in the system, the total active and reactive power loss was reduced and the voltage magnitude of all abuse was within the acceptable standard limits. From the simulation results percentage reduction in real power loss was 45.944%, 51.0277%, 58.7234%, and 58.8331%, while the percentage reactive power loss reduced was 52.267%, 59.279%, 62.9945%, and 62.4686% for 1-DG,2-DG,3-DG and 4-DG installation respectively. And also, base case minimum voltage was improved from 0.9155p.u to 0.95016p.u, 0.95341p.u, 0.95489p.u and 0.9571p.u. For all cases, the bus voltage of the system becomes within the acceptable range, i.e., between 0.95p.u to 1.05p.u.

Furthermore, a comparison analysis has also been performed to investigate the effectiveness of the proposed hybrid GA-PSO algorithm with other algorithms. The results obtained from the comparison indicate that in almost all cases the hybrid GA-PSO method gives a better system performance by minimizing total system power loss, voltage profile improvement, and better fitness values. Finally, a cost analysis has been done to determine the economic feasibility of the solution since, cost analysis is the necessary point while creating a solution to a problem. From scenario-II, case three (integrating 3-DG) at bus 26,72, and 98 with 1291 kW size for each bus was the best one in terms of reducing system power loss, and improving the voltage profile of the system as seen from the simulation results considering the technical and economic points of view. In this, cost-benefit analysis of the generated solution has been performed. The cost analysis showed that integration of 3-DG in the system needs an initial capital cost of 206,302,896.8 birr with a payback period of 4.782 years.

Thus, the objectives of the thesis work were achieved successfully and the implemented hybrid GA-PSO method was proved to be a better method for optimizing the location and size of multi-type DGs in power distribution networks with the aim of reducing both real and reactive power losses and improving network voltage profiles.

5.2 Recommendation

Different parties benefit directly and indirectly from this study endeavor. This research work will help EEU in reducing both active and reactive power losses in their networks and improve the voltage level at customers to the required limits. Therefore, based on the finding of this research, it is recommended to use DG to enhance the voltage profile and minimize power losses. Workers at Kombolcha-I substation and Kombolcha utilities have little experience in recording performance data for outgoing feeders and the data required for the researcher. Therefore, I recommended EEP/EEU to strengthen its data-gathering and documentation processes.

5.3 Future Work

Some of the future works are suggested as follows:

- This thesis work was only conducted on Kombolcha-I substation feeder (L3) lines, future works can use the same analysis to the remaining feeders.
- The effects of DG on the system short circuit level and harmonic distortion could be the subject of future research studies.
- Phase balance loading conditions were considered in this thesis work to meet the goal, but phase imbalance was not studied. Phase load imbalance would be attributed to the upcoming work.
- After programming the code in MATLAB 2021a software, a long iteration time was noted and hence a novel work is required to reduce this simulation time.
- The multi-objective function can be improved by taking into consideration other power system parameters like stability issues.

Research Fund Acknowledgment

This research thesis was funded by Adama Science and Technology University under the grant number ASTU/SM-R/733/23, Adama, Ethiopia.

REFERENCES

Abdulla,K., Mamun, A., Hossan, A., Arafat, Y., & Ahmed, S. (2015). *Feasibility Assessment of Wind Energy Prospect In Bangladesh And A Proposal of 2MW Wind Power Plant At ' Parky Saikat , Chittagong .'* 76–79.

Alam, A., Gupta, A., Bindal, P., Siddiqui, A., & Zaid, M. (2018). Distribution System with Distributed Generation Alam. *2018 International Conference on Power, Energy, Control and Transmission Systems (ICPECTS)*, 21–25.

Alemante, A. (2017). *Optimal Capacitor Placement on Primary Distrbution System for Loss Minimization Using Artificial Intelligent Techniques: Case study on Adama Town Distrbution System*. ASTU.

Alemu, A. (2020). *Voltage profile improvement and power loss minimization using Static Var Compensator (SVC) in Bahirdar Distribution system*.

Ankaliki,S.G.,Engineering,E.,Ananthapadmanabha,T.,&Engineer,E.(2021). *APPLICATION OF HYBRID TECHNIQUES FOR OPTIMAL POSITION AND SIZING OFDISTRIBUTEDGENERATIONUNITSIN*.*12*(2),90–99. https://doi.org/10.34218/IJEET.12.2.2021.009

Arefifar, S. A., Mohamed, Y. A.-R. I., & El-Fouly, T. (2014). Optimized multiple microgrid-based clustering of active distribution systems considering communication and control requirements. *IEEE Transactions on Industrial Electronics*, *62*(2), 711–723.

Avchat, H. S.,& Mhetre,S. (2020). Optimal placement of distributed generation in distribution network using particle swarm optimization. *2020 International Conference forEmergingTechnology,INCET2020*,*7*(11),1513–1522. https://doi.org/10.1109/INCET49848.2020.9154091

Chandel, P. (2016). *Energy Meter Tampering : Major Cause of Non- Technical Losses in Indian Distribution Sector*. 368–371.

Chatbordin, N., & Kulyos, A. (2013). Dependable capacity evaluation of wind power and solar power generation systems. *ECTI-CON, 10th International Conference*.

Chen, T. H., Chiang, L. S., & Yang, N. C. (2012). Examination of major factors affecting voltage variation on distribution feeders. *Energy and Buildings*, *55*, 494–499. https://doi.org/10.1016/j.enbuild.2012.08.021

Danishmal, M., Sarwari, D. M., & Serat, Z. (2022). *Investigation of Voltage Drop in the Primary Distribution Network of Ghazni City and Voltage Regulation in That Network 5. Adverse Effects of Excessive Voltage Deviation of High Voltage Consumers*

DifferentPartsoftheDistribution.*7*(3),39–45. https://doi.org/10.11648/j.es.20220703.11

Del Valle, Y., Venayagamoorthy, G. K., Mohagheghi, S., Hernandez, J.-C., & Harley, R. G. (2008). Particle swarm optimization: basic concepts, variants and applications in power systems. *IEEE Transactions on Evolutionary Computation*, *12*(2), 171–195.

Devi, S., & Geethanjali, M. (2014). Electrical Power and Energy Systems Optimal location and sizing determination of Distributed Generation and DSTATCOM using Particle Swarm Optimization algorithm. *INTERNATIONAL JOURNAL OF ELECTRICAL POWERANDENERGYSYSTEMS*,*62*,562–570. https://doi.org/10.1016/j.ijepes.2014.05.015

Esmaeilian, H. R., & Fadaeinedjad, R. (2014). Energy loss minimization in distribution systems utilizing an enhanced reconfiguration method integrating distributed generation. *IEEE Systems Journal*, *9*(4), 1430–1439.

Et. al., N. K. (2021). Optimal siting and sizing of multiple type DGs for the performance enhancement of Distribution System using Differential Evolution Algorithm. *Turkish Journal of Computer and Mathematics Education (TURCOMAT)*, *12*(2), 1140–1146. https://doi.org/10.17762/turcomat.v12i2.1135

Gallego, L. A., Member, S., Rider, M. J., Romero, R., & Garcia, A. V. (2009). *A Specialized Genetic Algorithm to Solve the Short Term Transmission Network Expansion Planning*. *5*, 1–7.

Gana, N. N., & Akpootu, D. O. (2013). Estimation of global solar radiation using four sunshine-based models in Kebbi, North-Western, Nigeria. *Pelagia Research Library Advances in Applied Science Research*, *4*(5), 409–421.

Ganguly, S., & Samajpati, D. (2017). Distributed generation allocation with on-load tap changer on radial distribution networks using adaptive genetic algorithm. *Applied Soft Computing*, *59*, 45–67.

Hailemariam,A.(2020).*POWER FLOW CONTROL AND BUS VOLTAGE ENHANCEMENT OF POWER TRANSMISSION SYSTEM USING UNIFIED POWER FLOW CONTROLLER (UPFC*.

Hammerschmitt, B. K., Affonso, J., Agnol, D., & Rigodanzo, J. (2020). *Non-Technical Losses Review and Possible Methodology Solutions*. 64–68.

Hassanat, A., Almohammadi, K., Alkafaween, E., & Abunawas, E. (2019). *Choosing Mutation and Crossover Ratios for Genetic Algorithms — A Review with a New Dynamic Approach*. https://doi.org/10.3390/info10120390

Hassanat, A., Almohammadi, K., Alkafaween, E., Abunawas, E., Hammouri, A., & Prasath,

V. B. S. (2019). Choosing mutation and crossover ratios for genetic algorithms—a review with a new dynamic approach. *Information*, *10*(12), 390.

Hussain, I., Khan, F., Ahmad, I., Khan, S., & Saeed, M. (2021). Power Loss Reduction via Distributed Generation System Injected in a Radial Feeder. *Mehran University ResearchJournalofEngineeringandTechnology*,*40*(1),160–168. https://doi.org/10.22581/muet1982.2101.15

Irfan, M., Ashraf, S., & Imtiaz, A. R. (2018). Sizing and siting of types I-IV DG Units using Chaos-assisted Gravitational search algorithm. *International Journal of Renewable Energy Research*, *8*(3), 1631–1640. https://doi.org/10.20508/ijrer.v8i3.8005.g7464

Jain, A., Gupta, A. R., & Kumar, A. (2014). *An Efficient Method for D-STATCOM Placement in Radial Distribution System*.

Juanuwattanakul, P., & Masoum, M. A. S. (2012). Increasing distributed generation penetration in multiphase distribution networks considering grid losses, maximum loading factor and bus voltage limits. *IET Generation, Transmission & Distribution*, *6*(12), 1262–1271.

Kalambe, S., & Agnihotri, G. (2014). Loss minimization techniques used in distribution network : bibliographical survey. *Renewable and Sustainable Energy Reviews, 29,* 184–200. https://doi.org/10.1016/j.rser.2013.08.075

Kalantari, M. (2011). *Placement of Distributed Generation unit and Capacitor Allocation in Distribution Systems using Genetic Algorithm*. *2*, 2–6.

Kanojia, S. S., & Rajyaguru, S. (2019). *Reactive Power Compensation for LV Distribution Network*. *6*, 1734–1741.

Kashyap, M., Kansal, S., & Kansal, R. (2018). *DGs IN RADIAL DISTRIBUTION SYSTEM*. *9*(3), 192–198.

Keoliya, J. A., & Vaidya, P. G. A. (2013). *Estimation Of Technical Losses In A Distribution System*. *2*(6), 2621–2626.

Khanday, M. A., & Malviya, R. (2019). *Optimal Placement and Sizing of STATCOM using PSO*. 1423–1428.

Khetrapal, P., Pathan, J., & Shrivastava, S. (2020). Power loss minimization in radial distribution systems with simultaneous placement and sizing of different types of distribution generation units using improved artificial bee colony algorithm. *International Journal on Electrical Engineering and Informatics*, *12*(3), 686–707. https://doi.org/10.15676/ijeei.2020.12.3.15

Khushalani, S., Member, S., Schulz, N., & Member, S. (2006). *Unbalanced Distribution*

PowerFlowwithDistributedGeneration.*June*. https://doi.org/10.1109/TDC.2006.1668508

Khushalani, & Schulz. (2006). Unbalanced distribution power flow with distributed generation. *2005/2006 IEEE/PES Transmission and Distribution Conference and Exhibition*, 301–306.

Kilonzi, J. C., & Odero, N. A. (2013). *A GA/IPSO based approach for System loss reduction and Voltage profile improvement Employing arithmetic Crossover and mutation.*

Kumar, B. (2020). *Optimal Distribution Network Reconfiguration to Improve the System Performances using PSO with*.

Kyule, M. M. (2020). *Improving the Voltage Stability of a Distribution System With Renewable Distributed Generation Using a Three Method Hybrid.* university of Nairobi.

Lalitha, M. P., & Reddy, N. S. (2011). *A Two Stage Methodology for Siting and Sizing of DG for Minimum Loss in Radial Distribution System using RCGA*. *25*(2), 10–16.

Leite, J. B., & Mantovani, J. R. S. (2016). *Detecting and Locating Non-technical Losses in ModernDistributionNetworks*.*3053*(c),1–11. https://doi.org/10.1109/TSG.2016.2574714

Maduforo, P. C., Emechebe, J. N., Eronu, E. M., & Benson, S. A. (2020). Sensitivity Based Approach for the Optimal Sizing and Allocation of Distributed Generation in a Radial Network. *European Journal of Engineering Research and Science*, *5*(6), 751–756. https://doi.org/10.24018/ejers.2020.5.6.1978

Mandefro, E. (2020). *PERFORMANCE ENHANCEMENT OF DISTRIBUTION SYSTEM USING OPTIMALLY ALLOCATED DISTRIBUTED GENERATION : - A CASE STUDY ON BAHIR DAR POWER DISTRIBU*.

Mandefro, E., & Bantiyrga, B. (2020). Optimal allocation of distributed generation for performance enhancement of distribution system using particle swarm optimization. In *Lecture Notes of the Institute for Computer Sciences, Social-Informatics and Telecommunications Engineering, LNICST: Vol. 308 LNICST*. Springer International Publishing. https://doi.org/10.1007/978-3-030-43690-2_30

Marneni, A., Kulkarni, A. D., & Ananthapadmanabha, T. (2015). Loss Reduction and Voltage Profile Improvement in a Rural Distribution Feeder using Solar Photovoltaic Generation and Rural Distribution Feeder Optimization using HOMER Abstract : *Procedia Technology*, *21*, 507–513. https://doi.org/10.1016/j.protcy.2015.10.036

Matos, S. P. S., Vargas, M. C., Fracalossi, L. G. V, Encarnação, L. F., & Batista, O. E.

(2021). Protection philosophy for distribution grids with high penetration of distributed generation☆. *Electric Power Systems Research*, *196*, 107203.

Messinis, G. M., & Hatziargyriou, N. D. (2018). *Review of non-technical loss detection methods*. *158*, 250–266.

Mithulananthan, N., Hung, D. Q., & Lee, K. Y. (2017). *Intelligent network integration of distributed renewable generation*. Springer.

Mohammadi, M., Nasab, M. A., & Branch, A. (2011). *PSO Based Multiobjective Approach for Optimal Sizing and Placement of Distributed Generation*. *2*(8), 832–837.

Ms. Rekha C M, D. S. C. B. (2022). Optimal Placement of Pso Based Photovoltaic (Pv) Distributed Generation (Dg) in a Distribution System. *Journal of Tianjin University Science and Technology*, *55*(03), 294–309. https://doi.org/10.17605/OSF.IO/PXAY4

Muhammad, M. A., Mokhlis, H., Naidu, K., Amin, A., Franco, J. F., & Othman, M. (2020). Distribution Network Planning Enhancement via Network Reconfiguration and DG Integration Using Dataset Approach and Water Cycle Algorithm. *Journal of Modern PowerSystemsandCleanEnergy*,*8*(1),86–93. https://doi.org/10.35833/MPCE.2018.000503

Muzathik, A. M. M., Nik, W. B. ., Ibrahim, K. ., Samo, K., Sopian, K., & Alghoul, M. . (2011). *DAILY GLOBAL SOLAR RADIATION ESTIMATE BASED ON SUNSHINE HOURS*. *6*(1), 75–80.

Niazi, G., & Lalwani, M. (2017a). PSO based optimal distributed generation placement and sizing in power distribution networks: A comprehensive review. *2017 International Conference on Computer, Communications and Electronics, COMPTELIX 2017*, *1*, 305–311. https://doi.org/10.1109/COMPTELIX.2017.8003984

Niazi, G., & Lalwani, M. (2017b). PSO based optimal distributed generation placement and sizing in power distribution networks: A comprehensive review. *2017 International Conference on Computer, Communications and Electronics (Comptelix)*, 305–311.

Ntombela, M., Musasa, K., & Leoaneka, M. C. (2022). Power Loss Minimization and Voltage Profile Improvement by System Reconfiguration, DG Sizing, and Placement. *Computation*, *10*(10). https://doi.org/10.3390/computation10100180

Ouali, S., & Cherkaoui, A. (2020). *An Improved Backward / Forward Sweep Power Flow Method Based on a New Network Information Organization for Radial*. *2020*.

Pandey, A. K., & Kirmani, S. (2019). *Multi-Objective Optimal Location and Sizing of Hybrid Photovoltaic System in Distribution Systems Using Crow Search Algorithm*. *9*(4).

Podder, S., Khan, R. S., Mohon, S. M. A. A., Hussain, M. J., & Basher, E. (2014). Solar radiation approximation using sunshine hour at patenga, Bangladesh. *8th International Conference on Electrical and Computer Engineering*, 321–324.

Prakash, D. B., & Lakshminarayana, C. (2018). *Multiple DG placements in radial distribution system for multi objectives using Whale Optimization Algorithm*. 2797–2806.

Rajalakshmi, J., & Durairaj, S. (2016). Review on optimal distributed generation placement using particle swarm optimization algorithms. *1st International Conference on Emerging Trends in Engineering, Technology and Science, ICETETS 2016 - Proceedings*. https://doi.org/10.1109/ICETETS.2016.7603088

Rani, B. J., & Reddy, A. S. (2019). Optimal allocation of dg using hybrid optimization technique for minimizing the power loss. *International Journal of Recent Technology and Engineering*, *7*(6), 1583–1591.

Rao, R. S., Ravindra, K., Satish, K., & Narasimham, S. V. L. (2013). *Power Loss Minimization in Distribution System Using Network Recon fi guration in the Presence of Distributed Generation*. *28*(1), 317–325.

Ray, R., & Gupta, A. R. (2022). *Power loss minimization and voltage profile improvement of radial and mesh distribution network using sine cosine optimization based DG allocation*. *14*(3), 64–73. https://doi.org/10.4314/ijest.v14i3.8S

Resen, A. K., Khamees, A. B., & Yaseen, S. F. (2020). Determination of wind shear coefficients and conditions of atmospheric stability for three Iraqi sites. *IOP Conference Series: Materials Science and Engineering*, *881*(1), 12161.

Rupa, J. A. M., & Ganesh, S. (2014). *Power Flow Analysis for Radial Distribution System Using Backward / Forward Sweep Method*. *8*(10), 1628–1632.

S, G. N., Khatod, D. K., & Sharma, M. P. (2016). *Distribution Network Power Loss Minimizationby Optimal DG Allocation*. *11*(5), 163–170. https://doi.org/10.9790/1676-110502163170

Saeidi, D., Mirhosseini, M., Sedaghat, A., & Mostafaeipour, A. (2011). Feasibility study of wind energy potential in two provinces of Iran : North and South Khorasan. *Renewable andSustainableEnergyReviews*,*15*(8),3558–3569. https://doi.org/10.1016/j.rser.2011.05.011

Salman, M., Hongsheng, S., Aman, M. A., & Khan, Y. (2022). Enhancing Voltage Profile and Power Loss Reduction Considering Distributed Generation (DG) Resources. *Engineering, Technology & Applied Science Research*, *12*(4), 8864–8871.

https://doi.org/10.48084/etasr.5046

Seet*, C. C., Pasupuleti, J., & Basir Khan, M. R. (2019). Optimal Placement and Sizing of Distributed Generation in Distribution System using Analytical Method. *International Journal of Recent Technology and Engineering (IJRTE)*, *8*(4), 6357–6363. https://doi.org/10.35940/ijrte.d5120.118419

Shaaban, M. F., & El-Saadany, E. F. (2012). Optimal allocation of renewable DG for reliability improvement and losses reduction. *IEEE Power and Energy Society General Meeting*, 1–8. https://doi.org/10.1109/PESGM.2012.6345054

Shivarudraswamy, R., Gaonkar, D. N., & Jayalakshmi, N. S. (2017). GA based optimal location and size of the distributed generators in distribution system for different load conditions. *1st IEEE International Conference on Power Electronics, Intelligent ControlandEnergySystems,ICPEICES2016*,2–5. https://doi.org/10.1109/ICPEICES.2016.7853256

Student, U. G., Medical, S., Medical, S., Sciences, T., Medical, S., & Sciences, T. (2018). *REVIEW ON OPTIMAL ALLOCATION OF DSTATCOM IN RADIAL*. *119*(16), 3207–3218.

Sultana, B., Mustafa, M. W., Sultana, U., & Rauf, A. (2016). Review on reliability improvement and power loss reduction in distribution system via network recon fi guration.*RenewableandSustainableEnergyReviews*,*66*,297–310. https://doi.org/10.1016/j.rser.2016.08.011

Talukder, S. (2011). *Mathematical Modelling and Applications of Particle Swarm Optimization*. *February*.

Taye, T. (2019). *Improvement of Distribution Feeder Loss and Voltage Profile (Case Study : Bella Substation Distribution Feeder)*.

Taylor, M., & So, E. Y. (2016). Solar PV in Africa: Costs and markets. *Bonn, Germany: IRENA*.

Thakur, R., & Chawla, P. (2015). *VOLTAGE DROP CALCULATIONS & DESIGN OF URBAN DISTRIBUTION FEEDERS*. 43–53.

Tizgui, I., Bouzahir, H., El Guezar, F., & Benaid, B. (2017). Wind speed extrapolation and wind power assessment at different heights. *2017 International Conference on Electrical and Information Technologies (ICEIT)*, 1–4.

Venugopal, D., & Jayalaxmi, A. (2015). *Optimal Placement of Facts Devices Using Particle Swarm Optimization Technique for the Increased Loadability of a Power System*. *10*(2), 20–26. https://doi.org/10.9790/1676-10232026

Verma, R., & Kashyap, M. (2021). DG Penetration in distribution networks: a review. *2021 7th International Conference on Advanced Computing and Communication Systems (ICACCS)*, *1*, 1144–1147.

Wang, D., Tan, D., & Liu, L. (2017). Particle swarm optimization algorithm : an overview. *Soft Computing*. https://doi.org/10.1007/s00500-016-2474-6

Werkie, Y. G., & Kefale, H. A. (2022). Optimal allocation of multiple distributed generation units in power distribution networks for voltage profile improvement and power losses minimization generation units in power distribution networks for voltage profile improvementandpower.*CogentEngineering*,*9*(1). https://doi.org/10.1080/23311916.2022.2091668

Yadav, A. K., & Chandel, S. S. (2015). Solar energy potential assessment of western Himalayan Indian state of Himachal Pradesh using J48 algorithm of WEKA in ANN-based prediction model. *Renewable Energy*, *75*, 675–693.

Yeh, T.-H., & Wang, L. (2008). A study on generator capacity for wind turbines under various tower heights and rated wind speeds using Weibull distribution. *IEEE Transactions on Energy Conversion*, *23*(2), 592–602.

Zaheer, E. J., Khan, D. M. I., & Hassan Jaskani, F. (2022). Optimization of Dg Unit Size and Placement in Radial Distribution Networks Using an Slfo-Bpso Hybrid Approach. *International Journal of Engineering Applied Sciences and Technology*, *6*(12), 20–31. https://doi.org/10.33564/ijeast.2022.v06i12.004

APPENDIXES

Appendix-A: Power Interruption Data for Kombolcha-I Substation 15 kV Feeders

Table Appendix-A: 2013 E.C and 2014 E.C Interruption

ETHIOPIAN ELECTRIC POWER CORPORATION

North Eastern Region Transmission Substation Operation and Maintenance Office

Substation Name: Kombolcha-I- 15 kV

Summarized Power Interruption Data for Kombolcha-I substation 15 kV Feeders in 2013 E.C and 2014 E.C

Summarized Power Interruption Data in 2013 E.C

Feeder Name	Voltage level (KV)	Frequency and duration	
		Total frequency (freq.int/yr.)	Total duration (Hours/yr.)
L1 (Kombolcha-II)	15	248	485.58547
L2 (Bati)	15	520	671.63715
L3 (Kombolcha-I)	15	627	982.2884
L4 (Harbu)	15	420	843.52323
L5 (BGI)	15	66	160.12144
L6 (Textile 1)	15	56	175.7005
L7 (Textile 2)	15	8	3.646
L8 (Industry Village)	15	100	197.9396

Summarized Power Interruption Data in 2014 E.C

Feeder Name	Voltage level (KV)	Frequency and duration	
		Total frequency (Freq.int/yr.)	Total duration (Hours/yr.)
L1 (Kombolcha-II)	15	201	353.12063
L2 (Bati)	15	520	987.83365
L3 (Kombolcha-I)	15	554	1212.2194
L4 (Harbu)	15	259	549.77993
L5 (BGI)	15	12	38.366966
L6 (Textile 1)	15	11	103.25026
L7 (Textile 2)	15	3	12.466667
L8 (Industry Village)	15	75	194.4671

Appendix-B: Single-Line Diagram of Kombolcha Feeder Three (Kombolcha-I)

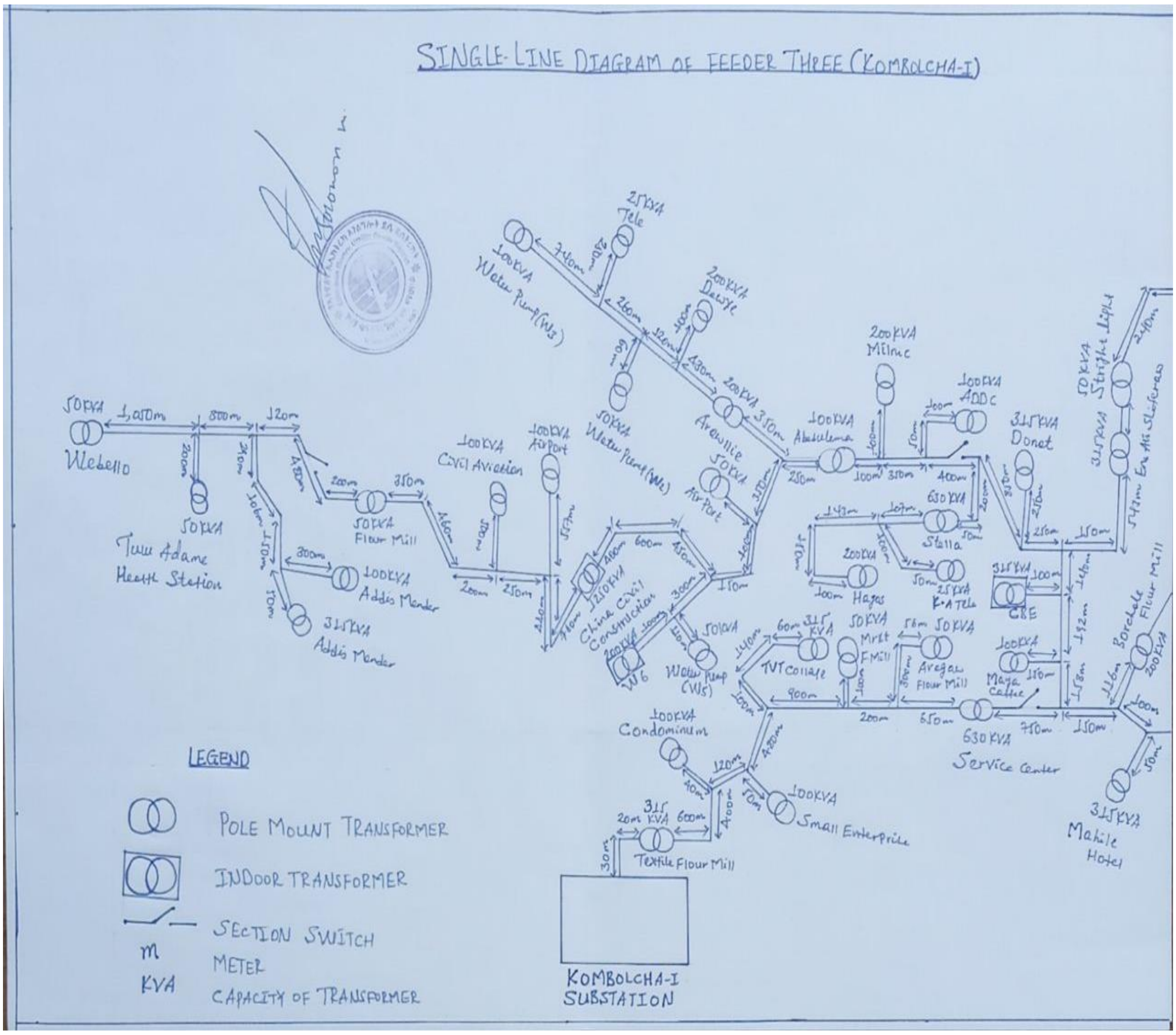

Cont…

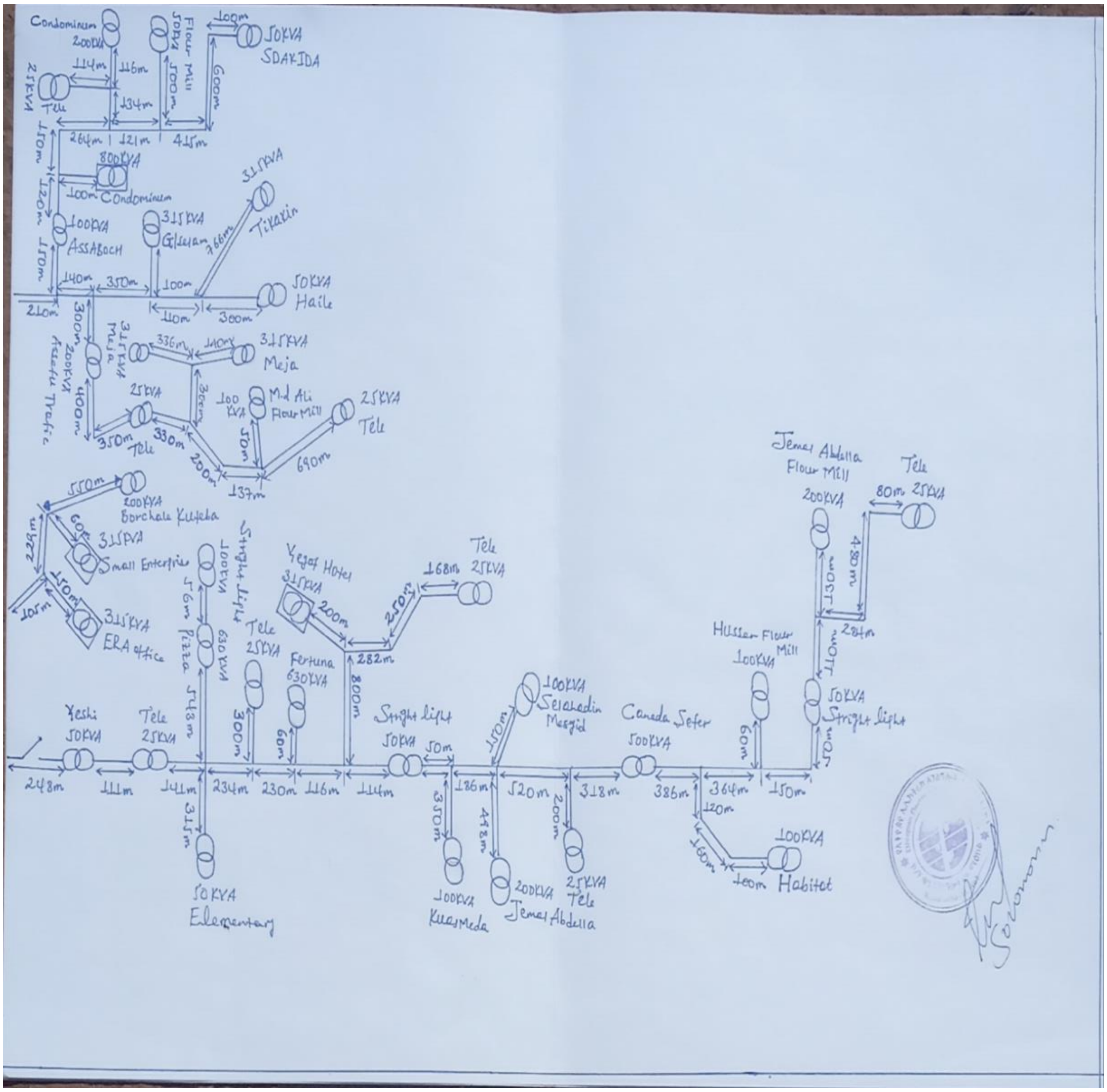

Appendix-C: Monthly Average Wind Speed(m/s) and Sunshine hour(hr.) of Kombolcha

at 2m above the ground

Average Monthely Wind run of kobolcha

month/year	2013	2014	2015	2016	2017	2018	2019	2020	2021	2022
jan	0.54	0.44	0.84	0.74	0.76	0.81	0.76	0.76	0.79	0.63
feb	0.66	0.44	0.88	0.86	0.82	0.79	0.93	0.77	0.78	0.74
mar	0.67	0.40	0.89	0.84	0.85	0.81	0.79	0.81	0.88	0.77
apr	0.64	0.45	0.99	0.76	0.83	0.72	0.68	0.75	0.87	0.79
may	0.52	0.36	0.85	0.75	0.68	0.81	0.79	0.68	0.74	0.82
jun	0.69	0.49	0.88	0.93	0.94	0.81	0.87	0.78	0.81	0.87
jul	0.48	0.47	0.92	0.80	0.95	0.76	0.82	0.71	0.73	0.51
aug	0.25	0.28	0.78	0.67	0.69	0.74	0.61	0.65	0.64	0.49
sep	0.23	0.22	0.62	0.58	0.59	0.59	0.61	0.57	0.55	0.46
oct	0.18	0.26	0.59	0.61	0.47	0.58	0.55	0.58	0.52	0.38
nov	0.28	0.50	0.59	0.66	0.58	0.59	0.60	0.67	xx	0.50
dec	0.35	0.69	0.69	1.18	0.81	0.67	0.65	0.72	0.61	0.56

Average Monthely Sunshine of kobolcha

month /year	2013	2014	2015	2016	2017	2018	2019	2020	2021	2022
jan	9.3	8.4	8.6	5.7	10.6	8.2	10.3	7.1	9.8	9.4
feb	9.8	6.7	9.7	9.1	7.3	8.4	9.0	7.9	7.6	9.1
mar	8.6	8.2	9.4	8.3	8.9	9.3	xx	7.6	10.2	xx
apr	8.5	8.4	10.1	6.3	9.4	xx	7.5	10.1	8.4	9.5
may	8.3	8.3	8.3	7.9	7.4	xx	8.6	8.7	7.6	10.0
jun	5.9	8.5	6.7	7.6	8.5	xx	7.8	7.1	6.8	10.4
jul	5.6	6.6	7.3	5.6	6.6	xx	6.4	4.2	3.6	4.8
aug	5.5	5.8	6.1	6.1	5.6	xx	4.7	1.2	4.9	4.5
sep	7.4	6.4	6.8	6.4	6.0	xx	5.2	xx	xx	6.2
oct	7.8	7.5	8.7	8.8	7.0	7.5	7.6	9.2	7.9	6.6
nov	8.5	8.4	8.0	9.1	8.5	7.6	7.3	9.1	xx	9.1
dec	9.7	9.3	6.5	9.2	8.2	9.2	7.9	9.2	xx	7.1

perepeared by, jemal alemu

signature

National Meteorological Agency

East Amhara Meteorological Service Center

Appendix-D: EEU Energy Tariff

Table Appendix-D: EEU Energy Tariff Amendment Study According to Consumer's Class

Tariff amendment	As of Dec. 18 onward	As of Dec. 19 onward	As of Dec. 20 onward	As of Dec. 21 onward
Tariff Category kWh /month	Birr/ kWh	Birr/ kWh	Birr/ kWh	Birr/ kWh
1. Residential tariff block				
1.1 1st block Up to 50 kWh	0.2730	0.2730	0.2730	0.2730
1.2 2nd block Up to 100 kWh	0.4591	0.5617	0.6644	0.7670
1.3 3rd block Up to 200 kWh	0.7807	1.0622	1.3436	1.6250
1.4 4th block Up to 300 kWh	0.9125	1.2750	1.6375	2.0000
1.5 5th block Up to 400 kWh	0.9750	1.3833	1.7917	2.2000
1.6 6th block Up to 500 kWh	1.0423	1.4965	1.9508	2.4050
1.7 7th block Above 500 kWh	1.1410	1.5877	2.0343	2.4810
2. General Tariff				
2.1 Flat Rate	1.0352	1.3982	1.7611	2.1240
3. Low Voltage Industry Tariff				
3.1 Flat Rate	0.8161	1.0544	1.2927	1.5310
3.2 Demand Charge rate	50.0000	100.00	150.0000	200.0000
4. Medium Voltage Industry Tariff 15kV & 33 kV				
4.1 Flat Rate	0.6047	0.8008	0.9969	1.1930
4.2 Demand Charge rate	36.8850	73.7700	110.6550	147.5400
5. High Voltage Industry Tariff Above 66 kV				
5.1 Flat Rate	0.5174	0.6540	0.7911	0.9280
5.2 Demand Charge rate	21.9100	43.8200	65.7300	87.6400
6. Street Light Tariff				
6.1 Flat Rate	1.0352	1.3982	1.7611	2.1240
7. Bulk Supply Tariff				
7.1 Demand Charge rate per kW	39.2908	78.5815	117.8723	157.1600
7.2 Generation Tariff. Monthly per kWh	0.2218	0.4435	0.6653	0.8870

Appendix-E: Power Loss for each Branch of Kombolcha Feeder Three at Base Case

Table Appendix-E: Base Case Active and Reactive Power Loss for each Branch

From bus	To bus	$P_{loss}(KW)$	$Q_{loss}(KVAr)$	From bus	To bus	$P_{loss}(KW)$	$Q_{loss}(KVAr)$
1	2	4.4482	4.6774	70	71	0.00057	0.00034
2	3	85.1071	89.4935	43	72	0.00014	8.41e-05
3	4	10.0728	10.5407	45	73	0.0060	0.0036
4	5	39.8896	41.9455	12	74	5.6196	3.3774
5	6	74.2289	78.0527	74	75	1.1639	0.6981
6	7	16.4275	17.2742	75	76	3.2517	1.94878
7	8	53.0205	55.8836	76	77	0.3051	0.18306
8	9	54.2889	57.0806	77	78	0.0435	0.0261
9	10	4.6944	4.9358	78	79	0.0016	0.00096
10	11	5.2938	5.5662	79	80	0.0087	0.0052
11	12	3.498	3.6782	78	81	0.0053	0.0032
12	13	2.127	2.2367	79	82	5.75e-05	3.5e-05
13	14	6.783	7.1098	76	83	0.221	0.13217
14	15	2.1167	2.226	83	84	0.15496	0.0929
15	16	1.7165	1.8043	84	85	0.0172	0.01035
16	17	0.4381	0.4607	85	86	0.0304	0.0182
17	18	1.0327	1.0860	86	87	0.0092	0.0055
18	19	0.5233	0.31393	87	88	0.0072	0.0043
19	20	1.14184	0.6845	84	89	0.0636	0.0357
20	21	1.1259	0.6754	86	90	0.0007	0.0004
21	22	4.9569	2.9725	90	91	0.0008	0.0005
22	23	0.2389	0.1433	90	92	0.00134	0.0008
23	24	0.0234	0.01406	87	93	2.18e-05	1.3e-05
24	25	0.08256	0.0262	77	94	0.3789	0.227
25	26	0.0339	0.01044	94	95	1.2777	0.4042
26	27	0.0059	0.0019	95	96	0.5453	0.1725
27	28	0.0052	0.0016	96	97	0.1181	0.0708
9	29	2.628	1.5768	97	98	0.0787	0.0472
29	30	1.1937	0.7160	98	99	0.0161	0.0097

30	31	2.4514	1.4704	96	100	0.0054	0.0017
31	32	1.0782	0.6467	100	101	0.0054	0.0017
32	33	1.357	0.8143	100	102	0.00027	8.7e-05
33	34	1.411	0.8465	98	103	0.0151	0.0091
34	35	1.3457	0.8227	3	104	0.0005	0.0003
35	36	0.3411	0.2045	4	105	5.2e-05	3.1e-05
36	37	0.2009	0.1205	5	106	0.00063	0.0004
37	38	0.0827	0.0493	6	107	7.12e-05	4.28e-05
38	39	0.2634	0.158	7	108	0.0002	0.00013
39	40	0.3633	0.2179	108	109	4.01e-05	2.4e-05
40	41	0.2148	0.12885	10	110	0.0112	0.0067
41	42	0.0561	0.0336	11	111	0.0119	0.0071
42	43	0.035	0.0212	13	112	0.0026	0.00156
43	44	0.0139	0.0083	112	113	0.0017	0.0010
44	45	0.0057	0.0035	14	114	0.1268	0.0761
45	46	0.0002	5.55e-05	114	115	0.0082	0.0049
46	47	2.93e-05	1.75e-05	115	116	0.0201	0.0121
47	48	1.58e-05	9.12e-06	116	117	0.0069	0.0042
29	49	0.062	0.0372	115	118	2.86e-05	1.72e-05
49	50	0.052	0.0312	15	119	0.0021	0.0012
50	51	0.05	0.03	16	120	0.0027	0.0016
51	52	0.0055	0.0033	18	121	0.1268	0.0761
50	53	0.0084	0.005	121	122	0.15	0.0475
51	54	0.0148	0.0089	122	123	0.01135	0.00359
30	55	0.00484	0.0029	123	124	0.0124	0.0039
33	56	0.0003	0.0002	124	125	9.84e-05	3.2e-05
56	57	0.0002	7.7e-05	122	126	0.0081	0.0025
33	58	0.2047	0.12283	123	127	0.00048	0.00015
58	59	0.00026	0.00015	124	128	0.0291	0.0092
34	60	5.67e-05	3.403e-05	20	129	0.00069	0.00042
35	61	0.03173	0.0186	21	130	0.0223	0.0135
36	62	0.1199	0.0719	130	131	0.00052	0.00031
62	63	0.0279	0.0167	130	132	0.004	0.00254

62	64	5.36e-05	3.213e-05	23	133	0.0109	0.006
64	65	7.94e-05	4.76e-05	24	134	0.0056	0.0034
38	66	0.0033	0.0019	26	135	0.0012	0.0007
39	67	0.024	0.0145	135	136	0.0006	0.0003
39	68	0.0027	0.0016	135	137	2.7e-28	1.6e-28
40	69	3.8e-05	2.28e-05	27	138	0.0004	0.0003
42	70	0.0013	0.00075				

Appendix-F: Voltage profile of all buses of Kombolcha Feeder Three at Base Case

Table Appendix-F: Base Case Voltage Profile for All Buses

Bus No.	Voltage Profile	Bus No.	Voltage Profile	Bus No.	Voltage profile	Bus No.	Voltage Profile
1	1	36	0.9315	71	0.9291	106	0.9751
2	0.9992	37	0.9312	72	0.9288	107	0.9617
3	0.9841	38	0.9310	73	0.9286	108	0.9587
4	0.9822	39	0.9306	74	0.9307	109	0.9587
5	0.9751	40	0.9298	75	0.9299	110	0.9371
6	0.9617	41	0.9293	76	0.9277	111	0.9355
7	0.9587	42	0.9291	77	0.9273	112	0.9332
8	0.9491	43	0.9288	78	0.9271	113	0.9332
9	0.9386	44	0.9287	79	0.9271	114	0.9290
10	0.9372	45	0.9287	80	0.9269	115	0.9289
11	0.9356	46	0.9286	81	0.9270	116	0.9288
12	0.9344	47	0.9286	82	0.9270	117	0.9287
13	0.9332	48	0.9286	83	0.9273	118	0.9289
14	0.92930	49	0.9373	84	0.9271	119	0.9278
15	0.9278	50	0.9372	85	0.9270	120	0.9265
16	0.9265	51	0.9370	86	0.9268	121	0.9249
17	0.9262	52	0.9369	87	0.9268	122	0.9244
18	0.9253	53	0.9371	88	0.9267	123	0.9243
19	0.9249	54	0.9368	89	0.9269	124	0.9241
20	0.9239	55	0.9368	90	0.9268	125	0.9241
21	0.9229	56	0.9339	91	0.9268	126	0.9243

22	0.9179	57	0.9339	92	0.9267	127	0.9243
23	0.9169	58	0.9333	93	0.9268	128	0.9238
24	0.9168	59	0.9333	94	0.9267	129	0.9239
25	0.9161	60	0.9328	95	0.9244	130	0.9228
26	0.91577	61	0.9317	96	0.9234	131	0.9228
27	0.9156	62	0.9308	97	0.9231	132	0.92277
28	0.9155	63	0.9307	98	0.9229	133	0.9168
29	0.9375	64	0.9308	99	0.9228	134	0.9167
30	0.9368	65	0.9308	100	0.9233	135	0.9157
31	0.9354	66	0.9309	101	0.9232	136	0.9156
32	0.9347	67	0.9304	102	0.9233	137	0.9157
33	0.9339	68	0.9306	103	0.9228	138	0.9156
34	0.9328	69	0.9298	104	0.9840		
35	0.9318	70	0.9290	105	0.9822		

Appendix-G: Sample MATLAB Code for the Research Work

Appendix-G1: MATLAB Program to Form BIBC Matrix

```
% This function used for the formation of the BIBC Matrix
function [bibc_matrix]=bibc_gen(linedata,busdata)
num_of_lines=length(linedata (:,2));
num_of_bus=length(busdata(:,1));
from_node=linedata(:,2);
to_node=linedata(:,3);
connect_matrix_lf=sparse(1:num_of_lines,from_node,ones(num_of_lines,1),
num_of_lines, num_of_bus);
connect_matrix_lt=sparse(1:num_of_lines, to_node, ones(num_of_lines, 1), num_of_lines,
num_of_bus) ;
connect_matrix_lt_lf=connect_matrix_lf+connect_matrix_lt;
connect_matrix_lt_lf1=connect_matrix_lt_lf'*connect_matrix_lt_lf;
connect_diag_mat=ones(num_of_bus)-eye(num_of_bus);% all element are one except
diagonal it is zero
connect_diag_mat1=connect_matrix_lt_lf1.*connect_diag_mat;
final_connect_mat=triu(connect_diag_mat1);
```

```
zero_matrix=zeros(num_of_bus);
zero_matrix1=zero_matrix(:,1); % columen matrix
for ind=1:num_of_bus
  node_order_val(:,ind)=sort([zero_matrix1(1:(num_of_bus-...
  length(graphtraverse(final_connect_mat,ind))));...
  graphtraverse(final_connect_mat,ind)']);
end
node_order_final=node_order_val;
for indr=1:length(node_order_final(1,:))
  for indc=1:length(node_order_final(1,:))
  order_node=node_order_final(indr,indc);
  if (order_node>0)
  bibc_matrix(order_node,indc)=1;
  bibc_matrix_ord(order_node,indc)=order_node
  if order_node==0
    bibc_matrix(indr,indc)=0;
    bibc_matrix_ord(indr,indc)=0;
  end
  end
  end
end
bibc_matrix_ord=bibc_matrix_ord;
```

Appendix-G2: MATLAB Program for Base Case Load Flow Algorithm

```
% This function is used to perform base case load flow
function finalres_out=without_DG()
tic
clc
clear
source_num=[1];
 LINEDATA=linedata_radial_bus(nbus);
 BUSDATA=busdata_radial_bus(nbus);
baseKV=15;baseMVA=100;
PBASE=baseMVA*1000;    % Change to KVA
ZBASE=(baseKV^2)/baseMVA;    % Base impedance
```

```
busdata_value=BUSDATA;linedata_value=LINEDATA;
linedata_value(:,4:5)=linedata_value(:,4:5)/ZBASE;   % per unit conversion
resistance_val=linedata_value(:,4);     % per unit resistance
reactance_val=linedata_value(:,5);     % per unit reactance
perunit_imped=complex(resistance_val,reactance_val);
busdata_value(:,2:3)=(busdata_value(:,2:3)/PBASE);  % Per unit conversion
imped_value=perunit_imped;
[bibc_matrix]=bibc_gen(linedata_value,busdata_value);  % calling bibc matrix
bibc_matrix(source_num,:)=[];
bibc_matrix(:,source_num)=[];
final_bibc_matrix=bibc_matrix';
% diag of column vector is happened
final_bcbv_matrix=final_bibc_matrix'*diag(perunit_imped);
final_dlf_matrix=final_bcbv_matrix*final_bibc_matrix;
complex_load_d=complex(busdata_value(:,2),busdata_value(:,3));  % complex power load
complex_load_g=zeros(size(busdata_value,1),1);
final_load_matrix=(complex_load_d-complex_load_g);   % ingected power Pi=Pd-Pg
final_load_matrix(length(source_num))=[];   % out of source node
initial_volt_value=ones(size(busdata_value,1)-length(source_num),1); % initial bus voltage
1.0 p.u
voltage_drop_value=initial_volt_value
% convergency with max iter
max_iter=100;
for ind_lop=1:max_iter
  %% backward sweep
  inject_current_data=conj(final_load_matrix./voltage_drop_value);   % injected current at
each bus
  IB=final_bibc_matrix*inject_current_data; %get the cumulative injected current flowing
through each branch
  old_volt=voltage_drop_value;
  volt_drop_each=final_dlf_matrix*inject_current_data;%Voltagedrop w.r.t. substation bus.
  voltage_drop_value=initial_volt_value-volt_drop_each;
  old_volt1=(old_volt);
  new_volt=(voltage_drop_value);
```

```
  % tolerance must definend
  error_volt_tolr=max(abs(old_volt1-new_volt));   %% must be defien max error
end
end
final_volt_data=[ones(length(source_num),1);voltage_drop_value];  % voltage profile
locvoltm=find(final_volt_data>1);   %if voltage is above 1 pu set as 1 pu
final_volt_data(locvoltm)=1;
from_node=linedata_value(:,2);
to_node=linedata_value(:,3);
for ind=1:length(from_node)
  %each branch voltage drop
  volt_diff_value(ind,:)=final_volt_data(from_node(ind))-final_volt_data(to_node(ind));
end
volt_diff_value1=abs(volt_diff_value); % magnitude of voltage drop for each branch
%% Loss calculation
ploss=((volt_diff_value1.^2).*resistance_val)./(abs(imped_value).*abs(imped_value))*10^
5; % Each Line Loss in kWs
loc1=find(~(isnan(ploss)));
qloss=((volt_diff_value1.^2).*reactance_val)./(abs(imped_value).*abs(imped_value))*10^
5; % Each Line Loss in kVAr
loc2=find(~(isnan(qloss)));
%apparent power of the branch
Br_power(:,1)=volt_diff_value(:,1).*conj(IB);
total_lossp=sum(ploss(loc1));
total_lossq=sum(qloss(loc2));
final_voltage=abs(final_volt_data); %
CVD=sum((1-final_voltage(:,1)).^2);
%% consruct the cell arrays
finalres_out{1}=total_lossp;
finalres_out{2}=total_lossq;
finalres_out{3}=final_voltage;
finalres_out{4}=ploss;
finalres_out{5}= CVD;
finalres_out{6}= qloss;
```

```
figure
plot(finalres_out{3},'rd-')
legend('Base Case/Without DG');
title('Voltage profile of Kombolcha feeder three at base case')
xlabel('Bus Number');
ylabel('Voltage (P.u)');
figure
plot(finalres_out{4},'rd-');
legend('Base Case/Without DG');
title('Active power loss');
xlabel('Bus Number');
ylabel('Active power (kW)');
figure
plot(finalres_out{4},'rd-');
legend('Base Case/Without DG');
title('Reactive power loss');
xlabel('Bus Number');
ylabel('Reactive power (kVAr)');
toc
 end
```

Appendix-G3: MATLAB Program for Load Flow Algorithm with DG Integration

```
% This function is used to perform load flow with DG
function finalres=Load_flow2(DG,Num_DG,Type_DG)
voltage_minimum=0.95;  % Minimum voltage deviation limit
voltage_maximum=1.05;  % Maximium voltage deviation limit
 current_maximum=2.834e-2% AAC 50mm2 temp 45 0c is 189A and base current 6.67kA
% % current_maximum = 189/6670; to convert current in to per unit
 dg_place=DG;
source_num=[1];
LINEDATA=linedata_radial_bus(nbus);
 BUSDATA=busdata_radial_bus(nbus);
baseKV=15;baseMVA=100;
PBASE=baseMVA*1000;VBASE=(baseKV^2)/baseMVA;
busdata_value=BUSDATA;linedata_value=LINEDATA;
```

```
linedata_value(:,4:5)=linedata_value(:,4:5)/VBASE;
resistance_val=linedata_value(:,4);
reactance_val=linedata_value(:,5);
actual_imped=complex(resistance_val,reactance_val);
busdata_value(:,2:3)=(busdata_value(:,2:3)/PBASE);
imped_value=actual_imped;
[bibc_matrix]=bibc_gen(linedata_value,busdata_value);
bibc_matrix(source_num,:)=[];
bibc_matrix(:,source_num)=[];
final_bibc_matrix=bibc_matrix';
final_bcbv_matrix=final_bibc_matrix'*diag(actual_imped);
final_dlf_matrix=final_bcbv_matrix*final_bibc_matrix;
complex_load_d=complex(busdata_value(:,2),busdata_value(:,3));% complex power load
complex_load_g=zeros(size(busdata_value,1),1);
%% DG location and size for example DG=2 dgplace=[L1 L2 S1 S2]
for ind=1:length(loc_value)
complex_load_g(loc_value(ind))=complex(PG/PBASE,QG/PBASE);
end
final_load_matrix=(complex_load_d-complex_load_g);
initial_volt_value=ones(size(busdata_value,1)-length(source_num),1);% initial bus voltage
voltage_drop_value=initial_volt_value;
max_iter=100;
 % error_volt_tolr
for ind_lop=1:max_iter
  %backward sweep
  inject_current_data=conj(final_load_matrix./voltage_drop_value); % injected current at each bus
  IB=final_bibc_matrix*inject_current_data; %get the cumulative injected current flowing through each branch
  old_volt=voltage_drop_value;
  volt_drop_each=final_dlf_matrix*inject_current_data; %voltage drops along each branch.
  voltage_drop_value=initial_volt_value-volt_drop_each;
  old_volt1=(old_volt);
  new_volt=(voltage_drop_value);
```

```
  error_volt_tolr=max(abs(old_volt1-new_volt));
end
final_volt_data=[ones(length(source_num),1);voltage_drop_value];
rvolt=real(final_volt_data);ivolt=imag(final_volt_data);
%% Voltage constraint
final_volt_data=complex(rvolt,ivolt);
from_node=linedata_value(:,2);
to_node=linedata_value(:,3);
for ind=1:length(from_node)
  volt_diff_value(ind,:)=final_volt_data(from_node(ind))-final_volt_data(to_node(ind));
end
volt_diff_value1=abs(volt_diff_value);
ploss=((volt_diff_value1.^2).*resistance_val)./(abs(imped_value).*abs(imped_value))*10^
5; % Each Line Loss in kWs
loc1=find(~(isnan(ploss)));
qloss=((volt_diff_value1.^2).*reactance_val)./(abs(imped_value).*abs(imped_value))*10^
5; % Each Line Loss in kVAr
loc2=find(~(isnan(qloss)));
P_loss=sum(ploss(loc1));Q_loss=sum(qloss(loc2));
finalvoltage=abs(final_volt_data);
CVD=sum((1-finalvoltage(:,1)).^2);
P_lossper=100*(400.9144-P_loss)/400.9144; % percentage active power reduction
Q_lossper=100*(404.8856-Q_loss)/404.8856; %percentage reactive power reduction
minvoltage=min(finalvoltage);  % minimum voltgae in P.u
maxVol_dev=max((1-finalvoltage)*100);  % maximum voltage deviation in percentage
f1=P_loss/PBASE;
f2=Q_loss/PBASE;
f3=CVD;
w1=0.8;
w2=0.1;
w3=0.1;
MOF=w1*f1+w2*f2+w3*f3;
finalres{1}=P_loss;
finalres{2}=Q_loss;
```

```
finalres{3}=finalvoltage;
finalres{4}=ploss;
finalres{5}=P_lossper;
finalres{6}=Q_lossper;
finalres{7}=minvoltage;
finalres{8}=maxVol_dev;
finalres{9}=MOF;
end
```

Appendix-G4: Main MATLAB Program to Call All Sub-Program

```
% This code is used to call all sub-program to determine optimal placements and size of DG
clc;
clear;
close all
tic
finalres_out=without_DG();  % Calling Base Case Load flow
%% Problem Definition
 Num_DG =1%input('Please Enter Number of DG [1 to 4]:')
 X= 3  %input('Enter the percentage value);
Type_DG=1;     %input ('please Enter the type of DG:-')
nVar=2*Num_DG;      % Number of Decision Variables
VarSize=[1 nVar];     % Size of Decision Variables Matrix
VarMin=[zeros(1,Num_DG) ones(1,Num_DG)]; % Lower Bound of Variables
VarMax = penetration(Num_DG,X);
MaxIt=100; % Maximum Number of Iterations
nPop=50;  % Population Size (Swarm Size)
VelMax=0.1*(VarMax-VarMin);
VelMin=-VelMax;
% PSO Parameters
wmax=0.9; %max inertia weight in w, wmax to control the balance b/n Gbest and Pbest
wmin=0.4; %min inertia weight in w, wmin to control the balance b/n Gbest and Pbest
c1=2.0; %Personal Learning Coefficient for accelerating the particle to reach the target
c2=2.0; %Global Learning Coefficient for accelerating the particle to reach the target
% GA parameters
pc=0.9; % Crossover Percentage or Crossover Probability
```

```
nc=2*round(pc*nPop/2);  % Number of Offsprings (also Parnets)
pm=0.02;  % Mutation Percentage or Mutation Probability
nm=round(pm*nPop);  %Number of Mutants
mu=0.02;  % Mutation Rate
beta=1;
empty_individual.Position=[];
empty_individual.Cost=[];
pop=repmat(empty_individual,nPop,1);
GlobalBest.Cost=inf;
empty_particle.Position=[];
empty_particle.Cost=[];
empty_particle.Velocity=[];
empty_particle.Best.Position=[];
empty_particle.Best.Cost=[];
for i=1:nPop
  % Initialize Position
  pop(i).Position=unifrnd(VarMin,VarMax,VarSize);
  % Evaluation
  particle(i).Position=pop(i).Position;
  % Initialize Velocity
  particle(i).Velocity=zeros(VarSize);
  % Evaluation value
  particle(i).Cost=pop(i).Cost;
  % Update Personal Best
  particle(i).Best.Position=particle(i).Position;
  particle(i).Best.Cost=particle(i).Cost;
  % Update Global Best
  if particle(i).Best.Cost<GlobalBest.Cost
  GlobalBest=particle(i).Best;
  end
end
Costs=[pop.Cost];
[Costs, SortOrder]=sort(Costs);
pop=pop(SortOrder);
```

```
% Store Best Solution
BestSol=pop(1);
% Array to Hold Best Cost Values
BestCost=zeros(MaxIt,1);
% Store Cost
WorstCost=pop(end).Cost;
for it=1:MaxIt
  P=exp(-beta*Costs/WorstCost);
  P=P/sum(P);
  popc=repmat(empty_individual,nc/2,2);
  for k=1:nc/2
  % Select Parents Indices
  i1=RouletteWheelSelection(P);
  i2=RouletteWheelSelection(P);
  p1=pop(i1);
  p2=pop(i2);
  % Apply Crossover
  [popc(k,1).Position,
popc(k,2).Position]=Crossover(p1.Position,p2.Position,gamma,VarMin,VarMax);
  % Evaluate Offsprings
  popc(k,1).Cost=Loadflow_DG(popc(k,1).Position,Num_DG,Type_DG);
    popc(k,2).Cost=Loadflow_DG(popc(k,2).Position,Num_DG,Type_DG);
  end
  popc=popc(:);
  % Mutation
  popm=repmat(empty_individual,nm,1);
  for k=1:nm
  % Select Parent
  i=randi([1 nPop]);
  p=pop(i);
  % Apply Mutation
  popm(k).Position=Mutate(p.Position,mu,VarMin,VarMax);
  % Evaluate Mutant
  popm(k).Cost=Loadflow_DG(popm(k).Position,Num_DG,Type_DG);
```

```
  end

% Create Merged or New Population
  pop=[pop
  popc
  popm];
  % Sort Population
  Costs=[pop.Cost];
  [Costs, SortOrder]=sort(Costs);
  pop=pop(SortOrder);
  % Update Worst Cost
  WorstCost=max(WorstCost,pop(end).Cost);
  pop=pop(1:nPop);
  Costs=Costs(1:nPop);
  % Store Best Solution Ever Found
  BestSol=pop(1);
  % Store Best Cost Ever Found
  for i=1:nPop
  if pop(i).Cost<=particle(i).Cost
  particle(i).Position = pop(i).Position;
  particle(i).Cost = pop(i).Cost;
  end
  Cx(i) = particle(i).Cost;
  end
  [BestCost(it),r]=min(Cx);
  GlobalBest.Cost=particle(r).Cost;
  GlobalBest.Position=particle(r).Position;
  BstCostGA(it)=BestCost(it);
  % Start PSO
for it=1:MaxIt
  for i=1:nPop
w(it)=wmin+((MaxIt - it)*(wmax - wmin))/(MaxIt-1);
  particle(i).Velocity = w(it)*particle(i).Velocity ...
  +c1*rand(VarSize).*(particle(i).Best.Position-particle(i).Position) ...
```

```
+c2*rand(VarSize).*(GlobalBest.Position-particle(i).Position);

% Apply Velocity Limits
particle(i).Velocity = max(particle(i).Velocity,VelMin);
particle(i).Velocity = min(particle(i).Velocity,VelMax);
% Update Position
particle(i).Position = particle(i).Position + particle(i).Velocity;
% Velocity Mirror Effect
IsOutside=(particle(i).Position<VarMin | particle(i).Position>VarMax);
particle(i).Velocity(IsOutside)=-particle(i).Velocity(IsOutside);
% Apply Position Limits
particle(i).Position = max(particle(i).Position,VarMin);
particle(i).Position = min(particle(i).Position,VarMax);
% Update Personal Best
if particle(i).Cost<particle(i).Best.Cost
particle(i).Best.Position=particle(i).Position;
particle(i).Best.Cost=particle(i).Cost;
% Update Global Best
if particle(i).Best.Cost<GlobalBest.Cost
  GlobalBest=particle(i).Best;
end
end
end
for i=1:nPop
if particle(i).Cost<=pop(i).Cost
pop(i).Position = particle(i).Position;
pop(i).Cost = particle(i).Cost;
end
Cx(i)=pop(i).Cost;
end
[BestCost(it),r]=min(Cx);
GlobalBest.Cost=pop(r).Cost;
GlobalBest.Position=pop(r).Position;
BstCostPSO(it)=BestCost(it);
```

```
  disp(['Iteration ' num2str(it) ': Best Cost = ' num2str(BestCost(it))]);
end
BestSol = GlobalBest;
finalres=Load_flow2(round(GlobalBest.Position,0),Num_DG,Type_DG);
%% Display all Results
disp('------------------------------------------------------------------------------------------');
disp('    Optimal Size and Location            ');
disp('------------------------------------------------------------------------------------------');
disp([' Number Of DG:            ' num2str(Num_DG)]);
disp(['Power Loss Before DG (KW):          ' num2str(finalres_out{1})]);
disp(['Power Loss Before DG (KVAr):        ' num2str(finalres_out{2})]);
disp(['Power Loss After DG (KW):        ' num2str(finalres{1})]);
disp(['Power Loss After DG (KVAr):        ' num2str(finalres{2})]);
disp(['Optimal          Location          of          DG(Bus          No.:                         '
num2str(round(GlobalBest.Position(Num_DG+1:end),0))]);
disp(['Optimal Size of DG (KW):    ' num2str(round(GlobalBest.Position(1:Num_DG),0))]);
disp([' Minimum Voltage(P.u):         ' num2str(finalres{7})]);
disp([' Maximum Voltage deviation(%):       ' num2str(finalres{8})]);
disp([' Active power reduction(%):         ' num2str(finalres{5})]);
disp([' Reactive power reduction(%):       ' num2str(finalres{6})]);
disp('------------------------------------------------------------------------------------------');
figure;
plot(BestCost,'LineWidth',2);
title('convergency curve')
xlabel('Iteration');
ylabel('Objective Function');
grid on;
figure
plot(finalres_out{3},'bo-')
hold on
plot(finalres{3},'gd-');
legend('Base Case Without DG',['With ', num2str(Num_DG), 'DG']);
title('Voltage profile of Kombolcha three Feeder')
xlabel('Bus Number');
```

```
ylabel('Voltage (P.u)');
figure
plot(finalres_out{4},'rd-');
hold on
plot(finalres{4},'bd-');
legend('Base Case Without DG',['With ', num2str(Num_DG), 'DG']);
title('Active power Loss');
xlabel('Bus Number');
ylabel('Active power (KW)');
figure
plot(finalres_out{6},'rd-');
hold on
plot(finalres{6},'bd-');
legend('Base Case Without DG',['With ', num2str(Num_DG), 'DG']);
title('Reactive power loss');
xlabel('Bus Number');
ylabel('Reactive power (kVAr)');
end
```